MODULATORS OF CALCIUM SIGNALLING IN NEURONAL PHYSIOLOGY AND DISEASE

by

Jeff Grant

A Thesis Submitted to the Faculty of Graduate Studies in

Partial Fulfilment of the Requirements of the Degree of

Doctor of Philosophy

Department of Pharmacology and Therapeutics

University of Manitoba

Winnipeg, Manitoba

© Copyright, 2008 by Jeff Grant

Abstract

This thesis focuses on the regulation of the ubiquitous second messenger Ca^{2+} in neuronal physiology and disease. Ca^{2+} signalling in neurons is regulated by ion channels located in the plasma membrane, as well as in the endoplasmic reticulum (ER) and mitochondrial membranes. Ca^{2+} signalling is essential for numerous cellular processes, including neuronal excitability, neurotransmitter release, synaptic plasticity, and induction of cell death. Age-related disruptions in Ca^{2+} signalling may contribute to decline of cognitive function and motor control associated with aging. Furthermore, disruption in neuronal Ca^{2+} signalling is implicated in several neurodegenerative disorders including Alzheimer's disease (AD), Parkinson's disease (PD), Huntington's disease (HD), and Amyotrophic Lateral Sclerosis (ALS). In this thesis, I studied neuronal Ca^{2+} signalling and how it is affected in neurodegenerative disease. First, I examined the role of the ER Ca^{2+} binding protein Calreticulin (CRT) in AD. CRT is involved in regulation of ER Ca^{2+} signalling and modulation of susceptibility to cell death. I found that there was an increase in the expression of CRT in *in vitro* and *in vivo* models of AD. However, increased levels of CRT did not alter susceptibility of neuronal cells to death induced by AD-related stressors. Second, I examined the role of X-Linked Inhibitor of Apoptosis Protein (XIAP) in the modulation of neuronal Ca^{2+} signalling. I found that overexpression of XIAP in neuronal cells modified Ca^{2+} signalling by decreasing Ca^{2+} flux through multiple plasma membrane and ER channels. These effects appear to be independent of caspase inhibition, which is one of the ways that XIAP can inhibit apoptosis. Third, I examined a compound found in green tea, L-theanine, a

glutamate receptor antagonist that is protective in models of excitotoxic neuronal injury. I found that 24 hour L-theanine treatment reduces the amount of Ca^{2+} released from neuronal intracellular stores in response to both glutamate stimulation and passive leak through ER channels. An acute 30 minute L-theanine treatment had similar effects. In conclusion, these observations further the understanding of the regulation of Ca^{2+} signalling in neurons and may lead to novel therapeutic strategies in neurodegenerative disease.

This thesis is dedicated to the memory of Dr. Nick Shepel

Your knowledge, insight, and mentorship will not be forgotten

"*Follow the science, not the hypothesis*"

Acknowlegments

I would like to thank my supervisor, Dr. Michael Mayne, and the members of my advisory committee, Dr. Paul Fernyhough, Dr. Fiona Parkinson, Dr. David Eisenstat, Dr. Ratna Bose, and Dr. Don Smyth, for the mentorship they have provided for me over the course of my degree. Their guidance and patience have been invaluable in the development of my research skills.

Many thanks to Dr. John Bradley, who has been instrumental in teaching me how to properly plan and execute my experiments, as well as how to clearly communicate my results. I appreciate the significant amount of time he has spent mentoring me.

Thanks to my fellow graduate students Charlene Supnet and Charmaine Noonan. Our informal scientific discussions were invaluable to the completion of my degree. I will always remember the great times we had in and out of the lab. Thank you to the technical staff of our lab whose efforts made working in the lab a thousand times easier.

I would like to thank the University of Manitoba, the Alzheimer's Society of Manitoba, the Alzheimer's Society of Canada, and the National Research Council of Canada for their financial support.

To my family, who taught me the value of hard work and dedication, and have been extremely supportive during my entire academic career. I will always be grateful for this.

Last, but not least, thanks to my wonderful love Jessica. Her sense of humor and energy always make me feel better when I am stressed or down. Thank you for encouraging me to be the best scientist I could possibly be. Without your love and support, I could not have achieved what I have.

TABLE OF CONTENTS

List of Figures

List of Abbreviations

AD - Alzheimer's disease

AHP – after hyper-polarization

ALS - amyotrophic lateral sclerosis

AMPA - 2-amino-3-(3-hydroxy-5-methylisoxazol-4-yl) proprionate

ANOVA - analysis of variance

ANT – adenine nucleotide translocase

APP - amyloid precursor protein

ATP - adenosine 5'-triphosphate

AUC - area under the curve

Aβ - amyloid β protein

BIR - baculovirus inverted repeat

BMPR -bone morphogenetic protein receptor

BSA - bovine serum albumin

cADPR - cyclic adenine diphosphate ribose

CaM – Calmodulin

CaM kinase - Ca^{2+}/calmodulin dependent protein kinase

cAMP – cyclic adenosine monophosphate

CCE – capacitative Ca^{2+} entry

CICR – Ca^{2+}-induced Ca^{2+} release

CNS - central nervous system

CRAC - Ca^{2+}-release-activated-Ca^{2+} channel

CRE - cAMP response element

CREB - cAMP response element-binding protein

CRT – calreticulin

CyP-D – Cyclophilin-D

DAP – depolarizing after-potential

DMEM/F12 - Dulbecco's modified Eagle's medium/F12

DNA - deoxyribonucleic acid

eGFP - enhanced green fluorescent protein

EOR - ER overload response

ER - endoplasmic reticulum

FBS - fetal bovine serum

GABA - gamma-aminobutyric acid

HBSS - Hank's balanced salt solution

HD - Huntington's disease

HEPES - 4-(2-hydroxyethyl)-1-piperazineethanesulfonic acid

H_2O_2 – Hydrogen peroxide

Hyg –hygromycin

IAP- inhibitor of apoptosis protein

IP_3 - inositol triphosphate

IP_3R - IP_3 receptor

JNK - Jun N-terminal kinase

Kd - dissociation constant

LTD - long term depression

LTP - long term potentiation

MEF- mouse embryonic fibroblasts

mGluR - metabotropic glutamate receptor

mHCX - mitochondrial $H+/Ca^{2+}$ exchanger

mNCX - mitochondrial $Na+/Ca^{2+}$ exchanger

MPTP - mitochondrial permeability transition pore

mRNA - messenger ribonucleic acid

MSN - medium spiny neuron

MTT - 3-(4,5-Dimethylthiazol-2-yl)-2,5-diphenyltetrazolium bromide

NAIP - neuronal apoptosis inhibitor protein

NB – neurobasal

NCRND8 - non-transgenic CRND8

NCS - neuronal Ca^{2+} sensor

NCX - Na^{+}/Ca^{2+} exchanger

NFAT - factor of activated T cells

Nf-κB - nuclear factor-kappa B

hILP - human IAP like protein

NMDA - N-methyl-D-aspartate

nNOS - neuronal nitric-oxide synthase

PAGE - polyacrylamide gel electrophoresis

PBS - phosphate-buffered saline

PBST - phosphate buffered saline with 0.1% tween-20

PCR - polymerase chain reaction

PD - Parkinson's disease

PMCA - plasma membrane Ca^{2+} ATPase

PS- presenilin

PVDF - polyvinylidene fluoride

RING - really interesting new gene

ROC - receptor-operated Ca^{2+} channels

RyR - ryanodine receptor

sAPP - secreted form of APP

SDS - sodium dodecyl sulfate

SERCA - sarco/endoplasmic reticulum Ca^{2+} ATPase

siRNA - small interfering RNA

SNpc - substantia nigra pars compacta

SOC - store-operated Ca^{2+} channel

SOD - superoxide dismutase

TBS - tris buffered saline

TBST - tris buffered saline with 0.1% tween-20

TCRND8 - transgenic CRND8

TGF-β - transforming growth factor beta

UP - mitochondrial Ca^{2+} uniporter

UPR - unfolded protein response

VDAC -voltage dependent anion selective channel

VGCC -voltage-gated Ca^{2+} channels

Wt - wild-type

XIAP - X-linked inhibitor of apoptosis protein

Chapter 1

General Introduction

The Ca^{2+} ion is a ubiquitous second messenger involved in multiple cellular processes [1]. This thesis examines the regulation of Ca^{2+} in neuronal cells, focusing on both endogenous and exogenous modulators of intracellular Ca^{2+}, and the possible role of these modulators in neurodegenerative disease. In the General Introduction I discuss the characteristics and mechanisms of cellular Ca^{2+} signalling, with particular emphasis on neurons. I then discuss neuronal processes regulated by Ca^{2+}. Finally, I discuss the effect of disruption of Ca^{2+} signalling in several neurodegenerative disorders of the brain. Figure 1.1 illustrates the different proteins responsible for regulation of neuronal Ca^{2+} signalling

1.1 Neuronal Ca^{2+} signalling: characteristics and mechanisms

1.1.1 The plasma membrane and neuronal Ca^{2+} signalling

At rest, the cytoplasmic resting Ca^{2+} concentration of neurons is approximately 100nM. Ca^{2+} sensitive processes are generally activated when the cytoplasmic concentration rises above 1000nM [1]. Cells invest considerable energy in maintaining low cytosolic Ca^{2+} levels, and loss of control of Ca^{2+} results in cellular dysfunction and death [2]. It is therefore essential to fully understand the system by which free Ca^{2+} is controlled in the cell, and what components of the system fail when Ca^{2+} is inappropriately controlled and cells die. There are several channels and transporters on the neuronal plasma membrane that function to modulate the amount of Ca^{2+} that enters the cytoplasm, and these are discussed below:

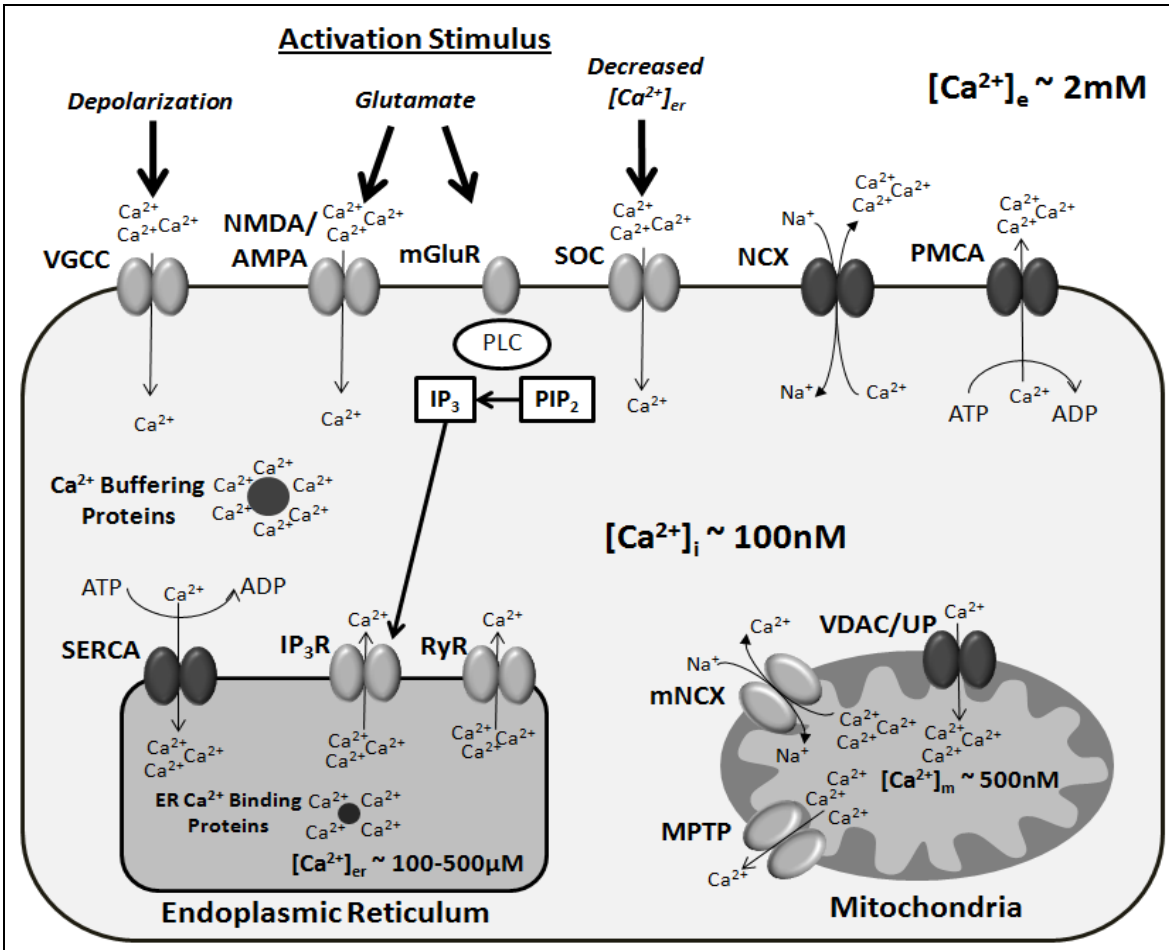

Figure 1.1. Mechanisms of Neuronal Ca^{2+} Signalling

At rest, neurons maintain a resting intracellular cytoplasmic $[Ca^{2+}]$ ($[Ca^{2+}]_i$) of roughly 100nM. A variety of stimuli can cause Ca^{2+} entry through plasma membrane channels such as voltage gated Ca^{2+} channels (VGCC), ionotropic glutamate receptors (NMDA/ AMPA), or store-operated channels (SOC). The ER is also a source of Ca^{2+} signals, maintaining a resting lumenal concentration ($[Ca^{2+}_{er}]$) of 100-500µM. The inositol triphosphate receptor (IP_3R) allows ER Ca^{2+} release upon IP_3 binding. An important source of IP_3 signals in neurons is through metabotropic glutamate receptors (mGluR) on the plasma membrane, which when activated cause phospolipase C (PLC) mediated conversion of phosphatidylinositol-4,5-bisphosphate (PIP_2) to IP_3. Ryanodine receptors (RyR) allow Ca^{2+} release from the ER when activated by increased levels of $[Ca^{2+}]_i$, a process termed Ca^{2+} induced Ca^{2+} release. The mitochondria, with resting Ca^{2+} levels ($[Ca^{2+}_m]$) of roughly 500nM, can also be a source of Ca^{2+} signals through channels such as the mitochondrial Na^+/Ca^{2+} exchanger (mNCX) and the mitochondrial permeability transition pore (MPTP). Cytoplasmic Ca^{2+} removal is needed to establish and maintain resting $[Ca^{2+}]_i$ after Ca^{2+} signals. The Na^+/Ca^{2+} exchanger (NCX) and plasma membrane Ca^{2+} ATPase (PMCA) move Ca^{2+} from the cytoplasm into the extracellular space. On the ER, the sarco/endoplasmic Ca^{2+} ATPase (SERCA) pumps Ca^{2+} from the cytoplasm into the ER lumen. The voltage dependent anion selective channel (VDAC) and the mitochondrial Ca^{2+} uniporter (UP) move Ca^{2+} from the cytoplasm through the outer and inner mitochondrial membranes into the mitochondrial lumen. Finally, Ca^{2+} buffering proteins in the cytoplasm and Ca^{2+} binding proteins in the ER also help to maintain resting Ca^{2+} levels.

1.1.1.1 Na^+/Ca^{2+} exchanger (NCX)

NCX is a bi-directional ion transporter on the plasma membrane that exchanges one Ca^{2+} ion for every three Na^+ ions, using energy from the Na^+ electrochemical gradient. Under resting conditions, the NCX moves Ca^{2+} out of the cell while allowing Na^+ into the cell. However, if the electrochemical gradient for Na^+ is reversed, as occurs during membrane depolarization, the NCX will then move Na^+ out of the cell while allowing Ca^{2+} into the cell [3]. There are three isoforms of NCX. NCX1 is expressed in multiple organs, including the brain, heart, kidney, skeletal muscle, and eye, while NCX2 and NCX3 are only found in the brain and skeletal muscle [4]. NCX transporters have a low affinity (K_d~1000 nM) for Ca^{2+}, but have high Ca^{2+}-binding capacity, resulting in a high turnover rate (~5000 ions/sec). This means that NCX binds and transports a relatively large amount of Ca^{2+} optimally at high cytoplasmic Ca^{2+} concentrations [5]. These properties are important for neuronal function, as the NCX works to return cytoplasmic Ca^{2+} to resting levels after large influxes due to an action potential. The NCX is also important for neuronal recovery after Ca^{2+} influx due to excitotoxic insult.

1.1.1.2 Plasma Membrane Ca^{2+} ATPase (PMCA)

The PMCA transporter uses energy from ATP hydrolysis to pump two Ca^{2+} ions out of the cytoplasm into the extracellular space for every molecule of ATP hydrolyzed [6]. In contrast to the NCX exchanger, PMCA has a high Ca^{2+} affinity (K_d~100nM), but low turnover rate (~250 ions/sec) for Ca^{2+} [7]. Therefore, PMCA is primarily responsible for maintaining cytoplasmic Ca^{2+} levels in neurons in the resting state. However, unlike

the NCX exchanger, PMCA is less effective at rapidly removing Ca^{2+} from the cytoplasm during action potentials or excitotoxic insult [8]. There are four major isoforms of the PMCA. PMCA1 mRNA was shown to be expressed in all tissues, thus is considered the housekeeping isoform of the protein [9] PMCA2 and PMCA3 expression was shown to be mostly limited to excitable tissues including the brain [9, 10], while PMCA4 is more widely expressed, also being found in the brain [11]. There are also several functional splice variants of all PMCA isoforms which have differential distributions in various tissues (for review see [12]). However, the functional consequences of these many isoform variants have yet to be determined.

1.1.1.3 Voltage-gated Ca^{2+} channels (VGCC)

VGCC open in response to depolarization of the plasma membrane, allowing an influx of Ca^{2+} into the cytoplasm down an electrochemical gradient. VGCC are heterooligomers formed from 5 protein subunits. The primary subunit of VGCC is the α_1 subunit, which forms the Ca^{2+} specific pore of the channel and is also responsible for voltage sensing. To date, 10 different isoforms of the α_1 subunit have been identified [13]. All VGCCs contain an α_1 subunit that forms a macromolecular complex with several other subunits; an intracellularly associated β subunit, which is believed to help stabilize the functional conformation of the α_1 subunit and enables the delivery of the channel from the ER to the plasma membrane. The β subunit also regulates the activation kinetics and voltage-dependence for activation of the α_1 subunit [14]; the α_2 and δ

subunits, which associate to each other by a disulfide bridge and may partially regulate expression of the α_1 subunit [15]; and finally the transmembrane spanning γ-subunit [13].

VGCCs are classified based upon the α_1 subunit and are grouped based on their electrophysiological characteristics. $Ca_v1.1$-$Ca_v1.4$ are defined as L- type Ca^{2+} channels. These channels are characterized by a high voltage threshold of activation (>-10mV), prolonged channel openings and slow inactivation [16]. Of this group, $Ca_v1.2$ and $Ca_v1.3$ are widely expressed in the brain and particularly modulate excitability and plasticity of hippocampal neurons [17]. $Ca_v2.1$, $Ca_v2.2$, and $Ca_v2.3$ are defined as P/Q-type, N-type, and R-type Ca^{2+} channels, respectively. P/Q and N-type channels exhibit a high voltage threshold of activation, similar to L-type channels, while R-type channels have an intermediate voltage threshold for activation (~-30mV) [18]. These three channel types are modulated by G-proteins. In the brain, P/Q-type channels are of particular importance in the cerebellum and brainstem, and are involved in synaptic transmission, neuronal excitability, gene expression, and neurotransmitter release [17]. Finally, $Ca_v3.1$- $Ca_v3.3$ are defined as T-type Ca^{2+} channels, and are characterized as having a low voltage threshold for activation (~70mV) and slow deactivation kinetics [18].

1.1.1.4 Receptor-operated Ca^{2+} channels (ROC)

Receptor operated channels (ROC) are defined as ion channels that open in response to a chemical messenger. A major ROC in terms of neuronal Ca^{2+} signalling is the ionotropic NMDA (N-methyl-D-Aspartate) receptor. The NMDA receptor is a heteromeric non-selective cation channel and is generally thought to be composed of two

NR1 subunits and two NR2 subunits [19]. Glutamate, along with the co-agonist glycine bind and activate NMDA receptors, allowing Na^+ and Ca^{2+} flux into the cell and K^+ flux out of the cell. Ca^{2+} flux through NMDA receptors acts as a second messenger to activate Ca^{2+}-dependent protein phosphorylation and gene transcription [20]. This is at least partially mediated by the c-terminus of the NR1 subunit of the NMDA receptor, as deletion mutants of this region lowered activation of these processes after NMDA receptor Ca^{2+} influx [21]. Ca^{2+} signalling through NMDA receptors is of particular importance in synaptic plasticity, providing Ca^{2+} signals involved in early modulation of synapses during learning and memory [22]. Ca^{2+} signalling through synaptic NMDA receptors has also been shown to promote neuronal survival by activating Ca^{2+}/calmodulin and CREB pathways [23], which in turn signal the nucleus to transcribe several pro-survival gene products [24]. A second class of ionotropic glutamate receptor is the AMPA (2-amino-3-(3-hydroxy-5-methylisoxazol-4-yl) proprionate) receptor. AMPA receptors are a homo- or hetero-tetrameric complex composed of various combinations of 4 types of subunit, GluR1-GluR4 [25]. AMPA receptors are also permeable to Ca^{2+}, unless they contain the GluR2 subunit [20]. Activation of Ca^{2+}-permeable AMPA receptors has been shown to activate transcription factors such as CREB [26] and AP-1 [27].

1.1.1.5 Store Operated Ca^{2+} channels (SOC)

Store operated Ca^{2+} entry replenishes intracellular stores by allowing Ca^{2+} influx through specific channels on the plasma membrane, termed SOC channels. Several types

of SOC channels are postulated to exist based upon electrophysiological studies [28], however the most extensively studied of these channels is the Ca^{2+}-release-activated-Ca^{2+} channel (CRAC). The exact nature of the CRAC channel has not been fully elucidated, however recent studies have identified the plasma membrane protein Orai1 to likely be at least one component of the CRAC channel [29-31]. Recently, STIM1, a protein found in the ER, was shown to be essential for capacitative Ca^{2+} entry through CRAC channels [32, 33]. STIM1 contains an EF Ca^{2+} binding domain, and it is believed that this domain senses depletion of ER Ca^{2+}. STIM1 then interacts with CRAC channels, signalling them to open and initiate capacitative Ca^{2+} entry [34]. Ca^{2+} signalling through SOC channels prevents depletion of intracellular stores, allowing sustained Ca^{2+} signals that are involved in gene transcription, cell metabolism and exocytosis [28].

1.1.1.6 Metabotropic Glutamate Receptors (mGluR)

Although metabotropic glutamate receptors do not directly allow Ca^{2+} flux across the plasma membrane, two isoforms of these receptors, mGluR1 and mGluR5, have been shown to modulate neuronal Ca^{2+} signalling. mGluR1 and mGluR5 are G-protein-coupled receptors which when stimulated activate phospholipase C, which in turn produces the second messenger inositol 1,4,5-trisphosphate (IP_3) [35]. IP_3 then stimulates Ca^{2+} release from ER stores by activating IP_3 receptor Ca^{2+} channels (IP_3R), which are important in several neuronal processes (see below).

1.1.2 The endoplasmic reticulum and neuronal Ca^{2+} signalling

The ER is a major sink for Ca^{2+} in neurons, acting to buffer Ca^{2+} signals by rapidly pumping Ca^{2+} into the ER lumen. The concentration of Ca^{2+} in the ER lumen can vary, depending on neuronal excitability, but usually it is in the micromolar range in resting cells [22]. In neurons, the ER is a continuous membrane system that extends from the nucleus in the cell soma all the way to dendrites and synapses, many tens of micrometers from the nucleus [36]. This membrane system is often in close contact with the neuronal plasma membrane which enables Ca^{2+} and second messenger signals from the plasma membrane to induce Ca^{2+} flux from the ER [22]. There are two major Ca^{2+} release channels on the ER membrane that are activated by these signals: the IP_3R and RyR channels. The SERCA Ca^{2+} pump on the ER membrane is responsible for Ca^{2+} uptake into the ER lumen. Finally, very recently presenilins (PS) have been shown to form passive Ca^{2+} leak channels on the ER membrane. Further detail for each of these proteins is provided below.

1.1.2.1 Inositol triphosphate receptors (IP_3R)

IP_3Rs are receptor operated Ca^{2+} channels located on the ER membrane, which when activated allow Ca^{2+} to flow out of the ER lumen into the cytoplasm down the electrochemical gradient [37]. The physiological ligand for IP_3Rs is IP_3, which is produced in the cytoplasm when agonists interact with specific G-coupled receptors on the plasma membrane (for example mGluR1), activating phospolipase C. IP_3 then diffuses through the cytoplasm, binding and activating IP_3R. IP_3Rs are composed of 4

subunits, with each subunit having one binding site for IP_3. Three mammalian isoforms of IP_3R have been identified to date [37]. IP_3Rs are widespread in the brain, with particular enrichment in cerebellar Purkinje cells, hippocampal CA1 pyramidal cells, and pyramidal cell bodies and proximal dendrites of the cortex [38]. Ca^{2+} release by IP_3Rs is modulated by the concentration of cytoplasmic Ca^{2+} [22], with low [Ca^{2+}] activating and high [Ca^{2+}] inhibiting the activation of IP_3Rs [39]. Levels of Ca^{2+} within the ER lumen also appear to modulate the sensitivity of IP_3Rs, with decreased levels of ER Ca^{2+} decreasing the sensitivity of the receptor to IP_3 [40].

1.1.2.2 Ryanodine Receptors (RyR)

RyRs are the second major class of Ca^{2+} -release channel located on the ER membrane. The major physiological agonist for RyRs is Ca^{2+}. An increase in cytosolic Ca^{2+} due to Ca^{2+} influx from either plasma membrane channels or Ca^{2+} release through channels in the ER membrane causes Ca^{2+} to bind to RyRs, which in turn open to allow Ca^{2+} release from the ER lumen, a process termed Ca^{2+}-induced Ca^{2+} release (CICR) [41]. CICR amplifies Ca^{2+} signals in response to action potentials or neurotransmitters in neurons [22]. RyR channels are composed of four identical subunits [41]. Three mammalian isoforms of RyR have been identified to date. All three isoforms are expressed in the brain, with RyR-2 being the most predominantly expressed [42]. Interestingly, RyRs are expressed at higher levels where IP_3R levels are lower, such as the dentate gyrus, CA3/4 areas of the hippocampus, and long thin apical dendrites of cortical pyramidal cells [38], suggesting that IP_3R and RyR Ca^{2+} pools may have

somewhat distinct roles in neuronal processes. There are several endogenous modulators of RyR activity, including ions (such as Ca^{2+}, Mg^{2+}, H^{+}, Fe^{2+}, and inorganic phosphate), adenine nucleotide, calmodulin, cyclic adenine diphosphate ribose and protein kinase-dependent phosphorylation, as well as the redox state of the cell [43].

1.1.2.3 Presenilin Ca^{2+} leak channels

Presenilins (PS), of which there are two isoforms, are ER and plasma membrane bound proteins that are involved in the cleavage and processing of several proteins including amyloid precursor protein (APP), the precursor to Aβ protein which is thought to be responsible for the pathogenesis of AD [44]. A recent study has shown that PS form low-conductance cation permeable ion channels in planar lipid bilayers. Also, this study demonstrated that knockout of PS in MEF cells resulted in overload of ER Ca^{2+} stores, which suggests that PS acts as a passive Ca^{2+} leak channel on the ER membrane [45]. Interestingly, familial AD associated mutations in PS-1 resulted in disruption of the PS-mediated Ca^{2+} leak, which may partially account for overload of Ca^{2+} in ER stores observed in certain models of AD [45].

1.1.2.4 Sarco/Endoplasmic reticulum Ca^{2+} ATPases (SERCA)

The SERCA pump is responsible for Ca^{2+} uptake into the ER lumen. Like PMCA channels (Section 1.1.2), SERCA pumps utilize energy from ATP hydrolysis to pump Ca^{2+} against an electrochemical gradient from the cytoplasm into the ER lumen, with a stoichiometry of two Ca^{2+} ions pumped per one molecule of ATP hydrolyzed [46]. There

are three isoforms of SERCA pumps, each of which exhibits different splice variants [47, 48]. The major isoform present in the brain is SERCA2b, which is found in the neurons of most brain regions [49].

1.1.3 Mitochondria and neuronal Ca^{2+} signalling

Mitochondria are the primary generators of energy in eukaryotic cells, and are widely distributed in the brain. Mitochondria are particularly concentrated in areas of the neuron that have high metabolic demand including the synapses, nodes of Ranvier, and myelination/demyelination interfaces [50]. In addition to generating ATP, mitochondria are also important in neuronal Ca^{2+} signalling. In particular, mitochondria can modulate the amplitude of Ca^{2+} signals by rapidly uptaking Ca^{2+} into the mitochondrial lumen [51]. Recent studies have also demonstrated that large global cellular Ca^{2+} signals are not required for mitochondria Ca^{2+} uptake, as local Ca^{2+} signalling can produce large spatially restricted increases in $[Ca^{2+}]$, and as such the mitochondria in these regions will take up Ca^{2+} [52]. There are several channels that regulate the amount of Ca^{2+} stored in the mitochondrial lumen:

1.1.3.1 Voltage dependent anion selective channel (VDAC)

VDAC is responsible for transport of Ca^{2+} from the cytoplasm across the mitochondrial outer membrane [53]. There are three mammalian isoforms of VDAC, and all three are found in the mitochondria of the brain [54]. Almost all metabolites and ions that cross the mitochondrial outer membrane must move through VDAC [55]. In the

open state, VDAC is weakly selective for anions, while the closing of VDAC is caused by both positive and negative potentials [55]. However, small ions such as Ca^{2+} can freely pass through the channel even in the closed state, while organic anions such as ATP, ADP, inorganic phosphate, and respiratory substrates such as pyruvate cannot [55].

1.1.3.2 Mitochondrial Ca^{2+} uniporter (UP)

This Ca^{2+} selective channel is responsible for allowing Ca^{2+} to pass through the inner mitochondrial membrane into the mitochondrial lumen [56]. The existence of this uniporter has been confirmed by electrophysiological studies, but the molecular features of the protein(s) have yet to be elucidated [57]. The UP requires an electrochemical gradient to allow Ca^{2+} to flow into the mitochondrial lumen [58]. When cytoplasmic Ca^{2+} concentration in the vicinity of the mitochondria exceeds roughly 500nM, flow through the uniporter increases such that Ca^{2+} influx into the mitochondria exceeds mitochondrial Ca^{2+} efflux mechanisms [59, 60]. Thus the uniporter allows the mitochondria to function as a Ca^{2+} sink.

1.1.3.3 Mitochondrial Na^{+}/Ca^{2+} exchanger (mNCX)

Several studies have demonstrated that mitochondria can efflux Ca^{2+} from the lumen to the cytoplasm in exchange for Na^{+} ions [61-63], although the molecular identity of this exchanger has yet to be elucidated. There is also evidence for the existence of a mitochondrial H^{+}/Ca^{2+} exchanger (mHCX) that moves protons into the mitochondrial lumen in exchange for Ca^{2+} ions [64].

1.1.3.4 Mitochondrial Permeability Transition Pore (MPTP)

The MPTP is a non-specific pore that forms at connecting junctions of the outer and inner mitochondrial membrane that allows ions and molecules up to a size of 1.5KDa to flow out of the mitochondria. The MPTP plays an important role in the induction of apoptosis and necrosis [65, 66]. Increased levels of Ca^{2+} (~ 1–3μM) within the mitochondrial lumen are critical for the formation of this pore [67]. Formation of the MPTP is also dependent on loss of mitochondrial membrane potential, accumulation of inorganic phosphate due to disruption of ATP production, and oxidative stress. Several components of the pore have been identified, including adenine nucleotide translocase (ANT), Cyclophilin-D (CyP-D), and VDAC [66].

The formation of the MPTP results in cytochrome C release from the mitochondria and also allows Ca^{2+} to flow out of the mitochondria, which can have several consequences to cellular function, including activation of Ca^{2+} dependent proteases such as calpain, and disruption of function of neighboring mitochondria because of Ca^{2+}overload [66].

1.1.4 Cytosolic Ca^{2+} binding proteins

Ca^{2+} that enters the cytoplasm is rapidly bound to Ca^{2+} buffering proteins such as parvalbumin and calbindin-D28k [1]. These cytosolic buffers can modulate the amplitude and duration of Ca^{2+} signals. For example, cerebellar purkinje neurons from parvalbumin and calbindin knockout mice exhibited increased amplitude of calcium

transients in dendritic shafts as compared to wild-type neurons [68]. Both parvalbumin and calbindin-D28k are widely expressed in the nervous system [69].

1.1.5 ER Ca^{2+} binding proteins

The major ER Ca^{2+}-binding protein in neurons and many other cell types is CRT, which has been shown to be involved in regulation of stored and releasable ER Ca^{2+} and ER protein folding and quality control [70]. The many functions of CRT as well as its role in AD are discussed in Chapter 2.

1.2 Ca^{2+} signalling and neuronal function

Several neuronal processes that are controlled or modulated by Ca^{2+} signalling are detailed below.

1.2.1 Neuronal Excitability

Ca^{2+} influx through VGCCs and release from ER Ca^{2+} channels can modulate plasma membrane potential and so affect neuronal excitability [22]. An example of this are after-hyperpolarizations (AHPs), which are hyperpolarizations of the neuronal plasma membrane that occur after an action potential. AHPs result from activation of two Ca^{2+} activated K^+ channels, termed gK_{Ca1} and gK_{Ca2} [71, 72]. gK_{Ca1} mediates fast AHPs during an action potential. Ca^{2+} entering through VGCCs activates gK_{Ca1}, which along with Na^+ channel inactivation rapidly restore the neuronal membrane to resting potential [72]. Slow AHPs, which can occur after fast AHPs are mediated by the opening of

gK_{Ca2}, which is caused by CICR through neuronal RyR channels [73, 74]. Recently, the cytoplasmic Ca^{2+} binding protein hippocalcin was shown to be the intermediary between Ca^{2+} release and gK_{Ca2} activation, acting as the Ca^{2+} sensor for gK_{Ca2} [75]. AHPs are thought to be important in regulating the rate of neuronal firing by interrupting high frequency neuronal discharges [22]. Finally, Ca^{2+} release from IP_3 stores was shown to be required for potentiation of inhibitory post-synaptic currents in cerebellar purkinje cells [76].

1.2.2 Neurotransmitter release

Neuronal Ca^{2+} signalling also plays an important role in both the mobilization and membrane fusion of synaptic vesicles containing neurotransmitters in synaptic terminals [77]. Ca^{2+} influx through VGCCs on the synaptic terminal occurs in response to action potentials. Neurotransmitters are stored in vesicles that are tethered to actin filaments via a protein called synapsin. Phosphorylation of synapsin by Ca^{2+}/calmodulin dependent kinase II disrupts the vesicle-actin interaction, and thus allows the synaptic vesicle to diffuse to and dock with SNARE complex on the plasma membrane [78]. Ca^{2+} entry through VGCCs also mediates assembly of the SNARE complex, an assembly of three proteins: the synaptic vesicle protein synaptobrevin and the plasma membrane proteins syntaxin and SNAP-25, which when assembled allows for vesicle-membrane fusion and subsequent neurotransmitter release [79]. A fourth protein, synaptotagmin, was identified to be the Ca^{2+}-sensor in SNARE assembly [80]. There is also evidence that

Ca^{2+} release from internal stores via IP_3 or RyR receptors may modulate neurotransmitter release at the synapse [81].

1.2.3 Learning and memory

The crucial role of Ca^{2+} as a second messenger in the brain is well illustrated in the role of Ca^{2+} in synaptic plasticity. Synaptic plasticity refers to the ability of neurons to alter the strength of the synaptic connection. An extensively studied form of synaptic plasticity is long-term potentiation (LTP), which is an increase in the strength of a synapse that can last from several minutes to several weeks [82]. Experimental LTP is induced in a postsynaptic neuron by inducing high-frequency stimulation of the presynaptic afferent, and is characterized by three sequential but distinct phases: The initial phase, which involves covalent modification (for example phosphorylation) of ion channels such as the AMPA receptor. The intermediate phase, which involves the translation and synthesis of new proteins from existing mRNA. Lastly, the sustained phase, which requires transcription of genes and subsequent protein synthesis [83]. Ca^{2+} entry through NMDA receptors or VGCCs, and a subsequent rise in Ca^{2+} concentration in the dendritic spine is the triggering event for the induction of LTP [84]. A crucial event is the Ca^{2+} mediated activation of calmodulin (CaM), an important regulatory protein that modulates the activity of several key signalling molecules involved in synaptic plasticity [85]. Ca^{2+} activates CaM by inducing a conformational change in the protein which enhances the interaction of CaM with downstream targets [86]. One such target is Ca^{2+}/calmodulin dependent protein kinase II (CaM kinase II). CaM kinase II modulates

early changes in LTP by altering both the conductance and distribution of AMPA receptors on the post-synaptic neuron [87, 88], with transient incorporation of Ca^{2+} permeable AMPA receptors into the plasma membrane occurring during LTP [89]. CaM kinase II may also regulate the enlargement of dendritic spines during LTP [90] and appears to be involved in regulating synthesis of dentritic proteins during late stage LTP [91]. CaM also can activate certain adenylyl cyclases [85], which are the enzymes responsible for production of cyclic AMP (cAMP). cAMP is important in learning and memory as it can activate the MAPK signal transduction pathway, which has been shown to be involved in LTP [92].

Ca^{2+} also modulates changes in gene expression in long-term memory via Ca^{2+}-mediated activation of cAMP response element-binding protein (CREB), a transcription factor that binds to and activates transcription from the cAMP response element (CRE) [93, 94]. CREB mediated gene transcription has been shown to be important in several neuronal processes, such as the establishment of long-term memory [95] and neuronal survival through neurotrophins [96]. Ca^{2+} entry through both VGCCs and NMDA channels in neurons was shown to activate this pathway [97, 98]. The mechanism by which Ca^{2+} mediates this activation is via phosphorylation of CREB that can occur by two separate pathways [99]. One pathway is via the interaction of Ca^{2+} with calmodulin and subsequent CaM kinase activation. CaM kinase IV in particular was shown to be responsible for CREB phosphorylation and activation in the brain, as mice deficient in CaM kinase IV had disrupted CREB phosphorylation and showed subsequent deficits in learning and memory [100-102]. CaM kinase IV also phosphorylates the CRE co-

activator CREB-binding protein, which enhances CRE transcription [103]. The other pathway by which Ca^{2+} can modulate the activatation of CREB is by activation of the MAP kinase pathway, as mentioned above [92]. Ras-ERK1/2 activates RSK2, a CREB kinase, which in turn phosphorylates CREB [104]. Interestingly, the CaM kinase pathway appears to modulate rapid activation of CREB, while the Ras-ERK1/2 pathway produces a slower, more prolonged activation of CREB [99].

Activation of the protein phosphatase calcineurin by CaM is also important in learning and memory. Activated calcineurin induces AMPA receptor endocytosis and internalization from the plasma membrane [105]. The resulting decreased AMPA receptor activity is involved in long term depression (LTD), which is a decrease in synaptic strength [106]. Calcineurin also is involved in the activation of the nuclear factor of activated T cells (NFAT) family of transcriptional activators, which regulate genes involved in learning and memory as well as neuronal survival [107].

Another group of proteins important in Ca^{2+}-mediated signal transduction during learning and memory are the Ca^{2+}-activated neuronal Ca^{2+} sensor (NCS) proteins. Like CaM, NCS proteins undergo a conformational change that causes activation when bound to Ca^{2+}. The most widely studied of the NCS proteins is NCS-1, which when activated modulates synaptic transmission [108], learning and memory [109, 110], Ca^{2+} channels [111, 112], neuronal growth [113] and neuronal survival [114]. Hippocalcin is another member of the NCS family, and has been shown to modulate mechanisms involved in learning and memory [115, 116] as well as neuronal survival [117]. There are several other members of this family of proteins that modulate a range of neuronal functions

[118]. Finally, caldendrins are another family of Ca^{2+}-activated second messengers that have recently been discovered to have important roles in neuronal Ca^{2+}-mediated signalling, including regulation of IP_3Rs [119] and VGCCs [120, 121]. Thus, there are several mechanisms by which Ca^{2+} can act in neurons to regulate learning and other neuronal processes.

1.2.4 Neuronal cell death

Neurons and all other cells of the body have a finely controlled Ca^{2+} homeostatic balance [1]. Subtle changes in this balance can modulate the susceptibility of neurons to cell death, while more gross changes in Ca^{2+} signalling can directly induce the death process. Apoptosis is a genetically controlled form of cell death that occurs in normal developmental and physiological processes. Over-induction of the apoptotic process is implicated in several diseases, including neurodegenerative disease [122]. Ca^{2+} is involved in the apoptotic process in several ways. In neurons, it has been demonstrated that overstimulation of NMDA receptors by glutamate leads to increased influx of Ca^{2+} which can initiate cell death pathways, a process which is termed excitotoxicity [123]. Cell death pathways induced by excitoxicity include induction of mitochondrial dysfunction, activation of MAP kinase apoptotic signalling, and modulation of the activity of Ca^{2+} sensitive enzymes such as calpain and calcineurin [124]. Increases in cytoplasmic Ca^{2+} concentration have been demonstrated to occur at both early and late stages of neuronal apoptosis [125].

In addition to Ca^{2+} influx, Ca^{2+} signalling from the ER has been implicated in apoptosis. For example, inhibition of IP_3R Ca^{2+} signalling was shown to protect cells from apoptosis [126]. It has been demonstrated that both overload and depletion of ER Ca^{2+} stores can also lead to induction of apoptosis. For example, extreme and/or prolonged alterations in the Ca^{2+} content of the ER can disrupt protein folding in the lumen of this organelle, resulting in activation of ER stress response pathways. One such pathway is the unfolded protein response (UPR) pathway which results in upregulation of several ER chaperone proteins [127]. Another is the ER overload response (EOR) which results in the production of several cytokines and interferons [128]. Both of these pathways are activated in an attempt to restore the normal protein folding function of the ER, but can also lead to induction of the apoptotic pathway [129]. Prolonged ER stress due to Ca^{2+} disruption can also lead to cleavage and activation of pro-caspase 12 by m-calpain, which subsequently activates other effector caspases, resulting in induction of apoptosis [122]. Changes in expression of the ER resident Ca^{2+} binding protein CRT has also been shown to alter sensitivity of cells to induction of apoptosis [130].

Mitochondrial Ca^{2+} handling is also implicated in induction of apoptosis, in particular with regards to Ca^{2+} mediated opening of the MPTP. Treatment of cells with a SERCA inhibitor caused increased mitochondrial Ca^{2+} uptake and Ca^{2+} mediated opening of MPTP, which subsequently lead to induction of apoptosis [131]. In contrast, treatment of cells with inhibitors of mitochondrial Ca^{2+} uptake or MPTP formation were shown to prevent the induction of apoptosis [122]. Opening of the MPTP results in disruption of mitochondrial membrane potential and uncoupling of the respiratory chain, resulting in

mitochondrial dysfunction [132]. This in turn causes release of cytochrome C from the mitochondria through the MPTP [133]. Cytochrome C then initiates Apaf-1/caspase-9 complex formation, which activates caspase-9, resulting in the apoptotic cascade [134].

Ca^{2+} can also activate a number of other molecules to induce apoptosis. One such molecule is the cysteine protease calpain, which has been shown to cleave several proteins involved in the modulation of apoptosis, including members of the Bcl-2 family, p53 transcription factors, and caspases [135]. Calpain can also irreversibly degrade several cytoskeletal and membrane proteins [136]. The protein phosphatase calcineurin, which is activated by Ca^{2+} through the Ca^{2+}/Calmodulin pathway, can induce apoptosis through dephosphorylation and subsequent activation of Bad, a pro-apoptotic member of the Bcl-2 family [137].

Necrosis, the uncontrolled form of cell death, may also be mediated by Ca^{2+}. Some studies have suggested that the magnitude of the Ca^{2+} disruption will determine which death pathway a cell will undergo, with smaller disruptions in Ca^{2+} promoting apoptosis and larger disruptions promoting necrosis [138].

1.3 Glial Ca^{2+} signalling

Ca^{2+} signalling is important for many physiological processes in glial cells. The term "glia" encompasses several cell types such as astrocytes, oligodendrocytes, and microglia [139]. Oligodendrocytes are responsible for forming the myelin sheaths around axons, while microglia are involved in inflammatory responses of the nervous system. Astrocytes have several functions in the nervous system, including mediating neuronal

differentiation and proliferation, as well as providing trophic support for neurons [140]. Of the various glial cells, astrocytes are the most studied in terms of Ca^{2+} signalling. Unlike neurons, astrocytes are non-excitable, thus use intracellular pools of Ca^{2+} for signalling instead of utilizing Ca^{2+} influx through VGCCs and ROCs. The two major channels responsible for astrocytic Ca^{2+} signalling are the IP_3Rs and the RyRs on the ER membrane [141]. Astrocytes display both spontaneous Ca^{2+} transients and Ca^{2+} signals resulting from communication from neighboring astrocytes and neuronal synapses. Interestingly, Ca^{2+} transients from a single astrocyte can propagate to neighboring astrocytes, creating "Ca^{2+} waves". The full details of the mechanisms of astrocyte-astrocyte Ca^{2+} signalling have not been fully elucidated, but current hypotheses include gap junction mediated diffusion of IP_3, or cell to cell ATP signalling through either direct cellular connection via gap junctions or exocytosis [142]. Neighboring neurons can elicit Ca^{2+} responses in astrocytes during synaptic transmission. Astrocytes possess receptors for several neurotransmitters (including glutamatergic, GABAergic, adrenergic, purinergic, serotonergic, muscarinic, and peptidergic receptors), and most of these receptors are G-protein coupled receptors that produce IP_3 when activated [143, 144]. This in turn will stimulate Ca^{2+} release from the ER via IP_3Rs.

Recent studies have demonstrated that astrocytic Ca^{2+} signalling can modulate synaptic activity. Ca^{2+} elevations in astrocytes can cause the release of specific neurotransmitters into the extracellular space, including glutamate, GABA, acetylcholine, and nitric oxide [145]. Release of these neurotransmitters can then modulate the synaptic activity of associated neurons, and this has been demonstrated in several *in vitro* and *in*

vivo settings [140]. Thus, Ca^{2+} plays a crucial role in the communication between neurons and astrocytes.

1.4 The role of Ca^{2+} in aging and neurodegenerative disorders

The above sections illustrate the crucial role of tightly controlled Ca^{2+} signalling in multiple neuronal processes. As such, disruptions in neuronal Ca^{2+} signalling can have a profound impact on the function of the brain. In this section I will review the role of altered neuronal Ca^{2+} signalling in aging-associated cognitive decline, and also in several neurodegenerative diseases.

1.4.1 Aging in the brain

Aging is associated with disruptions in learning and memory, which are common across numerous species [146]. At a cellular level, changes have been observed in terms of reduced neuronal excitability and reduction of LTP coupled with increases in LTD [147]. Subtle changes in neuronal Ca^{2+} signalling may at least in part mediate these age-related changes in neuronal function. Increased resting cytosolic Ca^{2+} concentration [148] and increased Ca^{2+} entry through VGCCs [149] have been observed in neuronal models of aging. Reductions in the Ca^{2+}-buffering capacity of the mitochondria [150] and the ER [151] have also been observed in aging models. In addition, several studies have shown that the rate by which Ca^{2+} is returned to resting concentration following a Ca^{2+} response is decreased in aged neurons [152]. This may be due to decreased expression and/or activity of the neuronal membrane PMCA [153]. Decreased Ca^{2+}

uptake through the mitochondrial uniporter due to loss of mitochondrial membrane potential has also been implicated in decreased Ca^{2+} removal from the cytoplasm [147]. These age-related changes in Ca^{2+} handling, along with reduced mitochondrial function, energy production and increased levels of oxidative stress, may serve to sensitize aged neurons to further disruptions in Ca^{2+} signalling due to toxic stimuli [154]. Indeed, disruption in Ca^{2+} signalling is observed in several age-related neurodegenerative disorders.

1.4.2 Alzheimer's disease

AD is an age-related neurodegenerative disorder characterized by progressive impairment of memory, mood, and coordination. Postmortem brains from patients who had AD exhibit striking deterioration in regions responsible for learning and memory, including the hippocampus, entorhinal cortex, basal forebrain, amygdala, frontal cortex, and inferior parietal cortex [155]. One of the pathological hallmarks of the disease is the presence of excessive amounts of Aβ peptide, which forms large deposits, or "plaques", in the brains of AD patients [155]. Another common feature is the presence of intracellular neurofibrillary tangles composed of hyperphosphorylated tau protein, a microtubule associated protein [155]. The current prevalent hypothesis for the pathology of this disease is referred to as the "amyloid hypothesis", which states that in AD, altered processing of APP causes overproduction of toxic Aβ peptides, resulting in disruptions in neuronal function and induction of neuronal death [156]. APP is an integral membrane protein that is cleaved into several products by proteolytic enzyme complexes called

secretases. There are 3 types of secretases, α, β, and γ secretase. Aβ is produced from APP by sequential cleavage by β-secretase and γ- secretase [157]. Strongly supporting the amyloid hypothesis is that the inherited form of AD, termed "familial" or "early onset" AD, is caused by mutations in γ-secretase enzyme complex components PS-1 or PS-2, which result in increased gamma secretase activity, or by mutations in APP itself, which enhance cleavage of APP by β and γ-secretase [156]. This results in increased production of the toxic $A\beta_{1-42}$ APP fragment, while decreasing production of a secreted form of APP (sAPP) that is thought to be involved in regulating synaptic plasticity and promotion of neuronal survival [156].

Analysis of post-mortem brain samples from AD patients revealed that altered Ca^{2+} signalling may be an important hallmark of AD. For example, it was demonstrated that levels of free and bound Ca^{2+} were increased in neurons exhibiting neurofibrillary tangles [158], and that these neurons also show increased levels of the Ca^{2+} activated protease calpain [159, 160]. The Ca^{2+} activated transglutaminase was shown to be increased in AD brains [161], and an increase in RyRs was observed as well [162].

Several studies conducted by Mattson and others have illuminated the mechanisms by which Aβ peptide may exert deleterious effects on neuronal Ca^{2+} signalling. Aβ exhibits a self-aggregation that ultimately results in deposition and plaque formation [156]. One of the byproducts of this aggregation is the production of hydrogen peroxide and hydroxyl radicals, an oxygen dependent process that is potentiated by metals such as Cu^{+} and Fe^{2+} [156, 163]. These byproducts can then in turn cause membrane lipid peroxidation that can impair the function of glucose and glutamate

transporters and membrane ATP-dependent Ca^{2+} exchangers, such as the Na^{+}/K^{+}-ATPase or the PMCA [164, 165]. This ultimately leads to increased neuronal basal Ca^{2+} levels and can render neurons susceptible to Ca^{2+} overload after glutamate stimulation [166]. Aβ has also been shown to increase Ca^{2+} entry through VGCCs [167].

Ca^{2+} release from neuronal intracellular stores is also changed in several models of AD. For example, several studies have shown increased Ca^{2+} release from ER stores in cells expressing familial AD PS mutations [168, 169]. Subsequent studies on cells expressing mutant PSs have shown increased levels of expression of RyRs coupled with increased Ca^{2+} release from RyR sensitive ER Ca^{2+} stores [170-172]. Our lab recently demonstrated that a mouse model expressing a mutant APP had increased neuronal levels of RyR-3 and exhibited increased neuronal ER Ca^{2+} release when stimulated with RyR specific agonists [173]. Astrocytes exposed to Aβ also exhibit increased Ca^{2+} release from intracellular stores, which results in enhanced astrocyte Ca^{2+} wave propagation [174].

Synaptic function seems to be especially affected by alterations of Ca^{2+} signalling in AD. The degree of synaptic degeneration in AD has been correlated to the severity of the disease [175]. Exposure of synaptosomes to Aβ resulted in impairment of the PMCA and increased Ca^{2+} levels after exposure to excitatory amino acids [164, 176]. Also, hippocampal slices from mice expressing mutant PS-1 showed increased after-hyperpolarizations, increased Ca^{2+} response to depolarization, and alterations in synaptic potentiation [177].

1.4.3 Parkinson's disease

PD is characterized by motor disturbances, loss of autonomic function, cognitive impairment, and depression [178]. These symptoms are associated with selective loss of dopaminergic neurons in the nigrostriatal pathway of the brain as well as less characterized loss of neurons from other regions of the brain [178]. The mechanisms of neuronal loss in PD have yet to be fully elucidated, but important aspects of PD appear to be oxidative stress and mitochondrial dysfunction which may be in part due to environmental toxin exposure [179]. Mutations within several genes are correlated with PD. Mutated α-synuclein, a protein of unknown function, was shown to be associated with an early onset form of PD [180], and the wild-type form of this protein is associated with the Lewy bodies that characterize brains of sporadic PD patients [178]. Mutations in the proteins Parkin, Pink-1, UCH-L1, and DJ-1 have also recently been linked to PD [179].

Changes in Ca^{2+} signalling may be associated with PD. It is thought that excitotoxicity and Ca^{2+} mediated nitric oxide production may contribute to the death of dopaminergic neurons in PD [181]. Neurons expressing high levels of the Ca^{2+}-buffering proteins calbindin and calretinin appeared to be resistant to cell death in PD [182, 183]. Finally, mutations in α-synuclein have been shown to increase neuronal plasma membrane ion permeability to several cations and anions, resulting in increase of basal Ca^{2+} levels and Ca^{2+} response due to depolarization [184].

1.4.4 Huntington's disease

Huntington's disease (HD) is an autosomal-dominant progressive neurodegenerative disorder characterized by involuntary movement, loss of coordination, cognitive decline and behavioral difficulties such as depression and psychosis. These symptoms are caused by selective loss of GABAergic medium spiny neurons (MSNs) in the striatum [185]. Mutations in the huntingtin gene resulting in expanded polyglutamine tracts have been identified as the cause of the disease [186]. These mutant forms of huntingtin deleteriously affect proteasomal function, ubiquitination, axonal transport, endocytosis, and synaptic transmission, as well as cause induction of apoptosis and alterations in gene transcription [187].

Several studies have also established that mutant huntingtin alters neuronal Ca^{2+} signalling [188]. For example, mitochondria from HD patients showed faster opening of the MPTP and subsequent loss of membrane potential compared with mitochondria from age-matched control patients [189, 190]. A subsequent study examining *in situ* mitochondrial Ca^{2+} handling using striatal neurons from mutant huntingtin knock-in mice showed that mitochondrial Ca^{2+} took longer to return to basal levels following stimulation with NMDA [191]. Neurons expressing certain forms of mutant huntingtin have also been shown to have larger Ca^{2+} signals through NMDA receptors [192, 193]. Finally, certain forms of mutant huntingtin have been shown to directly interact with IP_3R-1, which results in increased sensitivity of this receptor to IP_3 [194].

1.4.5 Amyotrophic lateral sclerosis

Amyotrophic lateral sclerosis (ALS) is characterized by progressive loss of muscle force, loss of breathing capacity, and limb spasticity. The symptoms result from progressive loss of cortical, spinal, and brainstem motor neurons [195]. Roughly 5-10% of ALS cases are familial in nature, while 20% of cases of the familial form of ALS are caused by mutations in the enzyme superoxide dismutase 1 (SOD-1). Several factors common to other neurodegenerative disorders are thought to be involved in the neuronal dysfunction and death of the motorneurons, including excitotoxicity [196], oxidative stress [197], and mitochondrial dysfunction [198].

Furthermore, changes in neuronal Ca^{2+} signalling are also implicated in the disease pathology. For example, motor neurons that expressed higher levels of the Ca^{2+}-buffering proteins calbindin or parvalbumin were more resistant to neurodegeneration in ALS [199]. Indeed, overexpression of these proteins conferred resistance to motor neuron death in ALS disease models [200, 201]. Neuronal cells expressing mutant SOD-1 were shown to have an increased cytoplasmic Ca^{2+} concentration [202], and increased Ca^{2+} entry through glutamate receptors, in particular Ca^{2+}-permeable AMPA receptors [203]. Thus, neurodegeneration in ALS may be in part due to increased free cytoplasmic Ca^{2+} levels as a consequence of increased Ca^{2+} entry through AMPA receptors. This in turn may cause an overload of mitochondrial Ca^{2+}, leading to increased oxidative stress and neurodegeneration [204].

1.5 Thesis objectives

As the above section has demonstrated, control of Ca^{2+} signaling in neurons is complex, and is crucial to optimal neuronal function. It is then therefore highly plausible that disruption of neuronal Ca^{2+} is associated with so many neurodegenerative diseases. However, there is much about the role and consequences of disruptions in neuronal Ca^{2+} signalling in neurodegenerative disease that is not well understood. It is imperative that ways to regulate these disruptions in Ca^{2+} signalling be discoved in order to prevent or treat neurodegenerative disease. This thesis has tested three separate hypotheses in order to investigate modulation of neuronal Ca^{2+} signalling and its role in neurodegeneration. Each of these studies are presented in separate chapters:

Chapter 2: CRT disrupts Ca^{2+} signalling and induces neurodegeneration in Alzheimer's disease. The objectives of this study were:

1) To determine if there are alterations in the levels of CRT in both an *in vitro* model and a mouse model of AD.

2) To determine the functional consequences of altered CRT levels in terms of neuronal Ca^{2+} signalling and cell death.

Chapter 3: XIAP modulates neuronal Ca^{2+} signalling. The objectives of this study were:

1) To determine if aspects of neuronal Ca^{2+} signalling are altered by XIAP overexpression in neurons.

2) To determine which specific aspects of Ca^{2+} signalling are affected by XIAP

3) To determine the mechanism by which XIAP alters neuronal Ca^{2+} signalling.

Chapter 4: L-theanine, a component of green tea, modulates neuronal Ca^{2+} signalling. The objectives of this study were:

1) To determine if aspects of neuronal Ca^{2+} signalling are altered by L-theanine treatment in neurons.

2) To determine which specific neuronal Ca^{2+} signalling mechanisms are affected by L-theanine treatment.

Chapter 2

The expression of Calreticulin is increased in *in vitro* and *in vivo* models of Alzheimer's disease

2.1 Abstract

CRT is the major Ca^{2+}-binding protein of the ER in non-muscle cells. CRT is involved in a variety of cellular processes including Ca^{2+} storage and release from the ER, the chaperoning and folding of proteins within the ER, as well as the induction of cell death. The expression of CRT is increased by general cell stress and dysregulation of Ca^{2+} signalling, however the physiological consequences of this induction are unclear. In AD, there is neuronal dysfunction and death, resulting in loss of memory, mood, and coordination. Deposition of toxic Aβ protein is thought to be responsible for many of the pathological effects seen in AD. In addition, oxidative stress is a prominent feature of the AD brain. Using a transgenic mouse model of AD, I found increased expression of CRT in the cortex at 12 weeks of age, with no change in CRT in the hippocampus. Furthermore, CRT expression is also increased in SH-SY5Y cells exposed to H_2O_2, $A\beta_{25-35}$ and $A\beta_{1-42}$ protein. Many studies have demonstrated that CRT regulates ER Ca^{2+} signalling, and disruption of ER Ca^{2+} signalling has been demonstrated in several models of AD. Therefore, to determine if increases in CRT in cells exposed to Aβ is causal in the changes in Ca^{2+} signalling observed in cells exposed to Aβ, I experimentally altered expression of CRT in SH-SY5Y cells and compared the resulting alterations in Ca^{2+} signalling to alterations observed after treatment with Aβ. I found few similarities between changes in Ca^{2+} signalling that occur with knockdown or overexpression of CRT and changes in Ca^{2+} signalling in cells exposed to Aβ . Overexpression of CRT did not affect the susceptibility of cells to toxicity from exposure to oxidative stress or toxic Aβ

protein. Further studies are needed to elucidate the consequences of increased CRT levels in models of AD.

2.2 Introduction

CRT, originally named High Affinity Ca^{2+} Binding Protein (HACBP) was discovered in 1974 in detergent extracts of the sarcoplasmic reticulum [205]. The CRT gene was cloned in 1989, which revealed an ER retention signal on the COOH-terminal sequence [206]. This indicated that CRT localized to the ER lumen, confirming a previous report that CRT was located primarily in the ER [206, 207]. Structural analysis of the CRT protein revealed two major Ca^{2+} binding domains. One is a high affinity, low capacity Ca^{2+} binding site located in the Proline rich (P)-domain, which binds 1mol Ca^{2+}/mol protein. The second is a low affinity, high capacity Ca^{2+} binding site in the carboxy-terminal (C)-domain, which binds about 25 mol Ca^{2+}/mol protein [208]. The C-domain is responsible for the ER Ca^{2+} storage function of CRT [209].

CRT is also a chaperone protein. CRT from liver ER extracts bound selectively to unfolded proteins, an interaction that was disrupted upon ATP hydrolysis, a property common to chaperone proteins [210]. Ca^{2+} was subsequently shown to be required for separation of CRT from unfolded proteins by ATP hydrolysis, demonstrating that the chaperone function of CRT can be regulated by changes in ER Ca^{2+} [211]. Furthermore, CRT was shown to bind to HIV gp120 protein in a manner similar to that of another ER chaperone, calnexin, suggesting that these proteins function in a similar manner [212]. Further studies have revealed that CRT, calnexin and another ER chaperone, ERp57,

function in concert to control protein folding and quality control within the ER [213, 214].

CRT gene transcription and protein synthesis is increased in situations of cell stress and/or toxicity, as well as in response to disruption of cellular Ca^{2+} signalling, particularly in the ER. For example, CRT transcription was upregulated in a variety of cell lines in response to heat shock, and rats exposed to hyperthermia showed increased CRT transcription and translation [215]. Tunicamycin, which inhibits protein glycosylation in ER and so causes accumulation of unfolded proteins also increased CRT mRNA levels [216]. Furthermore, in two separate studies, depletion of ER Ca^{2+} stores by treatment with the SERCA inhibitor thapsigargin also induced CRT mRNA expression [216, 217]. Thus, CRT is upregulated in several pathological settings.

The manner in which CRT modulates ER Ca^{2+} signalling is complex and remains controversial. For example, a number of studies have shown that overexpression of CRT increased IP_3-induced Ca^{2+} release [218, 219], while knockdown of CRT had the opposite effect of decreasing IP_3-induced Ca^{2+} release [209, 220]. Several studies have demonstrated that overexpression of CRT increased the stored ER Ca^{2+} [218, 219, 221-223]. Several studies have also shown that overexpression of CRT caused a reduction in the extent of CCE [218, 219, 221, 222, 224].

However, there are conflicting reports on the effect of CRT on Ca^{2+} signalling. For example, in two separate studies overexpression of CRT lowered or had no effect on Ca^{2+} release from ER stores [221, 224], while in another study, knockout of CRT did not alter Ca^{2+} release from ER stores [225]. Also contrary to previous reports, one study

demonstrated that overexpression of CRT increased CCE [223]. The role of CRT is also controversial in Ca^{2+} entry after oxidative stress. In one study, overexpression of CRT lowered the amount of Ca^{2+} that entered cells after oxidative stress [226], while another study found that CRT overexpression increased the amount of Ca^{2+} that entered the cell after oxidative stress [223]. It is unclear as to why contrasting effects of CRT on Ca^{2+} signalling are observed. The fact that a variety of different cell types were used for the various studies may be a factor, thus further studies will have to be performed to take into account these differences.

CRT also plays a role in cell death due to cellular stress. Early studies showed that CRT might have a protective role in the cell. Decreasing CRT expression resulted in increased susceptibility to ionomycin-mediated cell death in neuroblastoma cells [227], and CRT overexpression protected cells from oxidative stress mediated cell death [226].

In contrast, a more recent study using cardiomyoblasts demonstrated that overexpression of CRT actually increased induction of cell death in response to oxidative stress, while antisense knockdown of CRT prevented oxidative stress mediated cell death. [223]. In addition, another study demonstrated that fibroblasts derived from CRT knockout mice were resistant to UV radiation-mediated induction of apoptosis [228].

The conflicting effects of CRT on Ca^{2+} signalling and cell death are most likely the result of experiments performed with different drugs or stressors and different cell types. As such, it appears that CRT may have cell-type specific functions and/or functions that are altered depending on the type of stress the cell is exposed to.

Disruptions of neuronal Ca^{2+} signalling and subsequent neurodegeneration are well documented in AD. Since CRT is involved in ER Ca^{2+} signalling, I was interested in determining the role of CRT in AD. The first objective of this study was to determine if there were alterations in CRT expression in models of AD. To accomplish this I used the APP695 (KM670/671NL and V717F) mutant CRND8 mouse, as well as an *in vitro* model using SH-SY5Y neuroblastoma cells exposed to oxidative stress and β-Amyloid. I showed that in both models there is a significant increase in CRT. The second objective was to determine the physiological changes associated with altered CRT expression in neuronal cells. To accomplish this, I used siRNA mediated CRT knockdown and transient overexpression of CRT in SH-SY5Y neuroblastoma cells. I found that modulation of CRT expression does affect certain aspects of Ca^{2+} signalling. However these changes in Ca^{2+} signalling were not the same as those observed due to exposure to Aβ peptide. In addition, I found no significant alteration in susceptibility to AD-stressor induced cell death in CRT overexpressing cells. These data revealed that the changes in CRT expression in AD may not be causal in dysregulation of Ca^{2+} signalling.

2.3 Materials and Methods

2.3.1 Antibodies

CRT was probed with a specific mouse monoclonal IgG1 antibody (BD transduction laboratories) and β-Actin was probed with a specific goat polyclonal IgG antibody (Santa Cruz Biotechnology, Inc.). Secondary antibodies used for western analysis were peroxidase-conjugated Affinipure goat anti-mouse IgG (H + L) or rabbit

anti-goat IgG (H+L) (Jackson Immunoresearch Laboratories Inc.). Secondary antibodies used for immunofluorescence were Alexafluor 488 or Alexafluor 546-conjugated goat anti-mouse IgG (H+L) (Invitrogen).

2.3.2 Animals and cell culture

Human SH-SY5Y neuroblastoma cells (ATCC) were cultured in DMEM:F12 media with 10% fetal bovine serum (FBS), 1% penicillin/streptomycin (Invitrogen). APP695 (KM670/671NL and V717F) transgenic (T) CRND-8 mice were a gift from Dr. D. Westaway (University of Toronto) and a colony was established at the Atlantic Veterinary College, Charlottetown, PE. Transgenic (T) CRND-8 animals have a double mutation in the APP gene in which KM670/671NL and V717F amino acids are changed. Amyloid plaque deposits can be observed as early as 3 months of age, and are correlated with increased cognitive impairment [229]. For western analysis, animals were euthanized with Euthanyl (Sigma) at the specified ages, and cortical and hippocampal brain regions were dissected and quick-frozen on dry ice, then stored at -80ºC until further use. For primary neuronal cultures, non-transgenic (N)CRND8 female mice were bred with TCRND8 male mice (heterozygous for mutant APP). Pregnant females were sacrificed at embryonic day 16 and the embryos were removed and placed on ice. All embryos were genotyped for the APP695 double mutation by PCR (Platinum *Taq*DNA polymerase; Invitrogen) before cell dissociation and tissue pooling. The primers used for double mutant APP695 were as follows: 5_ TGT CCA AGA TGC AGC AGA ACG GCT ACG AAA A and 3_ AGA AAT GAA GAA ACG CCA AGC GCC GTG ACT. PCR

products were generated by 30 cycles of 94/68/72 °C (iCycler iQ real time PCR detection system ,Bio-Rad). Cerebral cortices were dissected from CRND8 fetuses and placed in Hank's balanced salt solution (HBSS, Invitrogen). NCRND8 and TCRND8 cortices were pooled separately. HBSS was removed and tissue was resuspended in warm trypsin solution (0.25% in HBSS, Invitrogen), and incubated for 10 min at 37ºC. An equal volume of HBSS + 10% FBS was then added to deactivate the trypsin. The tissue was triturated 10 times with a Pasteur pipette, and the cells were then aspirated and resuspended in Neurobasal media (Invitrogen) plus 10% FBS, 2% B27 supplement (Invitrogen), 5mM HEPES, 1mM L-glutamine, and 1% Gentamycin (Invitrogen), then counted, and plated at the desired density. Media was changed to Neurobasal plus 2% B27, 5mM HEPES, 1mM L-glutamine, and 1% Gentamycin 24 hours post-plating. Experiments were performed following 7-9 days of culture. All cells were cultured at 37ºC with 5% CO_2, and half the media was replaced with fresh media every 3 days. For all cell types, cells were plated at 1.5 x 10^6/well in 6 well plates for western analysis, 1.5 x 10^5/well in 24 well plates with coverslips for immunocytochemistry, and 6 x 10^5/well in 6 well plates for transfections, trypan blue viability assays, and Ca^{2+} imaging experiments.

2.3.3 Stressor treatment of SH-SY5Y cells and primary cortical neurons

Hydrogen peroxide (H_2O_2, Sigma) treatments were prepared from a 9.8M stock. $A\beta_{25-35}$ and $A\beta_{1-42}$ peptides (Bachem) were prepared as 200µM stock solutions in phosphate buffered saline (PBS, pH 7.4) and stored at -20ºC until use. All Aβ isoforms

were incubated overnight at 37^{o}C prior to application to allow fibril formation. Cells were treated with stressors for various concentrations and times of exposure. For western analysis, cell scrapers (VWR) were used to remove cells from the dishes after treatment. Cells were then spun down, supernatent was removed, and the cells were stored at -80ºC until further use.

2.3.4 Protein quantification, SDS-PAGE and Western analysis

Tissue or cells were homogenized in Laemmli buffer (0.5M Tris, 4% SDS, pH 6.8) containing protease inhibitor (Complete protease inhibitor, Roche), first using small pestles (Eppendorf) in an 1.5ml tube, then further homogenized by sonication for ~ 10 sec. Lysate was spun at maximum speed in a microcentrifuge to pull down insoluble protein. Supernatent was then placed in a fresh tube. Samples were diluted 1/10 - 1/1000 in laemmli buffer, then protein concentration was assayed for each sample in triplicate using the Lowry method (Biorad DC protein assay), with 0.2-1.6 mg/ml of BSA in laemmli buffer used to generate the standard curve for quantification. Absorbance after incubation with protein assay reagents was measured in a 96 well plate at a wavelength of 750nm using the Molecular Devices Spectramax M2 absorbance/fluorescence plate reader and analyzed using Softmax Pro 4.6 (Molecular Devices).

For SDS-PAGE, an equal volume of SDS-PAGE loading buffer (150mM Tris (pH 6.8), 1.2% SDS, 30% glycerol, 15% β-mercaptoethanol, 2.7μM bromophenol blue) was added to 40μg of each sample and boiled for 5 minutes, then loaded onto a 10% SDS-PAGE gel. Electrophoresis of gels was performed in running buffer (3.5mM SDS,

25mM Tris, 192mM glycine) at 100V until samples reached the stacking-separating interface, then run at 150V until adequate separation had occurred. Separating gels and PVDF membranes were then equilibrated in transfer buffer (38.6mM glycine, 47.9mM Tris, 1.28mM SDS, 20% Methanol (V/V)) for 5 minutes, then proteins were transferred to the PVDF membrane using a semi-dry transfer apparatus (Biorad) at 15V for 30 minutes. Membranes were blocked for 1 hour in blocking buffer (1% Roche blocking reagent solution in Tris Buffered Saline (TBS, 50mM Tris, 150mM NaCl, pH 7.5), then incubated overnight with anti-CRT antibody (1/2500 in 0.5% Roche blocking buffer) with rocking at 4ºC. Membranes were washed 3 times with TBST (0.1% Tween 20 in TBS) and incubated with horseradish peroxidase conjugated anti-mouse IgG antibody (1/10000 in 0.5% blocking buffer) for 1 hour at room temperature with rocking. Membranes were again washed 3 times with TBS, then exposed to chemiluminescent blotting substrate (luminescence substrate solution A and starting solution B mixed at 100:1 ratio, Roche) for 30 seconds and imaged on a Geldoc station (Biorad) for 60 seconds. Membranes were then stripped by two 5 minute incubations with stripping buffer (200mM glycine, 3.5mM SDS, 1% Tween 20, pH 2.2), then washed with two 10 minute incubations in PBS, 5 minutes in TBST, 1 minute rehydration in 100% methanol and finally 5 minutes in TBST. Membranes were then reprobed for β-Actin (primary antibody: 1/1000, secondary antibody, peroxidase conjugated ant-goat: 1/10000). Band density was measured using Scion image software (NIH). The average pixel intensity for a standardized region of interest was calculated for all bands and CRT data was normalized to the appropriate β-Actin band.

2.3.5 Knockdown of CRT

Serum containing media was removed from SH-SY5Y cells prior to transfection and replaced with DMEM/F12 containing no FBS or antibiotic. CRT small interfering RNA (siRNA) (Ambion) had the sequences 5'-GGAGCAGUUUCUGGACGGATT-3' and 5'-UCCGUCCAGAAACUGCUCCTT-3'. Scrambled non-specific siRNA (Ambion) was used as a negative control. For each experimental well, 100nM of siRNA (CRT specific or Negative control, unlabeled for western blot and cell viability experiments, Cy3^{TM} labeled for immunocytochemistry and Ca^{2+} imaging experiments) was mixed with 0.6% Lipofectamine 2000 in serum and antibiotic-free DMEM/F12 and incubated for 20 minutes at room temperature. The transfection mixture was then added to the appropriate well and incubated at 37ºC for 4 hours. Following this incubation, an equal volume of DMEM/F12 + 20% FBS was added to each well. 24 hours post-transfection, the transfection mixture was aspirated and replaced with DMEM/F12 with 10% FBS, 1% penicillin/streptomycin. To determine the effectiveness of CRT knockdown 2 methods were used: 1) 72 hours post-transfection, cells were scraped and CRT was assayed using western analysis, and 2) 48 hours post-transfection, cells were trypsinized (0.05% trypsin in HBSS), counted and re-plated on coverslips (poly-D-lysine coated) at 1.0×10^5 cells/well. After a further 24 hours, cells were fixed and immunocytochemistry was performed to assay CRT expression.

2.3.6 Transfection and overexpression of CRT

For Ca^{2+} imaging experiments, SH-SY5Y cells were transfected with mCherry (2µg/ml) or mCherry (2µg/ml) and CRT (8µg/ml). mCherry (gift, Dr. R. Tsien, Stanford) was cloned into gw1 plasmid (gift, Dr. S. Finkbeiner, UCSF) as follows: mCherry was PCR amplified from pSETmCherry using a 5' primer with a HindIII site (5' –CTG AAG CTT ATG GTG AGC AAG GGC GA - 3') and a 3' primer with a KpnI site (5' – AGT GGT ACC TTA CTT GTA CAG CTC GTC CAT GC - 3'). Following digestion of the pcr product and the gw1 plasmid with HindIII and KpnI, mCherry was ligated into gw1. CRT in pcDNA3.1 was a gift from Dr. Ihara, Nagaski University, Japan.

For immunofluorescence experiments, SH-SY5Y cells were transfected with pHyg-eGFP (BD Biosciences, 2µg/ml) or pHyg-eGFP (2µg/ml) and CRT (8µg/ml). pHyg-eGFP expresses enhanced green fluorescent protein, which allowed for the tracking of postively transfected cells. Prior to transfections, media was aspirated from cells and replaced with Opti-MEM reduced serum media (Invitrogen). Plasmids and Lipofectamine 2000 (0.6%) were incubated in Opti-MEM separately for 10 minutes at room temperature, then mixed and incubated at room temperature for 20 minutes. Transfection mixtures were then added to each well and cells were incubated at 37ºC for 4 hours. The media was then aspirated and replaced with DMEM/F12 with 10% FBS plus 1% penicillin/streptomycin. Cells were trypsinized and replated onto appropriate wells with poly-D-lysine coated coverslips 24 hours post-transfection. Transfected cells

were used for Ca^{2+} imaging experiments or immunofluorescence 48 hours post-transfection.

2.3.7 Immunocytochemistry

For immunocytochemistry, cells were washed once with PBS for 5 minutes, then fixed in ice cold 100% Methanol (Sigma) for 2 minutes. Fixed cells were then permeablized with 0.01% Triton-X 100 in PBS for 5 minutes and washed twice with PBS for 5 minutes. Cells were then blocked for 1 hour with blocking buffer (1% goat serum in PBS) at room temperature, and incubated with primary CRT antibody (1/250 dilution) in blocking buffer overnight at $4^{o}C$. After this incubation, they were washed 3 times with PBS for 5 minutes each and incubated with Alexafluor 488 or Alexafluor 546 conjugated secondary antibody (1/1000 dilution) at room temperature in the dark for 1 hour. A brief incubation (1 minute) with 1µg/ml Hoechst 33342 (Sigma) in PBS followed to stain the nuclei, followed by three 5 minute washes with PBS. Coverslips were mounted onto slides using Fluorosave reagent (Calbiochem) and imaged using an upright epifluorescent microscope (Axioskop 2 plus, with MBQ 52 ac Xenon lamp, Zeiss) equipped with a Zeiss Mrm Axiocam. All images were captures using Axiovision Release 4.2 software, and stored as 16-bit tiff files. Fluorescence intensity for each image was assessed using ImageJ software (NIH).

2.3.8 Single cell Ca^{2+} imaging

SH-SY5Y cells were loaded for 20 min at 37°C in Locke's solution (154mM NaCl, 3.6mM $NaHCO_3$, 5.6mM KCl, 1mM $MgCl_2$, 2.3mM $CaCl_2$, 5mM HEPES, and 5mM glucose, pH 7.2) containing fura-2 AM (1 µM, Invitrogen) and BSA (0.1% w/v). Coverslips of cells were placed in a laminar flow chamber (FCS2, Bioptechs, Butler, PA) and were perfused with a flow rate controlled by a peristaltic pump (0.5 ml/min; Instech, Plymouth Meeting, PA). Precise switching between perfusion solutions was achieved using solenoid valves (Valvelink 8 controller, Automate Scientific). Neurons were imaged with a heated 40x oil objective on an inverted epifluorescence microscope (Axiovert 200, Zeiss) equipped with a CCD digital camera (Axiocam MRm, Zeiss). Slidebook software (Intelligent Imaging Systems) controlled an excitation filter wheel for alternating excitation at 340 and 380 nm, and emitted light was collected through a custom dichroic block for fura-2, at a rate of 1 image pair/sec (Chroma). Average intensity for both 340nm and 380nm images was determined from regions of interest placed on cells. All data was analyzed by calculating the ratio between measured excitation at 340 nm vs. 380 nm, then converting the data to a measure of F/F_0, where: *F = ratio 340nm/380nm at time 'x'*, and *F_0 = ratio 340nm/380nm at time 'zero'$_0$, the first recorded ratio.* Two characteristics of Ca^{2+} responses were analyzed: Peak Ca^{2+} response (defined as $F_{max} - F_0$, where F_{max} = highest F value reached during a particular Ca^{2+} response) and area under the curve (A.U.C., defined as an integrative measurement of the Ca^{2+} responses). For calculation of resting cytoplasmic Ca^{2+}, 340nm/380nm fluorescence values were recorded for each cell for 5 seconds under resting conditions and averaged.

.

2.3.9 Cell viability assays

For trypan blue exclusion assay, following induction of cell death by stressor treatment, trypan blue exclusion was performed using an automated Vicell XR (Beckman Coulter). For the experiments measuring loss of Cherry fluorescence as an assessment of cell death, SH-SY5Y cells were transfected on 24 well plates with mCherry (2µg/ml) or mCherry (2µg/ml) and CRT (8µg/ml) as stated above. 24 hours post-transfection, the cells were treated with H_2O_2 for an additional 24 hours. The cells were then examined by immunocytochemistry as stated above. Transfected cells and nuclei were visually counted using ImageJ software.

2.3.10 Statistical Analysis

Data were analyzed using GraphPad Prism Version 4. Student's two tailed t-test or one way Analysis of Variance (ANOVA) with Tukey's post-test was performed to determine differences between means. Differences were considered significant at $P < 0.05$.

2.4 Results

2.4.1 CRT expression is increased in the cortex of transgenic CRND8 mice at ages that correlate with plaque deposition and cognitive decline

CRT expression was assayed using western analysis on cortical and hippocampal samples from transgenic (T) CRND8 mice and their Non-Transgenic (N)

CRND8 littermate controls. I observed a significant increase of cortical CRT in TCRND8 mice at 12 weeks and an increasing trend at 16 weeks of age compared to age-matched NCRND8 control cortical samples (Figure 2.1A). No significant difference was seen at 4 and 8 weeks. Furthermore, no significant difference in CRT expression was found in the hippocampus of TCRND8 mice compared with age-matched NCRND8 mice at all time points measured (8, 12 and 16 weeks of age) (Figure 2.1B).

2.4.2 CRT expression is increased in SH-SY5Y cells exposed to oxidative stress or Aβ protein in a dose dependent manner

Increased oxidative stress is a common hallmark in AD brain and accumulation of amyloid fibrils and subsequent plaque formation are major factors in the pathology of AD. Therefore, I investigated whether exposure to oxidative stress and Aβ could increase CRT expression in an *in vitro* neuronal cell model. As a model for oxidative stress, I exposed SH-SY5Y cells to H_2O_2 (25μM or 50μM) for 24 hours and measured CRT expression by western analysis. I observed a significant increase in CRT in cells treated with 50μM H_2O_2 as compared to untreated control cells (Figure 2.2A). To model damage caused to neurons in AD by exposure to amyloid fibrils, I treated SH-SY5Ys for 24 hours with either the toxic fragment of the Aβ protein, $A\beta_{25-35}$ (5-20μM), or with the full-length toxic $A\beta_{1-42}$ (5-20μM). As observed with cells treated with H_2O_2, there was a significant increase in CRT expression in SH-SY5Ys treated with 20μM of either $A\beta_{25-35}$ (Figure 2.2B) or $A\beta_{1-42}$ (Figure 2.2C) compared to untreated controls.

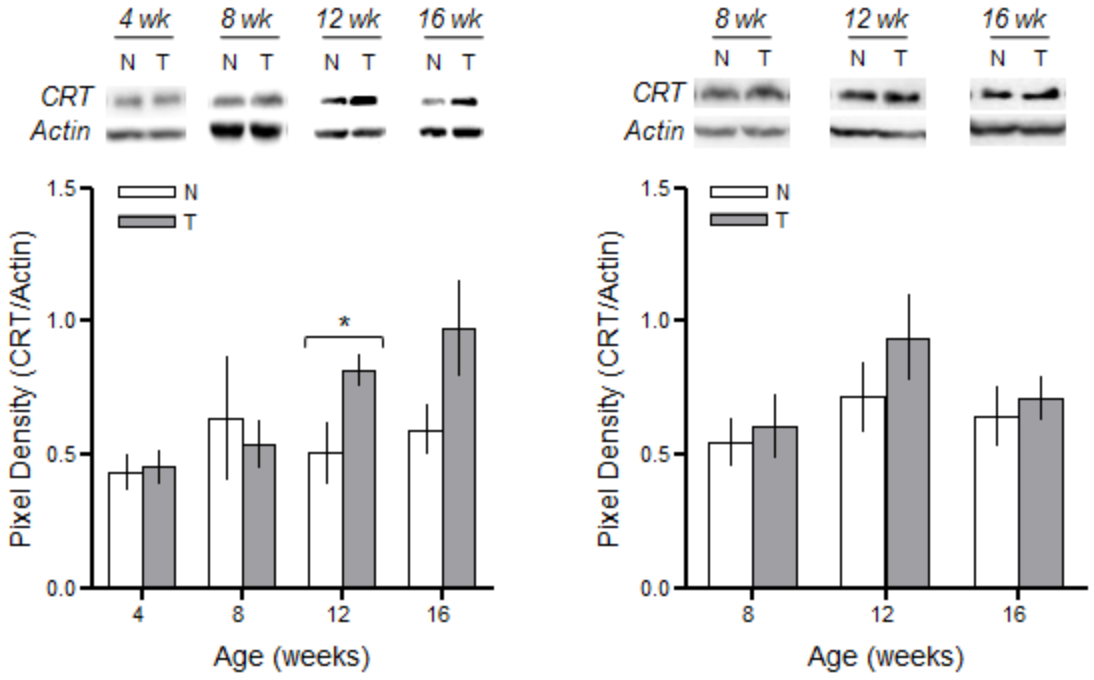

Figure 2.1. CRT is increased in cortex but not hippocampus of TgCRND8 mice at 12 weeks of age.

A. Western analysis on protein extract (40µg) from cortex from 4, 8, 12 and 16 week old transgenic (T) CRND8 mice compared to age-matched Non-Transgenic (N) controls. Blots were probed for CRT, then stripped and reprobed for β-actin. The top of the figure displays a representative blot, while the bottom chart represents quantification and normalization to β-actin of mean band intensity for multiple experiments. For this and all similar charts, bars represent mean +/- SEM (N- 4wk: n=10, 8wk: n=8, 12wk: n=6, 16wk: n=8, T- 4wk: n=10, 8 wk: n=8, 12 wk: n=7, 16 wk: n=10). ***** - $p<0.05$, student's two-tailed t-test. **B.** Western blot analysis on hippocampus from 8, 12 and 16 week old TCRND8 mice compared to age-matched NCRND8 controls (N- 8 wk: n=9, 12wk: n=7, 16 wk: n=8, T- 8wk: n=8, 12wk: n=8, 16wk: n=10).

2.4.3 CRT expression is not increased in primary cortical neurons treated with AD related stressors

I also investigated if stressor treatment of primary cortical neurons from NCRND8 mice would increase CRT expression similar to what was observed in the cortical region of TCRND8 mice (Figure 2.1A) and in SH-SY5Ys treated with AD

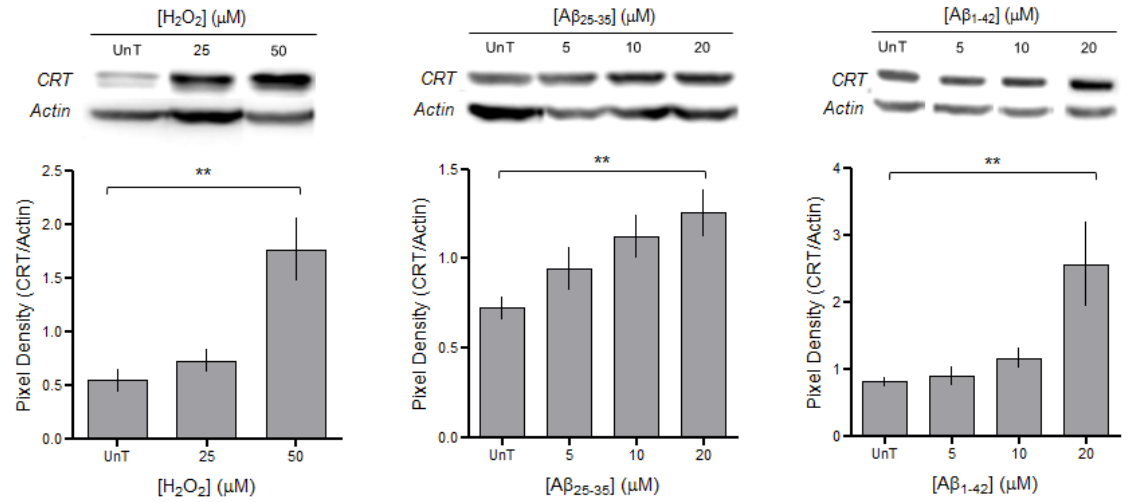

Figure 2.2. CRT is increased in SH-SY5Y cells following treatment with AD-related stressors.

Western analysis on protein extracts (40μg) from SH-SY5Ys pretreated for 24hrs with **A.** H_2O_2 (0-50μM), (n=5 for each treatment) **B.** $A\beta_{25-35}$ (0-20μM), (Untreated (UnT): n=14, 5μM: n=7, 10μM: n=8, 20μM: n=7), or **C.** $A\beta_{1-42}$ (5-20μM) , (UnT: n=12, 5μM: n=4, 10μM: n=5, 20μM: n=5, $A\beta_{42-1}$: n=3). For all three treatments (**A**-**C**), One way ANOVA, $p<0.01$, **-$p<0.01$ for 50μM H_2O_2, 20μM $A\beta_{25-35}$, or $A\beta_{1-42}$ vs. UnT, Tukey's multiple comparison test.

related stressors (Figure 2.2). However, I found no significant increase in CRT expression in neurons treated for 24 hours with H_2O_2 (25-100μM, Figure 2.3A) or $A\beta_{25-35}$ (20μM, Figure 2.3B). Interestingly, CRT expression was significantly decreased in neurons treated for 24 hours with $A\beta_{1-42}$ (10μM or 20μM, Figure 2.3C). Primary neurons were also treated with $A\beta_{1-42}$ for a variety of timepoints (4-48 hours) to determine if CRT expression may be induced by cellular stressors at a different rate in neurons as compared to SH-SY5Ys. No significant alteration in CRT expression was seen at any timepoints as compared to untreated controls (Figure 2.3D).

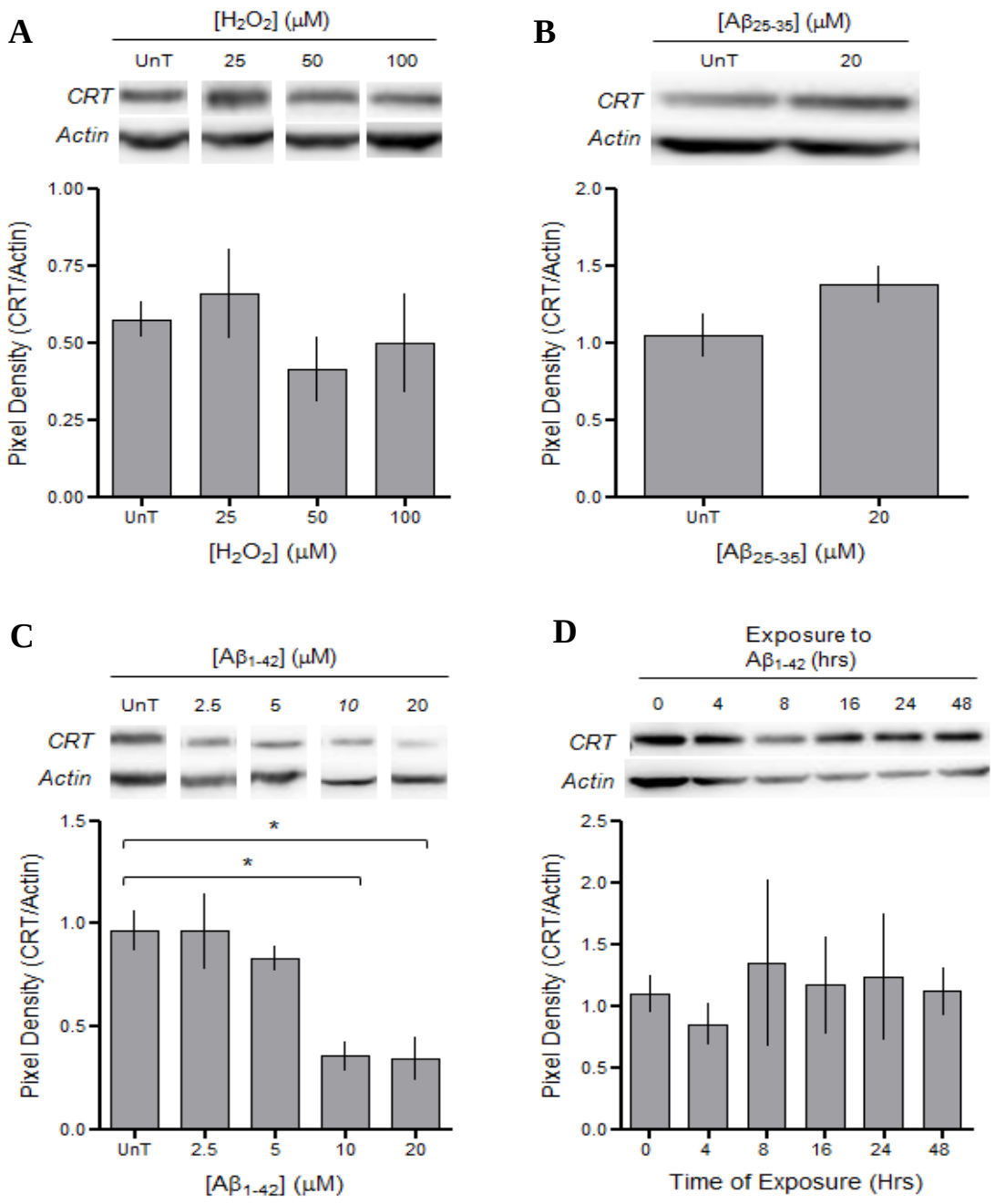

Figure 2.3. CRT is not increased in primary cortical neurons following treatment with AD-related stressors

Western analysis on protein extracts (40μg) from primary cortical mouse neurons pretreated for 24 hours with **A.** H_2O_2 (25-100μM), (Untreated (UnT): n=8, 25μM: n=3, 50μM: n=3, 100μM: n=3), **B.** $A\beta_{25-35}$ (20μM) (UnT: n=11, 20μM: n=11), or **C.** $A\beta_{1-42}$ (2.5-20μM) (UnT: n=7, 2.5μM: n=4, 5μM: n=3, 10μM: n=4, 20μM: n=4). **D**. CRT protein levels were measured by western blot using protein extracts from primary cortical neurons treated with 5μM $A\beta_{1-42}$ for 0-48 hours (n=3 for each treatment). *-$p<0.05$ vs. UnT (-), One way ANOVA with Tukey's multiple comparison test.

2.4.4 The effects of Aβ on Ca^{2+} signalling in SH-SY5Y cells

In the previous set of experiments I demonstrated an increase in CRT in the cortex of APP mutant mice and in SH-SY5Y cells treated with AD related stressors. Because increased expression of CRT has been shown to increase stored ER Ca^{2+} and alter the dynamics of ER Ca^{2+} signalling, I sought to determine if changes in Ca^{2+} signalling induced by Aβ would be comparable to changes in Ca^{2+} signalling induced by altered CRT expression. To determine the effect of Aβ exposure on Ca^{2+} release from ER stores in SH-SY5Ys, I pretreated cells for 24 hours with 20μM $A\beta_{25-35}$ (Figure 2.2). Ca^{2+} release from ER stores was induced by carbachol (1mM, 45 seconds, Figure 2.4A), or caffeine (20mM, 60 seconds, Figure 2.4B). Carbachol stimulates Ca^{2+} release from ER IP_3 receptors through muscarinic receptor activation and subsequent IP_3 second messenger generation [230]. Caffeine stimulates Ca^{2+} release from the ER through RyRs. Interestingly, I observed a significant decrease in area under the curve (A.U.C.) for carbachol induced intracellular Ca^{2+} responses in SH-SY5Ys treated for 24 hours with $A\beta_{25-35}$. In contrast, caffeine-induced Ca^{2+} responses were significantly increased in $A\beta_{25-35}$ treated cells as compared to untreated control cells (both A.U.C. and peak Ca^{2+} responses).

Previous studies have shown that there is a reduction in capacitative Ca^{2+} entry (CCE) in models of AD [231-233]. Similarly, previous studies have shown that overexpression of CRT also reduces CCE [218, 219, 221, 222, 224]. As such, I tested to see if treatment of SH-SY5Y cells with Aβ at a concentration that induced CRT

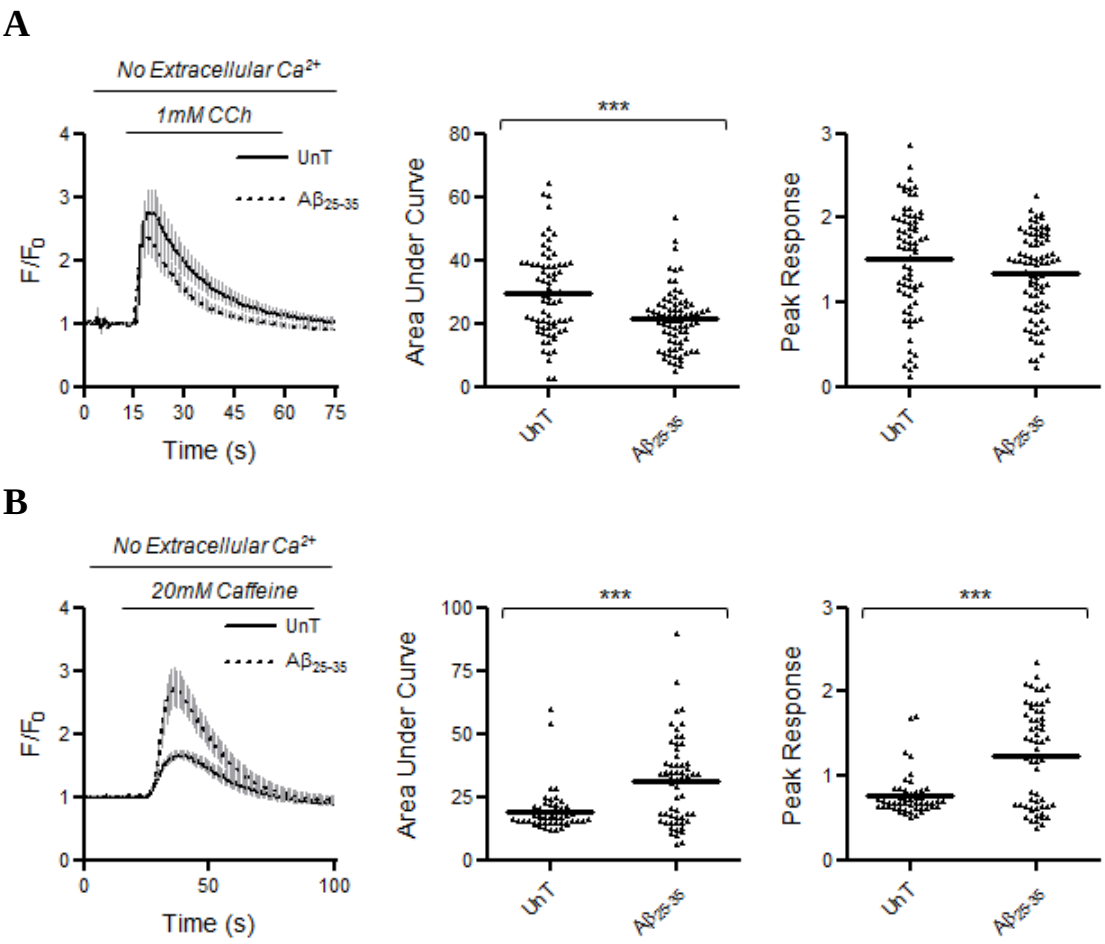

Figure 2.4. Treatment of SH-SY5Ys with Aβ alters Ca^{2+} response to carbachol and caffeine in the absence of extracellular Ca^{2+}.

A. Traces taken from a sample experiment for carbachol addition (1mM for 45 seconds) in the absence of extracellular Ca^{2+} in SH-SY5Ys pretreated for 24hrs with 20μM $Aβ_{25-35}$ compared to untreated (UnT) cells. Traces represent mean +/- SD for 28 cells (UnT) and 19 cells ($Aβ_{25-35}$) . Scatterplots represent individual values for cells from multiple runs (UnT – 71 cells, $Aβ_{25-35}$ - 80 cells) for area under curve (A.U.C.) and peak Ca^{2+} responses, with the horizontal line representing mean values. For A.U.C., *** - P<0.001 vs. UnT, Student's two-tailed t-test. **B**. Traces taken from a sample experiment for caffeine addition (20mM for 60 seconds) in the absence of extracellular Ca^{2+} in SH-SY5Ys pretreated for 24hrs with 20μM $Aβ_{25-35}$, compared to untreated (UnT) cells. Traces represent mean +/- SD for 15 cells (UnT) and 14 cells ($Aβ_{25-35}$). Scatterplots represent individual values for cells from multiple runs (UnT – 51 cells, $Aβ_{25-35}$ - 59 cells) for area under curve (A.U.C.) and peak Ca^{2+} responses, with the horizontal line representing mean values. For A.U.C. and peak responses *** - P<0.001 vs. UnT, Student's two-tailed t-test.

expression would alter the extent of CCE in these cells. SH-SY5Y cells were pretreated for 24 hours with 20μM $Aβ_{25-35}$. They were then treated with 1μM thapsigargin for 5

minutes in nominal extracellular Ca^{2+} in order to deplete ER Ca^{2+} stores. CCE was then induced by adding Ca^{2+} back to the extracellular medium. No significant difference in CCE was observed in $A\beta_{25-35}$ treated SH-SY5Ys as compared to untreated control cells in terms of both A.U.C. and peak responses (Figure 2.5A).

I next determined if exposure to Aβ could alter resting cytoplasmic Ca^{2+} concentrations in SH-SY5Y cells. Cells were again incubated with 20μM $A\beta_{25-35}$ for 24 hours and resting Ca^{2+} concentrations were then measured (expressed as the ratio of fluorescence at 340nm/380nm). No significant difference in resting Ca^{2+} concentrations was observed in $A\beta_{25-35}$ treated cells as compared to untreated control cells (Figure 2.5B).

2.4.5 The effects of modulation of CRT expression on Ca^{2+} signalling in SH-SY5Y cells

My previous data showed an increase in CRT expression in models of AD and altered carbachol and caffeine induced Ca^{2+} release in $A\beta_{25-35}$ treated SH-SY5Ys. In an attempt to determine if CRT is responsible for the changes in releasable Ca^{2+}, I experimentally manipulated the level of CRT expression and analyzed the effect on Ca^{2+} signalling. siRNA specific to CRT was used to knockdown levels of the protein in SH-SY5Ys. Cells were treated for 72 hours with either scrambled negative control siRNA (Neg, 100nM) or CRT specific siRNA (CRT, 100nM). A decrease in CRT expression was observed, as assayed by both western analysis (Figure 2.6A) and immunocytochemistry (Figure 2.6B). Once knockdown of CRT by siRNA was confirmed, I investigated the effects of CRT knockdown on Ca^{2+} signalling. In Figure

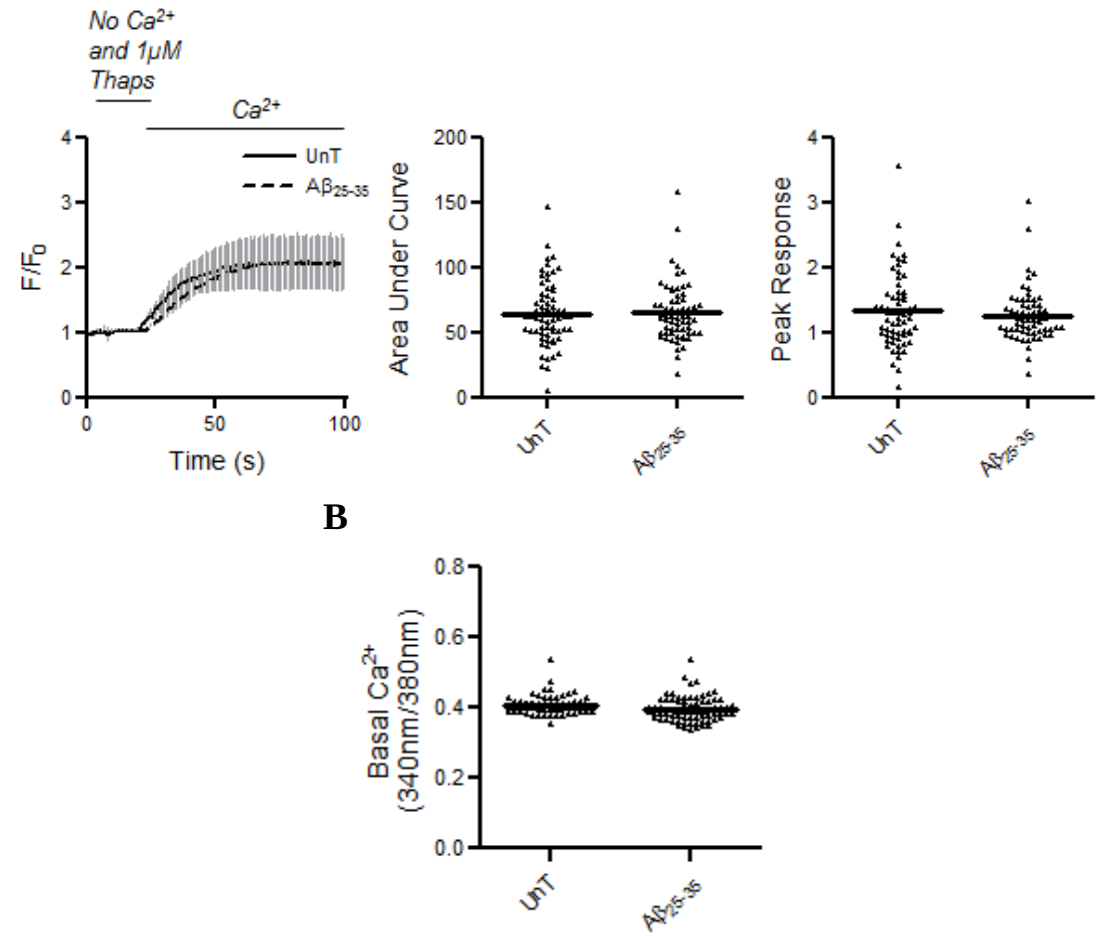

Figure 2.5. Treatment of SH-SY5Ys with Aβ does not alter capacitative entry or resting Ca^{2+} concentration in SH-SY5Y cells

A. Traces taken from a sample experiment for capacitative Ca^{2+} entry in after preincubation with thapsigargin (1μM for 5 minutes) in SH-SY5Ys pretreated for 24hrs with 20μM $A\beta_{25-35}$ compared to untreated (UnT) cells. Traces represent mean +/- SD for 23 cells (UnT) and 23 cells ($A\beta_{25-35}$). Scatterplots represent individual values for cells from multiple runs (UnT – 65 cells, $A\beta_{25-35}$ - 64 cells) for A.U.C. and peak Ca^{2+} responses, with the horizontal line representing mean values. **B.** Scatterplot represents individual resting cytoplasmic Ca^{2+} levels (as measured by calculating ratio of 340nm to 380nm fluorescence in each cell) taken from SH-SY5Ys treated with 20μM $A\beta_{25-35}$ (80 cells) or from untreated (UnT) controls (72 cells).

2.7A, Ca^{2+} response to carbachol (1mM, 45 sec) in nominal extracellular Ca^{2+} was measured in Negative control or CRT siRNA transfected SH-SY5Y cells. No significant difference in Ca^{2+} response in terms of A.U.C. or peak was observed in the two treatment

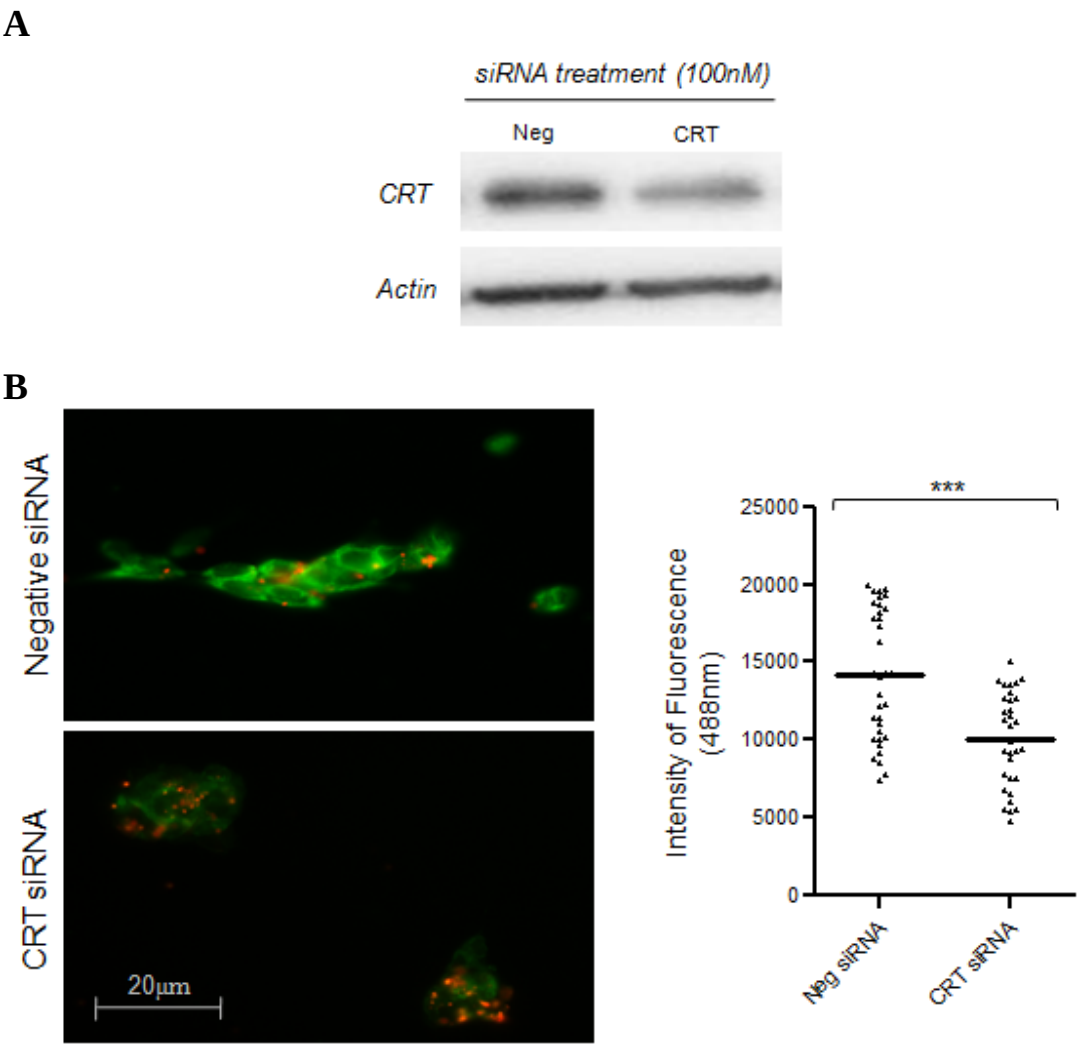

Figure 2.6. SiRNA mediated knockdown of CRT in SH-SY5Y cells.
A. Western analysis on protein extract from SH-SY5Ys treated with 100nM of non-specific negative control siRNA or CRT specific siRNA for 72 hours. Blots were probed with antibody specific for CRT then stripped and reprobed for β-actin. Three independent experiments were performed **B**. Overlayed Epifluorescent images taken with 40x objective on upright fluorescent microscope at excitation of 488nm for CRT protein (green fluorescence) and 546nm for Cy3 label (red fluorescence). SH-SY5Ys treated with 100nM Cy3-labeled siRNA (either non-specific Negative control or CRT specific) for 72 hours were fixed and probed for CRT. Mean fluorescent intensity for all background subtracted images was measured using ImageJ software (NIH). Scatterplot represents individual intensity values for each image, with solid line representing mean intensity for all images (Neg- 34 images, CRT - 33 images). *** - $P<0.0001$, student's two tailed t-test.

types. Figure 2.7B represents Ca^{2+} responses after stimulation with caffeine (20mM, 60sec) in nominal extracellular Ca^{2+} in negative control or CRT siRNA transfected SH-

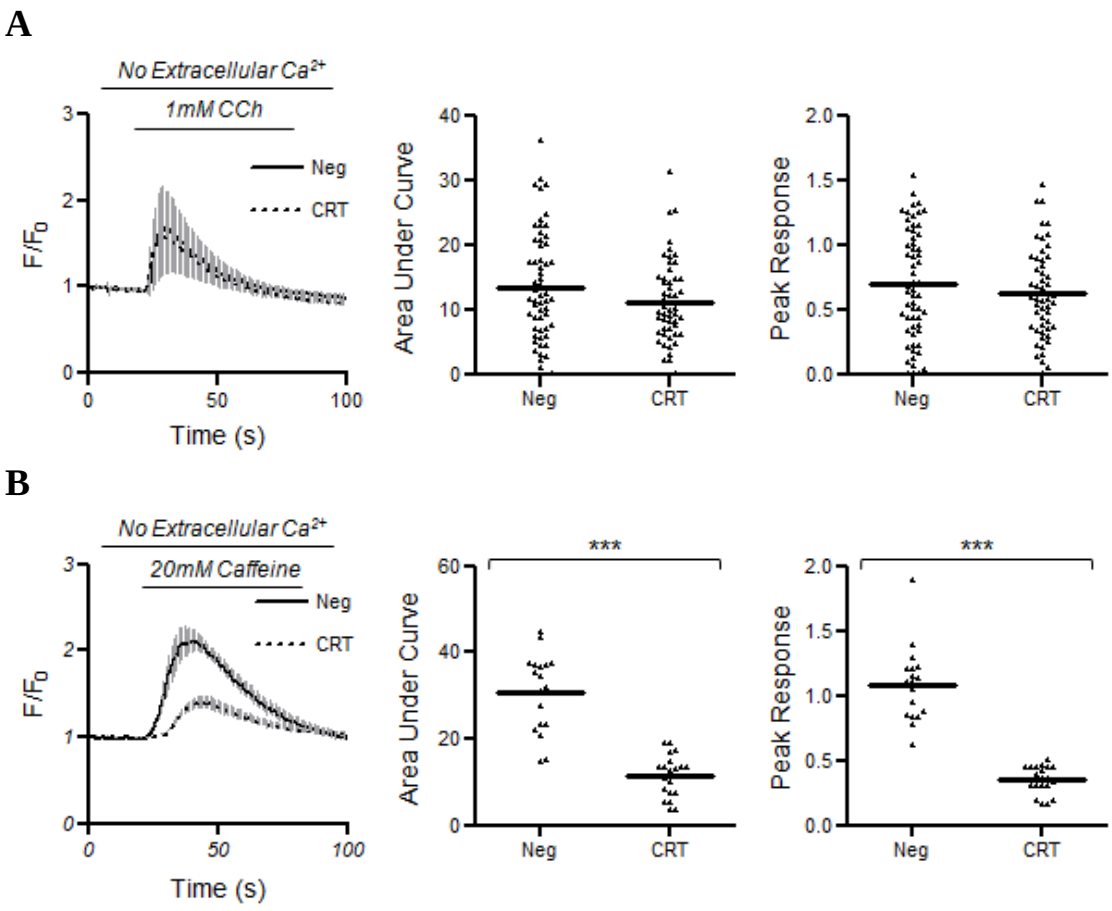

Figure 2.7. SiRNA mediated knockdown of CRT in SH-SY5Y cells does not alter ER Ca^{2+} response to carbachol but does decrease ER response to caffeine.

A. Traces taken from a sample experiment for carbachol addition (1mM for 45 seconds) in the absence of extracellular Ca^{2+} in SH-SY5Ys pretreated for 72hrs with 100nM of either negative control (Neg) or CRT specific (CRT) siRNA. Traces represent mean +/- SD for 21 cells (Neg) and 22 cells (CRT). Scatterplots represent individual values for cells from multiple runs (Neg – 60 cells, CRT - 53 cells) for A.U.C. and peak Ca^{2+} responses, with the horizontal line representing mean values. **B**. Traces taken from a sample experiment for caffeine addition (20mM for 60 seconds) in the absence of extracellular Ca^{2+} in SH-SY5Ys pretreated with siRNA in a manner identical to **A.** Traces represent mean ± s.d. for 11 cells (Neg) and 8 cells (CRT). Scatterplots represent individual values for cells from multiple runs (Neg – 18 cells, CRT - 20 cells) for A.U.C. and peak Ca^{2+} responses, with the horizontal line representing mean values. ***-$p<0.001$, student's two-tailed t-test.

SY5Y cells. A significant decrease in both A.U.C. and peak response was seen in cells treated with CRT siRNA as compared to cells treated with negative control siRNA. I then compared resting cytoplasmic Ca^{2+} concentrations in negative control or CRT

siRNA transfected cells. CRT knockdown did not affect resting Ca^{2+} concentration (Figure 2.8).

Figure 2.8. SiRNA mediated knockdown of CRT does not alter resting Ca^{2+} levels in SH-SY5Y cells
Scatterplot represents individual resting cytoplasmic Ca^{2+} levels from SH-SY5Y cells treated for 72 hours with 100nM of non-specific negative control siRNA (Neg, 91 cells) or 100nM CRT specific siRNA (CRT, 130 cells) with horizontal line representing mean value for each treatment

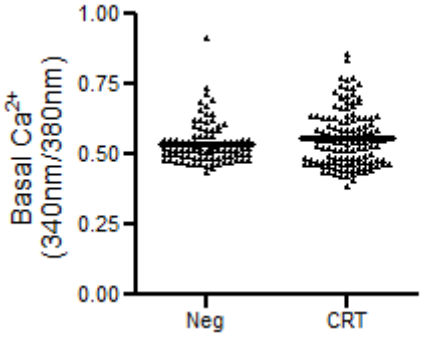

The second approach I used to determine the effects of CRT on Ca^{2+} signalling in SH-SY5Y cells was to overexpress CRT. eGFP was co-transfected with CRT to identify transfected cells, and 48 hours post-transfection, cells were fixed and CRT expression was determined by immunocytochemistry (Figure 2.9) . I observed overexpression of CRT in all cells with green fluorescence indicating that all transfected cells expressed both plasmids. In cells transfected with eGFP alone, there was no corresponding increase in CRT expression as compared to untransfected cells. This co-transfection protocol was then used to investigate the effect of CRT overexpression on Ca^{2+} signalling.

For these Ca^{2+} imaging experiments, SH-SY5Y cells were co-transfected with CRT and mCherry, a monomeric red fluorescent protein derived from dsRed protein of the *Discosoma* species [234], This allowed for determination of which cells co-expressed CRT and mCherry by utilizing the red fluorescence filter on our Ca^{2+} imaging inverted microscope. Ca^{2+} responses to carbachol (1mM, 45 sec) in nominal extracellular Ca^{2+} were measured in SH-SY5Ys co-transfected with mCherry and pCRT, or with mCherry alone. No significant difference in Ca^{2+} response was observed between the two

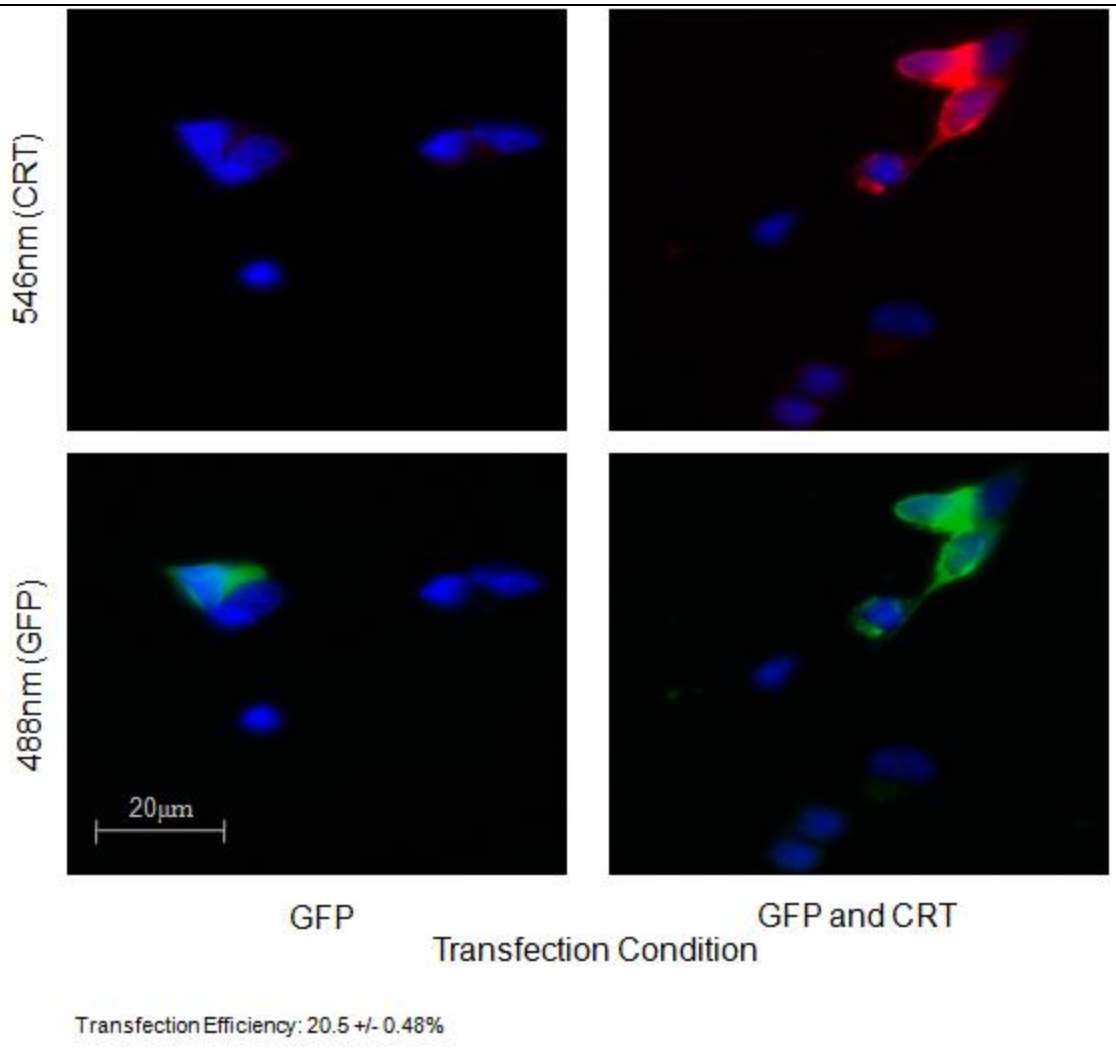

Figure 2.9. Transient overexpression of CRT in SH-SY5Y cells

Top and bottom left panels represent overlayed images of eGFP (2µg/ml) transfected SH-SY5Ys obtained under 40x objective using upright fluorescent microscope. Blue fluorescence represents hoescht 33342 stained nuclei, fluorescing under DAPI filter (~350nm). Top left panel represents cells fluorescing red under Rhodamine filter (~546nm) for CRT protein. Bottom left panel represents the same cells fluorescing for eGFP under FITC filter (~488nm). Top and bottom right panels represent overlayed images of eGFP (2µg/ml) and CRT (8µg/ml) co-transfected SH-SY5Ys obtained under 40x objective using upright fluorescent microscope. Again, nuclei were stained with Hoescht 33342. Top right panel represents red CRT fluorescence, while bottom left panel represents same cells with eGFP green fluorescence, with all pictures obtained under same conditions as images of cells transfected with eGFP alone. Transfection efficiency was calculated by dividing total transfected cells by total cells for three independent experiments.

treatment types (Figure 2.10A). I next designed experiments to determine if there was a difference in caffeine response from ER stores. As such, I exposed mCherry transfected and mCherry/pCRT co-transfected cells to caffeine (20mM, 60sec) in nominal extracellular

Ca^{2+} and measured Ca^{2+} responses. Unfortunately, even after several independent experiments, I could not elicit any Ca^{2+} response from caffeine for unknown reasons, contrasting with my previous experiments (data not shown). Attempts to induce a Ca^{2+} response from RyR stores using the RyR agonist ryanodine were also unsuccessful (data not shown). To test if CRT overexpression affected CCE, cells transfected with mCherry alone or mCherry/CRT were treated with 1μM thapsigargin for 5 minutes in nominal extracellular Ca^{2+} in order to drain ER Ca^{2+} stores. CCE through store-operated Ca^{2+} channels was then induced by adding Ca^{2+} back to the extracellular medium. As illustrated in Figure 2.10B, I observed a significant decrease in the extent of CCE in CRT overexpressing cells as compared to cells transfected with mCherry alone, in terms of both A.U.C. and peak response. Finally, I determined if overexpression of CRT would affect cytoplasmic resting Ca^{2+} concentrations. Figure 2.11 shows that there was no significant difference in resting Ca^{2+} concentrations in CRT transfected cells as compared to cells transfected with mCherry alone.

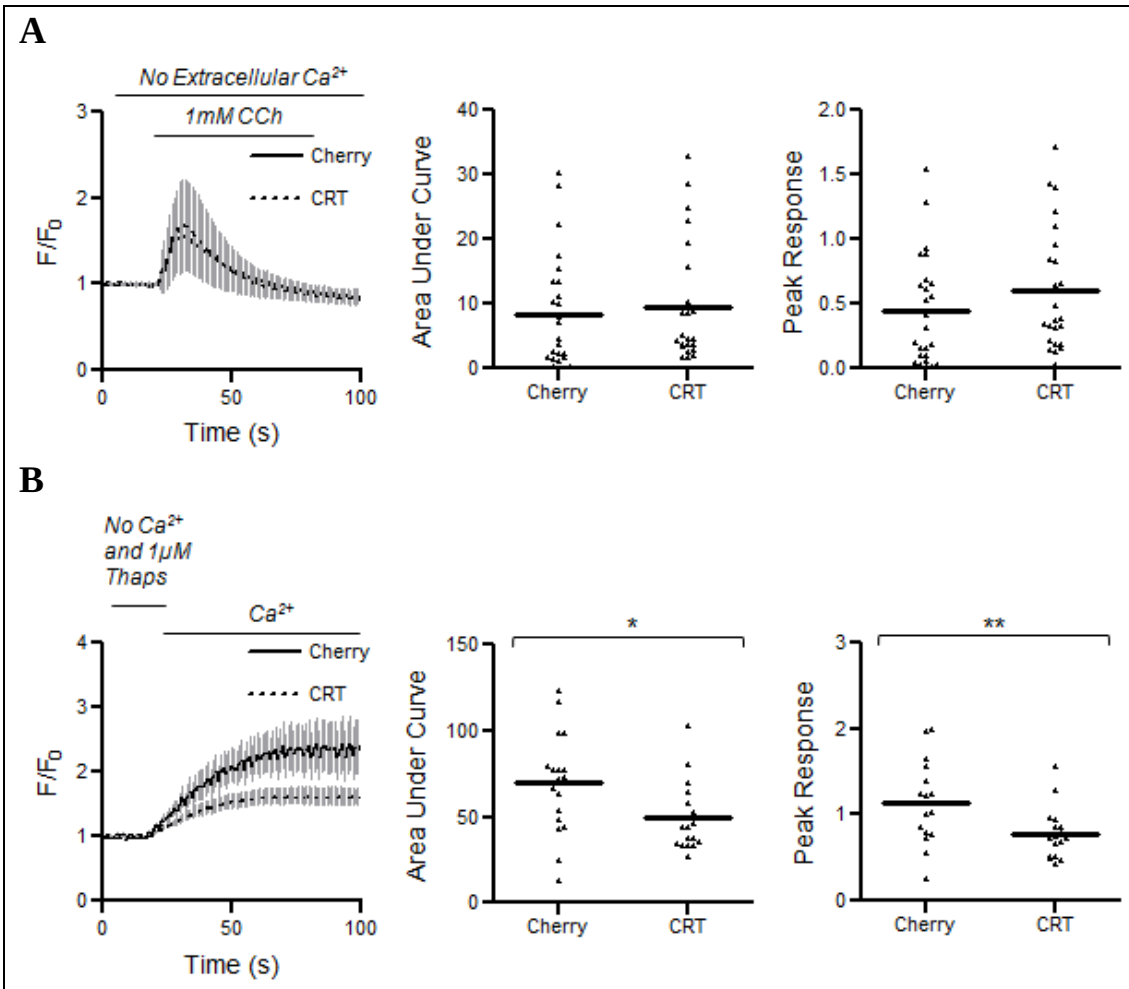

Figure 2.10. Overexpression of CRT in SH-SY5Y cells does not alter ER Ca^{2+} response to carbachol but does decrease extent of capacitative calcium entry.

A. Traces taken from a sample experiment for carbachol addition (1mM for 45 seconds) in the absence of extracellular Ca^{2+} in SH-SY5Ys transfected with either mCherry (2μg/ml) alone (Cherry) or mCherry and pCRT (CRT). Traces represent mean +/- SD for 5 cells (Cherry) and 4 cells (CRT). Scatterplots represent individual values for cells from multiple runs (Cherry – 25 cells, CRT - 24 cells) for A.U.C. and peak Ca^{2+} responses, with the horizontal line representing mean values. **B**. Traces taken from a sample experiment for capacitative Ca^{2+} entry in after preincubation with thapsigargin (1μM for 5 minutes) in SH-SY5Ys transfected with either mCherry (2μg/ml) alone (Cherry) or mCherry (2μg/ml) and pCRT (8μg/ml) (CRT). Traces represent mean +/- SD for 5 cells (Cherry) and 8 cells (CRT). Scatterplots represent individual values for cells from multiple runs (Cherry – 18 cells, CRT - 18 cells) for A.U.C. and peak Ca^{2+} responses, with the horizontal line representing mean values. *-$p<0.05$, student's two-tailed t-test, **-$p<0.01$, student's two-tailed t-test

Figure 2.11. Overexpression of CRT in SH-SY5Y cells does not alter resting Ca^{2+} levels in SH-SY5Y cells.

Scatterplot represents individual resting cytoplasmic Ca^{2+} levels from SH-SY5Y cells transfected for 48 hours with either mCherry (2µg/ml) alone (Cherry, 25 cells) or mCherry (2µg/ml) and pCRT, (8 µg/ml, CRT, 24 cells) with horizontal line representing mean value for each treatment.

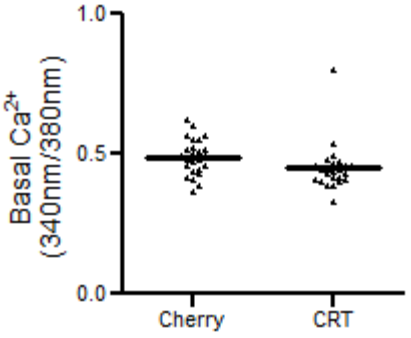

2.4.6 Overexpression of CRT does not alter susceptibility to cell death by AD related stressors in SH-SY5Ys

CRT is involved in modulation of cell death in several cell types in response to cellular stress, although the exact role CRT plays is contested. I determined if overexpression of CRT altered the extent of cell death induced in SH-SY5Ys after exposure to oxidative stress and Aβ. SH-SY5Ys were transfected for 24 hours with either mCherry alone (2µg/ml), or co-transfected with mCherry (2µg/ml) and pCRT (8µg/ml). The cells were then treated with a range of concentrations of either H_2O_2 (0-300µM) or $A\beta_{25-35}$ (0-20µM) for 24 hours. Cell death was then measured by trypan blue exclusion, a measure cellular membrane integrity. No significant difference was seen in trypan blue exclusion in cells co-transfected with mCherry/pCRT as compared to cells transfected with mCherry alone after treatment with either H_2O_2 or $A\beta_{25-35}$ (Figure 2.12A, left and right panels, respectively). One possible confounding factor for the above toxicity experiments was that any effects of CRT overexpression on stressor susceptibility may have been masked by the high number of untransfected cells (~80%) due to the low transfection efficiency. To address this, I designed an experiment to

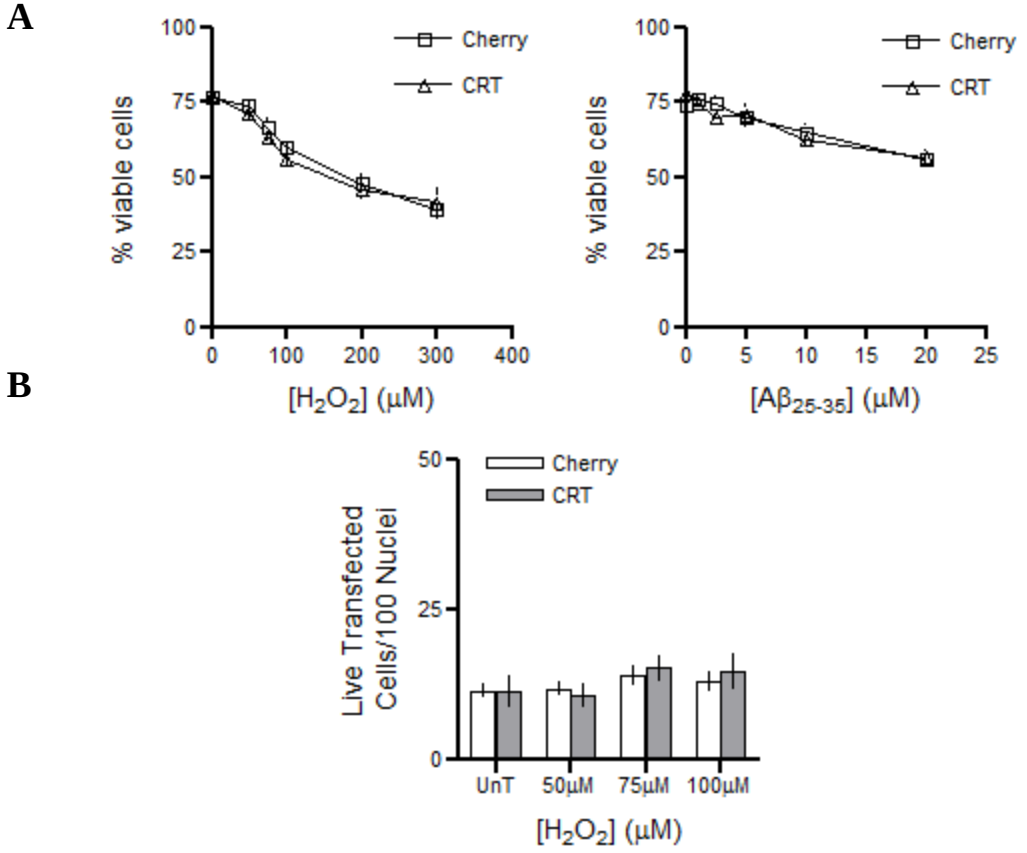

Figure 2.12. Overexpression of CRT in SH-SY5Y cells does not alter susceptibility to toxicity from exposure to AD related stressors.

A. Left panel measures % viability by trypan blue exclusion in SH-SY5Ys transfected with either mCherry (2μg/ml) alone (Squares) or mCherry (2μg/ml) and pCRT (8μg/ml) (Triangles) after 24 hour exposure to various concentrations of H_2O_2 (0-300μM). Right panel measures the same after 24 hour exposure to various concentrations of $A\beta_{25-35}$ (0-20μM). % viability was assessed by dividing total unstained cells by total cell count. **B**. Total number of transfected SH-SY5Y cells after 24 hour exposure to H_2O_2 (0-100μM). SH-SY5Ys were transfected with either mCherry (2μg/ml) alone (white bars) or mCherry (2μg/ml) and pCRT (8μg/ml, grey bars). Transfected counts were normalized to total nuclei in the given field.

directly assess cell death in mCherry/pCRT overexpressing cells relative to untransfected cells using an upright fluorescent microscope. A previously published study has demonstrated cells transfected with fluorescent protein will lose their fluorescence upon induction of cell death [235] . Therefore, if CRT affects susceptibility to cell death, mCherry/pCRT co-transfected cells would exhibit a change in the total number of

fluorescent cells relative to total number of cells after induction of cell death by stressor treatment. I counted cells expressing fluorescent

Cherry protein in mCherry or mCherry/pCRT transfected cells after 24 hour treatment with H_2O_2 (0-100μM). Total number of cells (transfected and untransfected) in a particular field was measured by counting Hoescht 33324 stained nuclei. Although increasing concentrations of H_2O_2 caused cell death to an extent similar to that seen in Figure 2.12A (data not shown), there was no significant change in the number of Cherry expressing cells relative to total cells after H_2O_2 treatment in SH-SY5Ys transfected with mCherry/pCRT, indicating that overexpression of CRT did not affect the susceptibility of SH-SY5Ys to cell death (Figure 2.12B).

2.5 Discussion

In the above studies, I have shown that the ER resident Ca^{2+} binding protein CRT is upregulated in both an animal model as well as a cell culture model of AD. The animal model utilized in this study was the mutant APP695 CRND8 mouse, which due to altered APP processing, produces significantly increased amounts of $A\beta_{1-42}$ starting at 8 weeks of age. These mice then show development of plaques at roughly 8 weeks of age in cortical regions of the brain and in the hippocampus by just over 12 weeks of age and significant reductions in cognitive ability at roughly 11 weeks of age [229]. Qualitatively, the increased expression of CRT that was observed in the cortex of these mice by western analysis correlates well with cognitive decline. CRT has been previously shown to be upregulated in long-term sensitization training in a neuronal, model of learning and

memory [236]. Given the strong correlation between decline in cognitive ability and increase in CRT expression, it is plausible that increased in CRT expression may be a compensatory response to detrimental effects of Aβ deposition and plaque formation on learning and memory. Thus, future studies addressing the role of CRT in mammalian learning and memory, such as a study examining the effect of modulation of CRT expression on LTP, would be prudent and informative. No significant increase in hippocampal CRT expression was observed in TCRND8 mice at 8-16 weeks of age. This result was somewhat surprising, because plaque formation is seen in the hippocampus of these mice at this time. One possible explanation for lack of CRT induction in the hippocampus is that the timeframe in which I examined CRT expression did not extend out for a sufficiently long period. Plaque formation in the hippocampus of TCRND8 mice occurs at a later interval than plaque formation in the cortex [229]. Another possibility is that CRT is not highly inducible in hippocampal regions of the brain. Future experiments examining CRT expression in brain slices from multiple animal models of AD as well as from post-mortem brains of AD patients at multiple stages of disease severity would be the best way to answer these questions, as they would allow for determination of which specific areas of the brain CRT expression is increased.

When H_2O_2 or Aβ proteins were added to SH-SY5Y neuronal cell cultures I observed a significant increase in CRT expression. This is in line with previous studies that have shown that CRT expression is upregulated under conditions of cellular stress and disruption of cellular Ca^{2+} signalling, as both of these conditions occur upon exposure to oxidative stress and Aβ. However, when these same stressors were applied

over a range of concentrations and exposure times to primary cortical neurons from non-transgenic mice, upregulation of CRT expression was not observed, and in fact a lowering of CRT expression was seen in neurons treated with $A\beta_{1-42}$. A previous study showed a similar result with decreased expression of CRT in the parietal grey matter neurons of AD brains [237]. The reasons for this are unclear, however one could speculate that increases in CRT observed in the cortex of TCRND8 mice were occurring in glial cells and not neurons. Perhaps the best way to determine this would be to examine CRT expression in brain slices from multiple animal models of AD as well as from post-mortem brains from AD patients, to observe if CRT expression is altered differentially in neurons and glial cells.

In this study, carbachol-induced Ca^{2+} release from ER stores was significantly reduced in SH-SY5Y cells pretreated with $A\beta_{25-35.}$ Other studies have also demonstrated that direct exposure of cells to oxidative stress [238] or Aβ peptides [239] inhibited cholinergic signal transduction and subsequent carbachol mediated Ca^{2+} release through IP_3R stores. Possible explanations for this decreased cholinergic signal transduction are reduced surface expression of cholinergic receptors or increased IP_3 metabolism. Further studies are required to determine this mechanism, such as examination of the expression/function of proteins involved in cholinergic signal transduction and IP_3 release and metabolism. I also observed increased Ca^{2+} release from RyR stores in cells exposed to $A\beta_{25-35}$, which is also in line with previous studies involving models of AD [171, 173]. CCE was unchanged in SH-SY5Y cells treated with $A\beta_{25-35}$. Previous studies have shown an inhibition of CCE in models of AD, however all these studies involved AD

models of mutant PS-1, which I did not utilize in this study [231-233, 240]. My results suggest that the inhibition of CCE in mutant PS-1 models is not due to the overproduction and deposition of Aβ, but rather some other change in cell function induced by mutant PS-1.

In SH-SY5Y cells with siRNA mediated reduction of CRT expression, I observed a significant decrease in caffeine induced Ca^{2+} response from RyR stores. This result could suggest the involvement of increased CRT expression in the increased caffeine mediated Ca^{2+} response in SH-SY5Y cells treated with $A\beta_{25-35}$. Unfortunately, I was unable to determine if overexpression of CRT had the opposite effect to knockdown of CRT in terms of caffeine mediated Ca^{2+} responses, as I was unable to induce Ca^{2+} responses to caffeine in the cells during this set of experiments for unknown reasons. Given that previous studies have shown upregulation of RyR(s) in models of AD [171, 173], it would be interesting in future studies to determine if CRT has an effect on RyR expression/function. Similar to what was seen in $A\beta_{25-35}$ treated cells, there was no significant difference in resting Ca^{2+} levels in CRT knockdown or overexpressing SH-SY5Ys. However, I did observe a significant decrease in CCE in CRT overexpressing cells, similar to what has been observed in previous studies [218, 219, 221, 222, 224]. Given that I have shown increased CRT expression in cells exposed to oxidative stress and Aβ protein, I anticipated inhibition of CCE in the $A\beta_{25-35}$ treated cells. This was not the case. As stated above, previous studies that have shown an inhibition of CCE in models of AD, however all these studies involved PS-1 mutants, not cells exposed to exogenous Aβ [231-233, 240]. A likely explanation is that changes CCE could not be

observed in the $A\beta_{25-35}$ treated cells because CRT levels are increased to a much lesser extent in $A\beta_{25-35}$ treated cells than in transfected CRT-overexpressing cell. Another explanation is that there may be unknown mechanisms that can compensate for any changes in CCE that induction of CRT after stressor treatment may cause. For example, increased Ca^{2+} efflux from the ER through RyR channels could empty ER stores and allow for greater CCE.

Since CRT has been previously shown to modulate the sensitivity of cells to induction of cell death by exposure to stressors, I designed experiments to determine if overexpression of CRT would alter (increase or decrease) the sensitivity of SH-SY5Y cells to cell death from exposure to oxidative stress or Aβ protein. However, I observed no significant difference in induction of cell death after exposure to oxidative stress or Aβ in CRT overexpressing cells as compared to control cells. Thus, the increased CRT in models of AD is likely not contributing to induction of cell death. Exactly what the effects of this increase in CRT in AD are remain to be determined. Since CRT is known to be involved in ER protein folding and quality control [213, 214], it is possible that changes in CRT after exposure to AD-related stressors may be an attempt of the cell to compensate for disruptions in ER protein folding. Further experiments determining the role of changes in CRT expression in disruptions of ER protein folding function in models of AD would be informative.

It should also be acknowledged that there are several limitations to consider when utilizing a neuroblastoma cell line such as SH-SY5Y cells as an experimental model. Neuroblastoma cells are useful in that they can easily and indefinitely grow in *in vitro*

culture conditions and that they generally represent a single cell type, which allows for increased reproducibility of results. However, the tumor origins of neuroblastoma cells means that they have significant genotypic differences compared to neurons found in an *in vivo* setting. Long term growth of neuroblastoma cells can result in further genetic aletrations due to selective pressures of *in vitro* culture conditions. Finally, neuroblastoma cells tend to exhibit a metabolic emphasis on growth and proliferation rather than differentiated function, thus may not fully exhibit neuronal functions such as excitability or neurotransmitter release [241]. This may explain why differences were observed between results from SH-SY5Ys and primary cortical neurons in this study.

In summary, I have demonstrated in this study that there is increased CRT expression in the cortex but not the hippocampus of 12 and 16 week old TCRND8 mice. Exposure of SH-SY5Y neuroblastoma cells to stressors associated with AD, such as oxidative stress and Aβ protein, also increased CRT expression. Further studies examining the consequence of increased CRT expression in AD are required.

Chapter 3

X-Linked Inhibitor of Apoptosis Protein Modifies Neuronal Ca^{2+} Signalling

3.1 Abstract

X-linked inhibitor of apoptosis protein (XIAP), a member of the IAP family of anti-apoptotic proteins, has been shown to inhibit apoptosis through several distinct mechanisms, including inhibition of caspases 3, 7 and 9, as well as by induction of signalling pathways such as the JNK1 and NF-κB pathways. Disruption of neuronal Ca^{2+} signalling and subsequent induction of apoptotic pathways have been implicated in several models of neuronal injury and neurodegeneration. XIAP has been shown to be protective against Ca^{2+} mediated induction of the apoptotic pathway, as well as protective in models of neuronal disease. In this study I demonstrate that XIAP overexpression alters several aspects of Ca^{2+} signalling in two overexpression models: in primary cortical neurons from a XIAP-overexpressing mouse, and in primary cortical neurons transiently transfected with a XIAP-dsRed plasmid. In these two models, XIAP overexpression significantly lowered the neuronal Ca^{2+} response to the neurotransmitter glutamate. XIAP overexpression also lowered the extent of Ca^{2+} release from ER Ca^{2+} channels, entry through both NMDA receptors and VGCCs and the extent of CCE through SOC. XIAP also lowered Ca^{2+} entry due to oxidative stress in neurons from XIAP overexpressing mice, suggesting that XIAP may be able to directly protect cells from damage and death from stressors that cause dysregulation of Ca^{2+}. Furthermore, the effect of XIAP on Ca^{2+} signalling was not exclusive to primary cortical neurons as XIAP-overexpressing glia also showed lower Ca^{2+} responses. Inhibition of caspases with the pan-caspase inhibitor Z-VAD-FMK did not alter neuronal Ca^{2+} response to glutamate,

suggesting that XIAP affects neuronal Ca^{2+} signalling in a manner independent of caspase inhibition. It appears therefore that an increase in XIAP expression can reduce potentially toxic increases of cytoplasmic Ca^{2+} independent of caspase inhibition. Further studies are required to fully understand the means by which XIAP suppresses Ca^{2+} signalling.

3.2 Introduction

X-linked inhibitor of apoptosis protein (XIAP), also known as human IAP-like protein (hILP), is a 57kDa member of the IAP family of anti-apoptotic genes which is ubiquitously expressed in human tissues [242]. Structurally, XIAP contains two distinctive features: three amino-terminal baculovirus IAP repeat domains (BIR 1-3) and a carboxy-terminal RING finger domain [242]. XIAP inhibits apoptosis by multiple mechanisms, based on the different functions of the BIR and RING domains. One important mechanism by which XIAP inhibits apoptosis is by inhibiting the cleavage and activation of pro-caspases 3, 7 and 9. XIAP binds directly to the pro-enzymes via it's BIR domains [243-245].

XIAP has also been shown to regulate the activity of several proteins associated with signal transduction in apoptotic or pro-survival pathways. For example, XIAP was shown to physically associate with TGF-β R1 receptor through the BIR domain, resulting in activation of transcription from TGF-β responsive promoters [246]. XIAP also has been shown to enhance TAB1, TAK1 and BMPR1A complex formation via interaction with all three of these proteins, which subsequently activates JNK1 signalling [247] as

well as NF- κB dependent transcription [247-251]. This interaction appears to be essential for XIAP to protect against certain forms of apoptosis, as dominant negative TAK1 or JNK attenuated XIAP mediated protection against TNFα [247]. Interestingly, disruption of the caspase inhibiting activity of XIAP by point mutations in BIR caspase binding domains did not affect the ability of XIAP to activate NF-κB, TGF-β1/Smad4, or JNK1 activities [251]. This indicated that the ability of XIAP to disrupt apoptosis via interaction with caspases is distinct from the ability of XIAP to modulate signal transduction through these pathways. A summary of the structure and function of XIAP is illustrated in Figure 3.1.

XIAP has been shown to be protective in several models of neurodegenerative disease. For example, XIAP overexpression was shown to be neuroprotective in models of excitotoxic and ischemic injury to the brain, attenuating neuronal loss and improving neurological function as compared to control animals [252-255]. One study showed that XIAP was downregulated in cells treated with low concentrations of Aβ protein [256]. XIAP overexpression was also shown to protect dopaminergic neurons of the substantia nigra pars compacta (SNpc) in *in vitro* and *in vivo* models of PD [257]. In both *in vitro* and *in vivo* models of ALS, XIAP was shown to be downregulated and subsequent overexpression of XIAP protected against mutant SOD1 mediated cell death, and improved long term survival in a SOD mutant mouse model [258, 259]. In addition, XIAP was shown to prevent cell death in axotomized retinal ganglion cells *in vivo* [260].

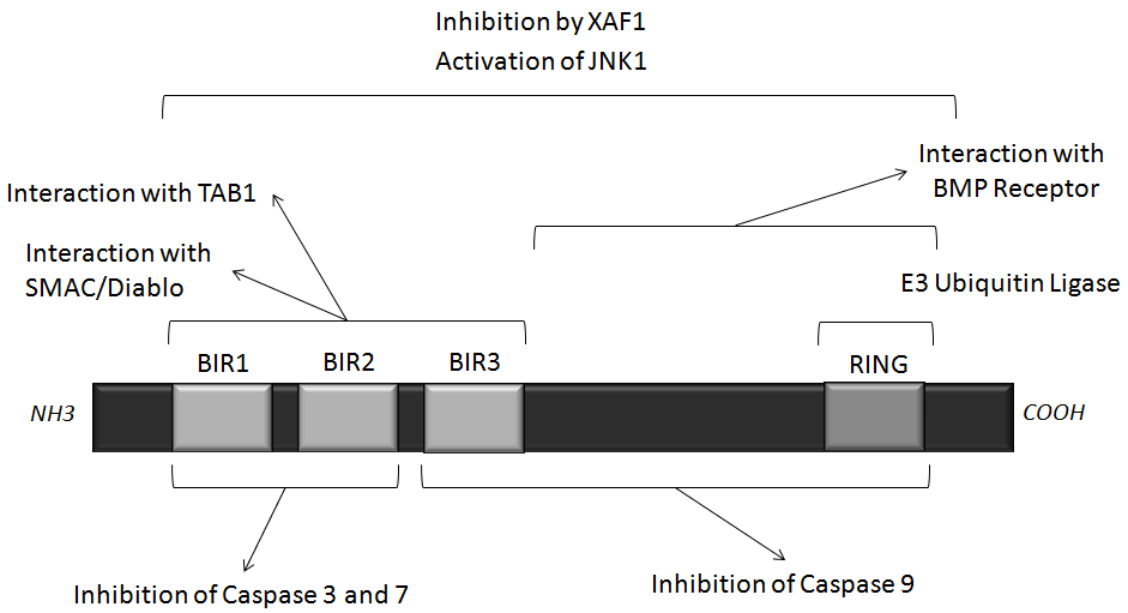

Figure 3.1. The structure and function of XIAP

A diagram of the 2-dimensional structure and function of full-length XIAP protein (adapted from Holcik, 2001). Note that although there are 3 distinct amino-terminal BIR domains and one carboxy-terminal RING-finger domain, these domains do not act independently in the many functions of XIAP. Inhibition of caspases 3 and 7 occur through interaction with BIR1 and BIR2, while inhibition of caspase 9 requires BIR3 and the RING domain. Also note that the BIR domains are responsible for interaction with Smac/DIABLO and TAB1, while the RING domain functions as an ubiquitin ligase. The unnamed domain of XIAP located between the BIR and RING domains is also essential for certain functions of XIAP, as it acts in concert with the BIR domains to allow XIAP mediated activation of JNK1, mediate interaction with the XIAP-inhibitor protein XAF1, and also is required along with the RING domain to allow XIAP interaction with the BMP receptor.

Disruption of Ca^{2+} signalling and subsequent induction of neuronal dysfunction and death have been implicated in many models of neurodegenerative disorders [261-264]. Interestingly, one study has shown that depletion of ER Ca^{2+} stores by thapsigargin induced XIAP protein expression in neuronal SH-SY5Y cells [265]. In addition, knockdown of XIAP sensitized SH-SY5Y neuroblastoma cells to thapsigargin induced cell death [265] . Another member of the IAP family, Neuronal Apoptosis Inhibitory Protein, or NAIP, was shown to be protective against ionomycin and

thapsigargin mediated cell death in NSC-34 motor neuron-like cells [117]. NAIP was subsequently shown to interact strongly with hippocalcin, a neuron specific Ca^{2+} binding protein, and this interaction was enhanced in the presence of Ca^{2+} [117].

In this study, I demonstrate that XIAP overexpression in a mouse overexpression model or in transiently transfected neurons alters several aspects of neuronal Ca^{2+} signalling. XIAP overexpression lowered the amount of stored Ca^{2+} in the ER and subsequent release from ER channels. XIAP overexpression also lowered the extent of Ca^{2+} entry through plasma membrane Ca^{2+} channels, lowered CCE, and increased cytoplasmic resting Ca^{2+} levels. Similarly, XIAP lowered the amount of Ca^{2+} that enters neurons after exposure to oxidative stress. Similar effects of XIAP on Ca^{2+} signalling were also detected in primary glia cells from XIAP-overexpressing mice. Treatment of neurons with the potent caspase inhibitor ZVAD-FMK did not affect Ca^{2+} signalling, indicating that the effects XIAP exerts on Ca^{2+} handling are independent of caspase inhibition.

3.3 Materials and Methods

3.3.1 Antibodies

XIAP protein was probed with hILP/XIAP-specific mouse monoclonal IgG1 (BD transduction laboratories). Secondary antibody used for immunofluorescence was Alexafluor 488-conjugated goat anti-mouse IgG (H+L) (Invitrogen).

3.3.2 Animals and cell culture

Human SH-SY5Y neuroblastoma cells (ATCC) were cultured in DMEM: F12 media with 10% FBS, 1% penicillin/streptomycin (Invitrogen), and plated at 8 x 10^5 cells on 60mm coverslips.

A C57/Bl6 mouse colony was maintained at the Atlantic Veterinary College, University of Prince Edward Island. Transgenic XIAP-overexpressing mice were created by Dr. Peter Liston at the Apoptosis Research Center, University of Ottawa, and a colony was maintained at the Sir Charles Tupper Building, Dalhousie University. The animals were generated by microinjection of human full length XIAP with an N-terminal 6 x myc tag into C3H X C57BL/6 fertilized oocytes. The animals were then back-crossed ~16 times against wild-type C57/Bl6 mice. Expression of the human XIAP transgene is controlled by a ubiquitin promoter, which allows for XIAP expression in all tissue types. For primary neuronal cultures, non-transgenic female mice were bred with XIAP overexpressing male mice (heterozygous for human XIAP). Pregnant females were sacrificed at embryonic day 16 and embryos were removed and placed on ice. Embryos were genotyped for the human XIAP gene by PCR (Platinum *Taq*DNA polymerase; Invitrogen) before cell dissociation and tissue pooling. The sequences of primers used for human XIAP were as follows: 5_GGA TCC TCT GAT GCT GTG AGT TCT GAT AGG AAT TTC CC and 3_GAC TCG AGC TAA GTA GTT CTT ACC AGA CAC TCC TCA AG. PCR products were generated by 30 cycles of 94/68/72 °C and analyzed by agarose gel electrophoresis. Dissection of cortices and preparation of XIAP neuronal cultures was performed as described for TCRND8 cultures in Chapter 2. Experiments

were performed following 7-9 days of *in vitro* culture. For primary glia cultures, cerebellum from (N) XIAP or (T) XIAP day 3-5 neonates were dissected and placed separately into HBSS. The tissue was dissociated by incubation in 0.25% trypsin for 30 min at 37ºC. Following this, cells were then centrifuged at 1000rpm for 5 minutes and trypsin was removed. The pellet was then resuspended in DMEM:F12 media with 20% FBS, 1% antibiotic/antimycotic. Cells were counted and plated at 1 x 10^5 cells/flask in $80cm^2$ flasks and incubated at 37ºC at 5% CO_2. One week following plating, media was changed such that FBS concentration was lowered to 15%. Once glia reached roughly 70% confluence, they were trypsinized and plated at 1 x 10^5 cells on 60mm coverslips for Ca^{2+} imaging experiments.

3.3.3 Single cell Ca^{2+} imaging

Primary cortical neurons, primary glia, or SH-SY5Y cells were imaged and data was analyzed as described in Chapter 2.

3.3.4 Immunocytochemistry

Neuronal cultures plated on poly-d-lysine coated coverslips were washed once with PBS for 5 min, then fixed in ice cold 100% Methanol for 2 minutes. Fixed cells were then permeablized with 0.01% Triton-X 100 in PBS for 5 minutes and subsequently washed twice with PBS for 5 minutes. The cells were blocked for 1 hour with blocking buffer (1% goat serum in PBS) at room temperature and incubated with primary XIAP antibody (1/100 dilution) in blocking buffer overnight at 4ºC. After this incubation, cells

were washed 3x with PBS for 5 minutes each and incubated with Alexafluor 488 conjugated secondary antibody (1/1000 dilution) in blocking buffer at room temperature in the dark for 1 hour. A brief incubation with 1μg/ml Hoechst 33342 (Sigma) in PBS followed to stain the nuclei, followed by a three 5 minute washes with PBS. Coverslips were mounted onto slides using Fluorosave reagent (Calbiochem) and imaged using an upright epifluorescence microscope (Axioskop 2 plus, with MBQ 52 ac Xenon lamp, Zeiss). All images were recorded using Axiovision software (version 4.2), and subsequently exported as 16-bit tiffs. Fluorescence intensity for each image was assessed using ImageJ software (NIH).

3.3.5 Neuronal XIAP-Dsred transfections

Transfections were performed on C57/Bl6 neurons at 5-6 DIV at $8x10^5$ cells/dish on poly-d-lysine coated 60mm coverslips for Ca^{2+} imaging and at 1.5 x 10^5cells/well on coverslips for immunocytochemistry. Prior to transfections, conditioned neurobasal (NB) media (Invitrogen) was removed and replaced with OptiMEM (Gibco). An equal volume of NB containing no FBS was added to the conditioned media and the cells were returned to this medium following the transfection. XIAP-dsred (8 μg) and Lipofectamine 2000 (final concentration of 0.6%) were incubated in Opti-MEM separately for 10 minutes at room temperature and then mixed and incubated for a further 20 minutes. Transfection mixtures were then added to each well and cells were incubated at 37ºC for 4 hours. The media was then replaced with conditioned media. Ca^{2+} imaging/XIAP immunocytochemistry was performed 48 hours post-transfection.

3.3.6 Statistical Analysis

Data were analyzed using GraphPad Prism, version 4. For Ca^{2+} imaging of neurons and glia from XIAP overexpressing mice and littermate controls, student's two-tailed t-test was performed to determine the difference between mean area under the curve (A.U.C.) and peak Ca^{2+} response from multiple independent experiments. For Ca^{2+} imaging of transiently transfected wild-type neurons, control values from untransfected neurons for each independent experiment were averaged and compared to values from XIAP-transfected neurons in the same experiment using student's paired t-test. Differences were considered significant at $P < 0.05$.

3.4 Results

3.4.1 Overexpression of XIAP reduces glutamate-induced Ca^{2+} response and glutamate-induced Ca^{2+} release from intracellular stores

XIAP exerts anti-apoptotic effects through multiple mechanisms, and XIAP and other IAP family members have been shown to protect cells from death induced by disruption of Ca^{2+} signalling [117, 265]. Given this, I wished to determine if an increase in the expression of XIAP may affect intracellular Ca^{2+} signalling. I was particularly interested in Ca^{2+} responses induced by the neurotransmitter glutamate, which plays an important role in excitotoxic mechanisms of neurodegenerative disease [166]. Using cultured cortical neurons from XIAP-overexpressing mice I observed that Ca^{2+} responses to glutamate (250 µM, 60 seconds) were significantly reduced compared with Ca^{2+}

responses in wild-type mice, in terms of both area under the curve (A.U.C.) and the peak Ca^{2+} response (Figure 3.2A). I next determined if XIAP overexpression could affect glutamate-induced release of Ca^{2+} from intracellular stores, as increased Ca^{2+} release from ER stores is another important hallmark of neurodegenerative diseases such as AD. I stimulated neurons with glutamate (250μM, 60 seconds) in Ca^{2+}-free extracellular medium (nominal extracellular Ca^{2+}). I noted a significant reduction in the Ca^{2+} response to glutamate in XIAP-overexpressing neurons as compared to wild-type neurons for both A.U.C. and peak Ca^{2+} response (Figure 3.2B). This suggests that XIAP may have either decreased the amount of stored releasable Ca^{2+} within the neurons, or decreased mGluR mediated signalling from the plasma membrane.

To further explore the effect of XIAP overexpression on neuronal Ca^{2+} signalling, I transiently overexpressed XIAP by transfecting cortical neurons from C57/Bl6 mice with a XIAP-dsRed fusion protein. I confirmed overexpression of XIAP in these neurons by detection of dsRed-positive cells (Figure 3.3). As a result of transient overexpression of XIAP-dsRed, I noted a significant reduction in glutamate induced Ca^{2+} responses (Figure 3.4), similar to what was observed in cortical neurons from XIAP-overexpressing transgenic mice (Figure 3.2).

3.4.2 The amount of releasable Ca^{2+} in intracellular stores is decreased upon overexpression of XIAP

Glutamate stimulates metabotropic glutamate receptors to elevate $InsP_3$ which releases intracellular Ca^{2+} from the ER IP_3Rs. This in turn stimulates RyRs to release

additional Ca^{2+} through CICR. Two possible mechanisms may explain how XIAP overexpression reduces glutamate-induced release of Ca^{2+} from intracellular stores.

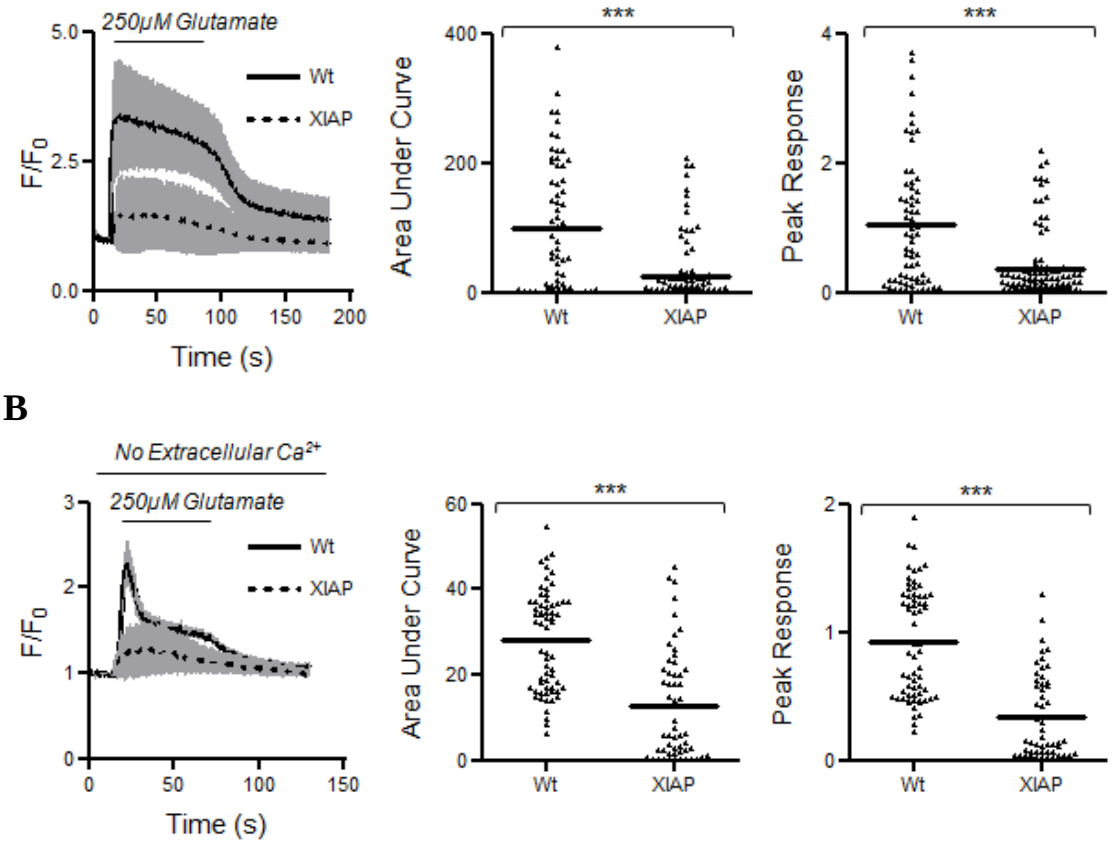

Figure 3.2. Glutamate-induced Ca^{2+} responses are reduced in neurons from XIAP-overexpressing mice.

A. Ca^{2+} traces taken from a sample experiment for glutamate addition (250μM for 60 seconds) in wild-type (Wt) or XIAP-overexpressing (XIAP) primary mouse cortical neurons. For these and all sample traces shown, 340nm / 380nm ratios were normalized to the first value of each trace (F/F_0); Traces represent mean ± s.d. for 13 neurons (Wt) and 25 neurons (XIAP). Scatterplots represent individual values for cells from three or more runs (Wt – 65 neurons, XIAP – 104 neurons) for area under curve (A.U.C.) and peak Ca^{2+} responses, with the horizontal line representing mean values. For A.U.C. and peak responses, *** - $P<0.0001$, Student's t-test **B**. Traces taken from a sample experiment for glutamate addition (250μM for 60 seconds) in nominal extracellular Ca^{2+} in wild-type (Wt) or XIAP-overexpressing (XIAP) primary mouse cortical neurons. Traces represent mean ± s.d. for 30 neurons (wild-type) and 17 neurons (XIAP). Scatterplots represent individual values for cells from three or more runs (Wt – 65 neurons, XIAP – 54 neurons) for area under curve (A.U.C.) and peak Ca^{2+} responses, with the horizontal line representing mean values. For A.U.C. and peak responses, *** - $P<0.0001$, Student's t-test

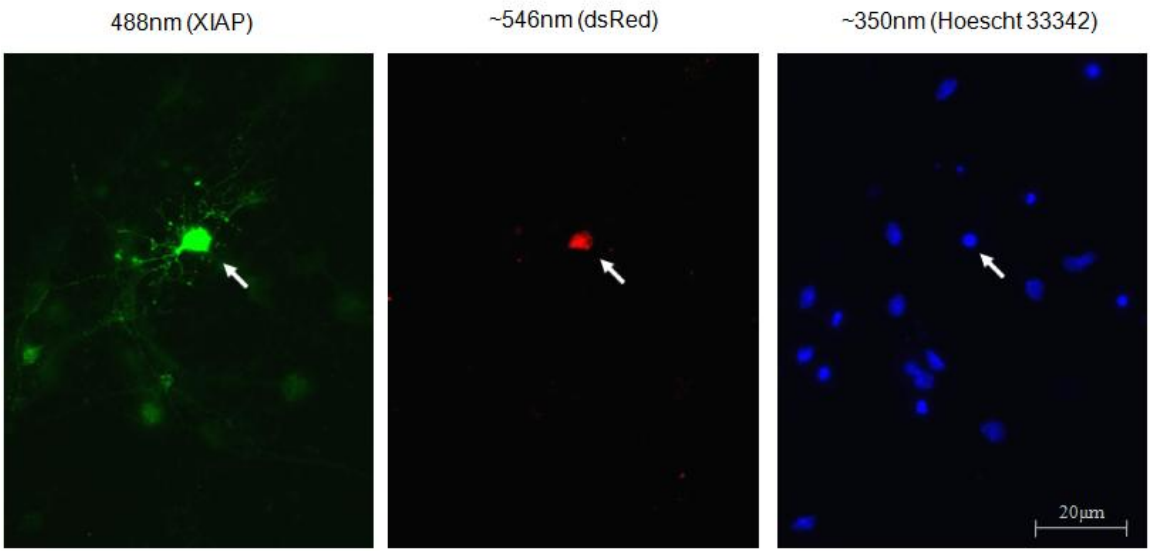

Figure 3.3. Transfection of XIAP-dsRed into primary cortical neurons.

Fluorescent sample images (under 40x objective) of neurons (day 5-6 old) transfected with XIAP-dsRed plasmid DNA, fixed and immunostained with primary antibody specific for XIAP (1/100 dilution) and then probed with goat-antimouse IgG labeled with alexafluor 488 (1/1000 dilution). Neurons were then nuclear-stained with Hoescht 33342 (1µg/ml) and mounted onto slides. Left panel represents alexafluor 488 labeled XIAP protein. Middle panel represents dsRed fluorescence (~546nm) in the same neurons. Right panel represents fluorescent nuclei of the same neurons. White arrow in all three images points to XIAP-dsRed plasmid transfected neuron.

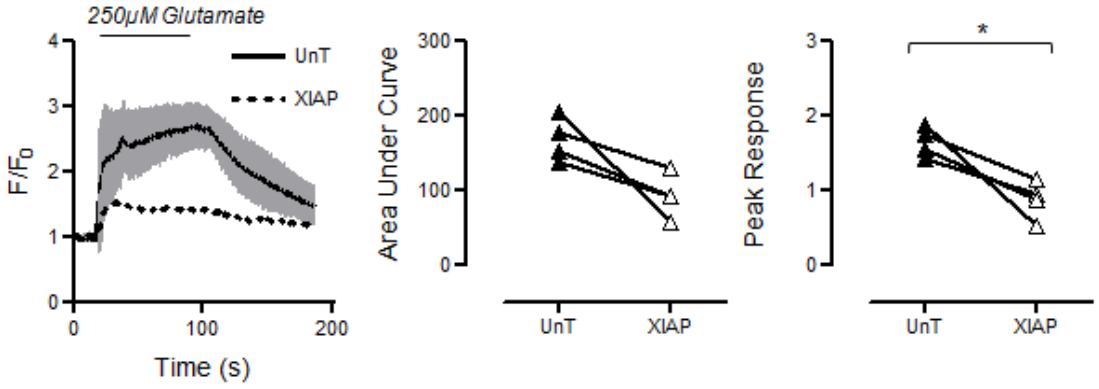

Figure 3.4. Glutamate-induced Ca^{2+} response is reduced in neurons transiently transfected with XIAP-dsRed.

Ca^{2+} traces taken from a sample experiment for glutamate addition (250µM for 60 seconds) in primary mouse cortical neurons. The trace shows the response of a single XIAP transfected neuron and mean ± s.d. for 11 surrounding untransfected (UnT) neurons. Quantification and comparison of the area under the curve (A.U.C.) and peak calcium response was for 4 independent experiments; results for this and all transfection experiments show averaged untransfected values versus transfected values for each independent run. * - $P<0.05$, Student's paired t-test.

Firstly, XIAP may reduce the amount of stored Ca^{2+} available for release from intracellular Ca^{2+} stores. Secondly, an increase in XIAP may not decrease the total amount of stored Ca^{2+}, but instead decrease the extent of release from ER Ca^{2+} channels such as IP_3R or RyR. To determine if XIAP overexpression would lead to a decrease in the release of Ca^{2+} from ER stores from these channels, I treated neurons that had been perfused in nominal extracellular Ca^{2} with the irreversible SERCA pump inhibitor, thapsigargin. By inhibiting SERCA pumps, thapsigargin induces a gradual leak of Ca^{2+} from the intracellular Ca^{2+} stores. I observed decreased Ca^{2+} response to thapsigargin in neurons from XIAP overexpressing mice as compared to wild-type control neurons (Figure 3.5A). Both A.U.C. and peak responses to thapsigargin were significantly decreased in XIAP neurons. In XIAP-dsRed transfected neurons I observed a similar decrease in release from intracellular stores upon thapsigargin stimulation in the absence of extracellular Ca^{2+} (Figure 3.5B), with a significant decrease in both A.U.C. and peak responses as compared to untransfected neurons from the same run.

The decrease in Ca^{2+} leak from the ER seen in XIAP overexpressing neurons when stimulated with thapsigargin in Ca^{2+} free media may be due to a decreased concentration of Ca^{2+} in ER stores. To test this, neurons were exposed to the Ca^{2+} ionophore ionomycin (25μM) in the absence of extracellular Ca^{2+} in order to empty intracellular stores in a channel-independent manner. XIAP overexpressing mouse neurons exhibited a very small decrease in Ca^{2+} response to ionomycin (Figure 3.6A), with a slight trend towards decrease in A.U.C. and small significant decrease in peak Ca^{2+} response. Similarly, XIAP-dsRed transiently transfected neurons showed a small

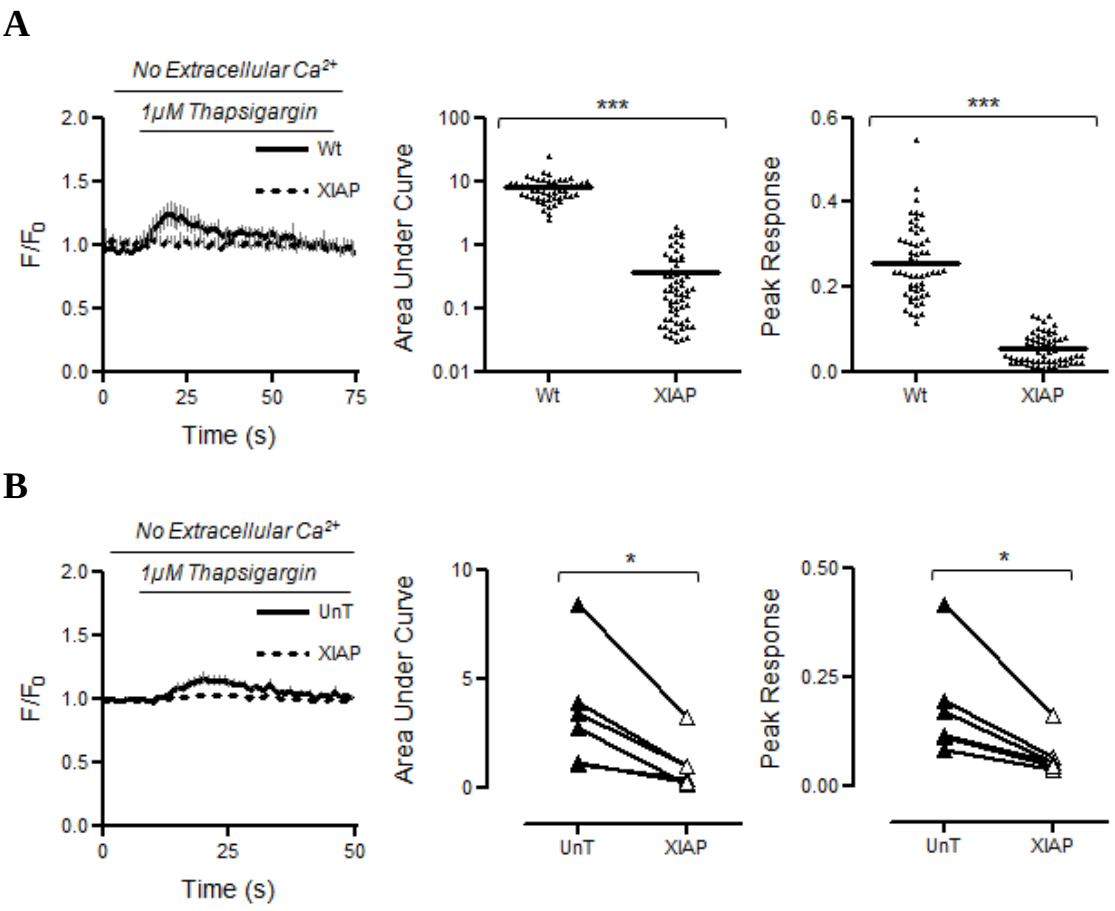

Figure 3.5. The amount of releasable ER Ca^{2+} is reduced in XIAP-overexpressing neurons and in neurons transiently transfected with XIAP-dsRed.

A. Ca^{2+} traces taken from a sample experiment for thapsigargin addition (1μM for 60 seconds) in wild-type (Wt) or XIAP-overexpressing (XIAP) primary mouse cortical neurons. Traces represent mean ± s.d. for 18 neurons (Wt) and 28 neurons (XIAP). Scatterplots represent individual values for cells from three or more runs (Wt – 53 neurons, XIAP – 60 neurons) for area under curve (A.U.C.) and peak Ca^{2+} responses, with the horizontal line representing mean values. For A.U.C. and peak responses, *** - P<0.0001, Student's t-test. **B**. Ca^{2+} traces taken from a sample experiment for thapsigargin addition (1 μM for 60 seconds) in XIAP transiently transfected neurons. The trace shows the response of a single XIAP transfected neuron and mean ± s.d. for 5 surrounding UnT neurons. Quantification of the peak Ca^{2+} response and the area under the curve (A.U.C.) was from 5 independent experiments; * - P<0.05 Student's paired t-test.

decrease in response to ionomycin as compared to untransfected controls (Figure 3.6B), with a significant decrease in A.U.C. and trend towards decrease in peak Ca^{2+} response, indicating that XIAP overexpression caused a marginal overall reduction in stored Ca^{2+}.

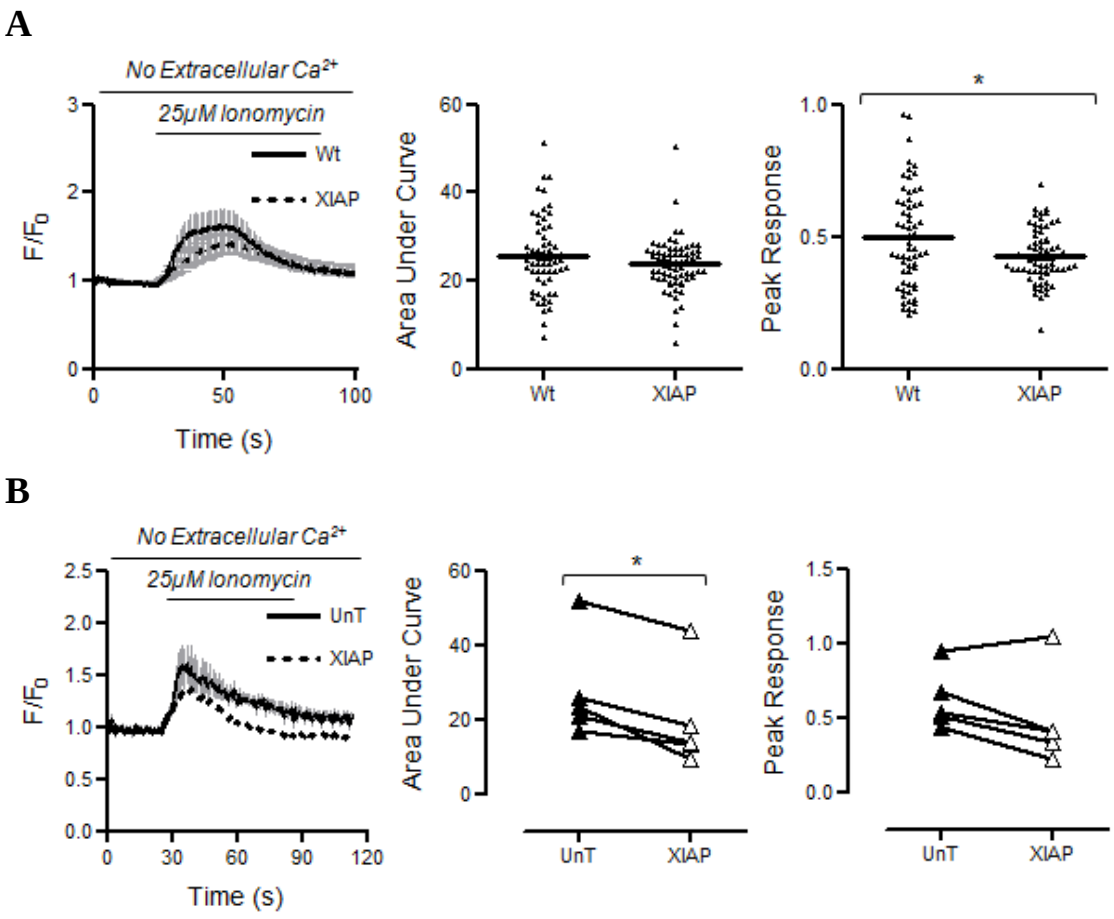

Figure 3.6. The amount of stored intracellular Ca^{2+} is reduced in XIAP-overexpressing neurons and in neurons transiently transfected with XIAP-dsRed

A. Ca^{2+} traces taken from a sample experiment for ionomycin addition (25μM for 60 seconds) in wild-type (Wt) or XIAP-overexpressing (XIAP) primary mouse cortical neurons. Traces represent mean ± s.d. for 15 neurons (wild-type) and 22 neurons (XIAP). Scatterplots represent individual values for cells from three or more runs (Wt – 62 neurons, XIAP – 68 neurons) for area under curve (A.U.C.) and peak Ca^{2+} responses, with the horizontal line representing mean values. For peak responses, * - $P<0.05$, Student's two tailed t-test. **B**. Traces taken from a sample experiment for ionomycin addition (25μM for 60 seconds) in XIAP transiently transfected neurons. The trace shows the response of a single XIAP transfected neuron and the mean value ± s.d. for 6 surrounding UnT neurons. Quantification of the peak Ca^{2+} response and the area under the curve (A.U.C.) was from 5 independent experiments. For A.U.C.** - $P<0.01$ Student's paired t-test.

3.4.3 XIAP lowers Ca^{2+} response from plasma membrane channels independent of release from intracellular stores

I also wished to determine if XIAP altered any aspect of Ca^{2+} signalling from plasma membrane Ca^{2+} channels independent of release from intracellular stores. To address this question, I first used pharmacological treatments to block the contribution of intracellular stores in neuronal Ca^{2+} responses to glutamate. XIAP-dsRed transiently transfected neurons were pretreated with dantrolene (10μM, 10 minutes) which blocks Ca^{2+} release from the ER by inhibition of IP_3R and RyR channels. The neurons were then stimulated with 250μM glutamate in the presence of extracellular Ca^{2+}. I observed a decrease in neuronal Ca^{2+} entry in XIAP overexpressing neurons as compared to untransfected neurons (Figure 3.7A), with a significant decrease in both A.U.C. and peak Ca^{2+} response.

As an independent confirmation of this, I treated XIAP-dsRed transfected neurons with the irreversible SERCA inhibitor thapsigargin (1μM, 10 minutes) in the absence of extracellular Ca^{2+} in order to drain ER Ca^{2+} stores by passive leak through IP_3R and RyR channels. Ca^{2+} was then added back to the medium and the neurons were stimulated with 250μM glutamate. Again, I observed a decrease in neuronal Ca^{2+}entry in XIAP-dsRed neurons as compared to controls (Figure 3.7B), with a significant decrease in both A.U.C. and peak responses.

Furthermore, I selectively stimulated NMDA receptors in XIAP-dsRed transfected neurons using NMDA (30μM, 60 seconds) in the presence of the NMDA co-agonist glycine (10μM). This approach allowed me to look at Ca^{2+} entry directly through

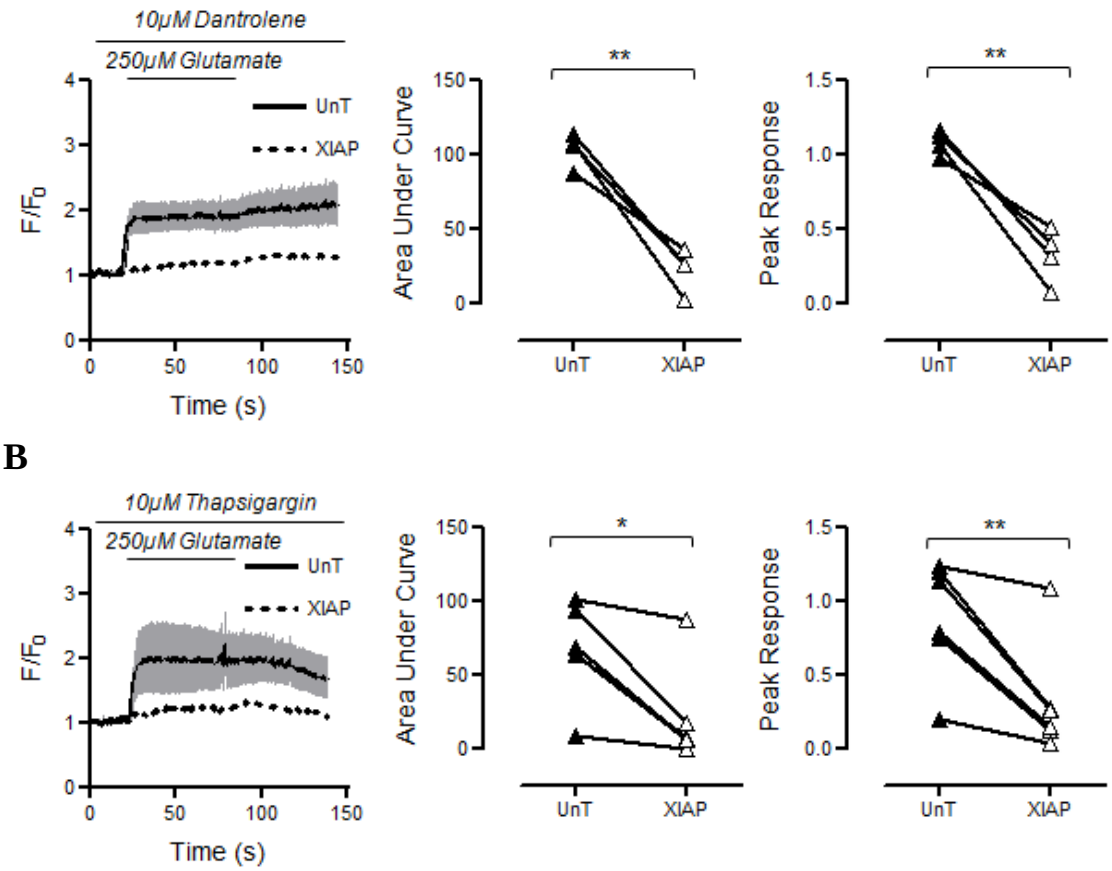

Figure 3.7. Ca^{2+} entry from glutamate activated plasma membrane Ca^{2+} channels is reduced in neurons transiently transfected with XIAP-dsRed

A. Ca^{2+} traces taken from a sample experiment for glutamate addition (250μM for 60 seconds) after a 10 minute dantrolene pretreatment (10μM) in XIAP transiently transfected neurons. The trace shows the response of a single XIAP transfected neuron and mean ± s.d. for 3 surrounding UnT neurons. Quantification of the peak Ca^{2+} response and the area under the curve (A.U.C.) was from 4 independent experiments. **B.** Ca^{2+} traces taken from a sample experiment for glutamate addition (250μM for 60 seconds) after a 10 minute thapsigargin (1μM) pretreatment in the absence of extracellular calcium in XIAP transiently transfected neurons. The trace shows the response of a single XIAP transfected neuron and mean ± s.d. for 6 surrounding UnT neurons. Quantification of the peak Ca^{2+} response and the area under the curve (A.U.C.) was from 6 independent experiments. For A.U.C. and peak responses, * - $P<0.05$, ** - $P<0.01$, Student's paired t-test.

plasma membrane NMDA receptors without concurrent stimulation of metabotropic glutamate receptors. I observed decreased Ca^{2+} response to NMDA in XIAP transfected

neurons as compared to untransfected neurons (Figure 3.8A), with a significant decrease in both A.U.C. and peak Ca^{2+} responses.

To determine if XIAP also affects Ca^{2+} entry through VGCCs, XIAP-dsRed transiently transfected neurons were depolarized with KCl (90mM for 30 seconds). I observed a decrease in Ca^{2+} response to KCl in XIAP transfected neurons as compared to untransfected controls (Figure 3.8B), with a significant decrease in both A.U.C. and peak Ca^{2+} responses.

3.4.4 XIAP alters neuronal capacitative Ca^{2+} entry

Since depletion of ER Ca^{2+} stores activates CCE and since I observed a decrease in ER Ca^{2+} upon XIAP overexpression, I examined the effect of XIAP overexpression on CCE. I treated XIAP-dsRed transfected neurons with thapsigargin (1μM for 10 minutes) in the absence of extracellular Ca^{2+} to deplete ER stores, then added back extracellular Ca^{2+} and measured Ca^{2+} entry into the cytoplasm. XIAP transfected neurons exhibited reduced CCE as compared to untransfected control neurons (Figure 3.9), with a significant decrease in A.U.C. of the Ca^{2+} response in XIAP neurons. A trend towards decreased peak response in XIAP neurons was seen as well.

3.4.5 XIAP overexpression increases neuronal cytoplasmic resting Ca^{2+} concentrations

To determine if XIAP could alter resting cytoplasmic Ca^{2+} concentrations, I measured basal Ca^{2+} levels in neurons from XIAP overexpressing mice and dsRED-

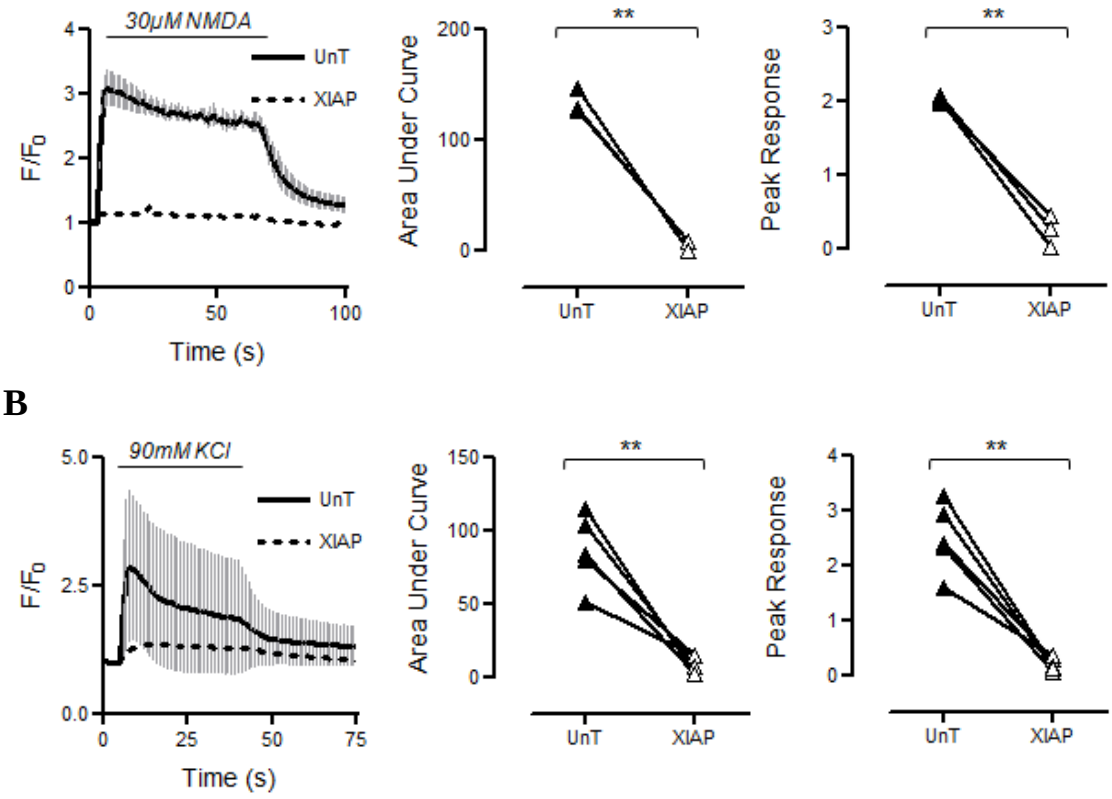

Figure 3.8. Ca^{2+} entry from NMDA and voltage operated calcium channels is reduced in neurons transiently transfected with XIAP-dsRed

A. Ca^{2+} traces taken from a sample experiment for NMDA addition (30μM for 60 seconds in the presence of 10 μM glycine) in XIAP transiently transfected neurons. The trace shows the response of a single XIAP transfected neuron and mean ± s.d. for 3 surrounding UnT neurons. Quantification of the peak Ca^{2+} response and the area under the curve (A.U.C.) was from 3 independent experiments. **B.** Ca^{2+} traces taken from a sample experiment for KCl addition (90μM for 30 seconds) in XIAP transiently transfected neurons. The trace shows the response of a single XIAP transfected neuron and mean ± s.d. for 5 surrounding untransfected neurons. Quantification of the peak Ca^{2+} response and the area under the curve (A.U.C.) is from 5 independent experiments. For A.U.C. and peak responses, ** - $P<0.01$, Student's paired t-test.

XIAP transiently transfected neurons, as well as their respective controls. I observed that in both neurons from XIAP-overexpressing mice (Figure 3.10A) and XIAP-dsRed transiently transfected neurons (Figure 3.10B), there was a small significant increase in

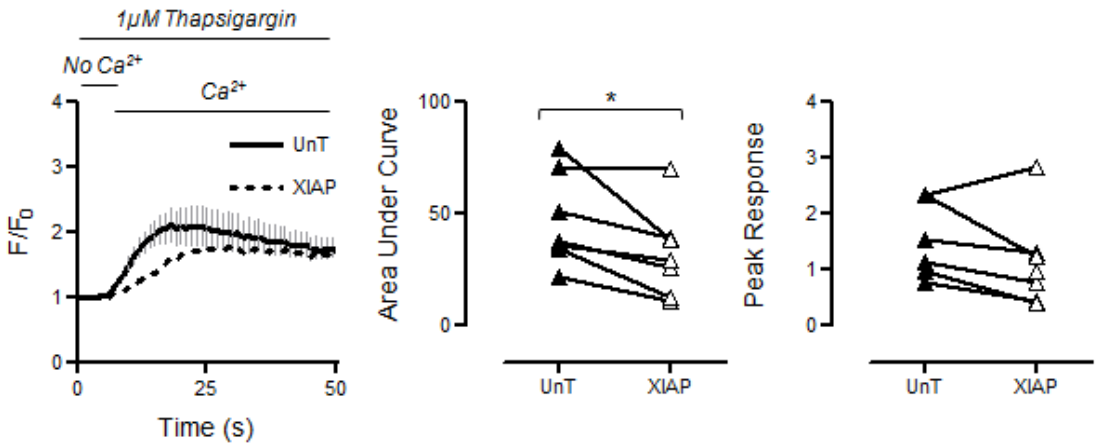

Figure 3.9. XIAP alters neuronal capacitative Ca^{2+} entry in neurons transiently transfected with XIAP-dsRed

Ca^{2+} traces taken from a sample experiment for reintroduction of Ca^{2+} into the extracellular medium after thapsigargin pretreatment (1μM for 10 minutes) in the absence of extracellular Ca^{2+} in XIAP transiently transfected neurons. The trace shows the response of a single XIAP transfected neuron and mean ± s.d. for 5 surrounding untransfected neurons. Quantification of the peak Ca^{2+} response and the area under the curve (A.U.C.) is from 6 independent experiments. For A.U.C. * - P<0.05, Student's paired t-test.

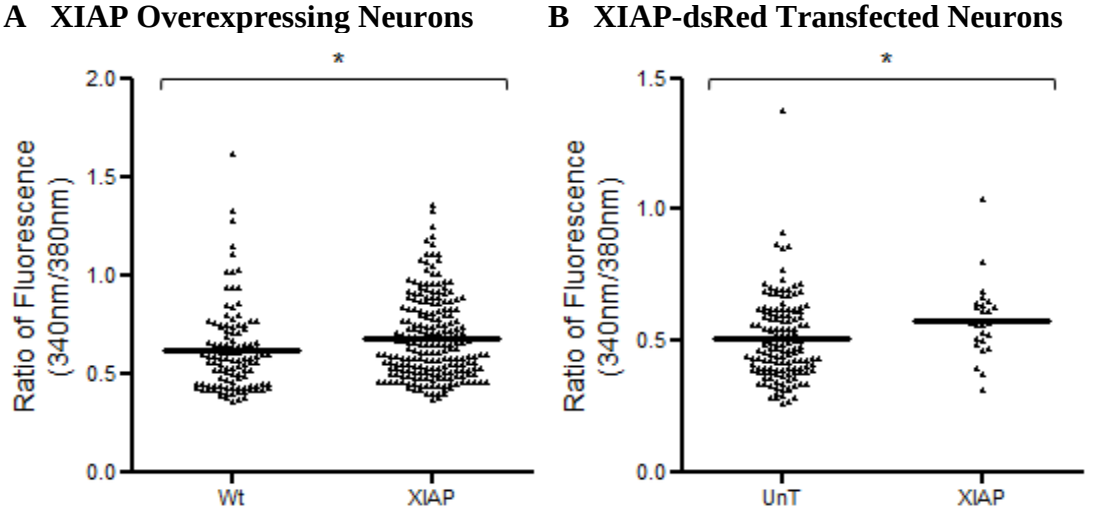

Figure 3.10. XIAP overexpression increases neuronal cytoplasmic resting Ca^{2+} concentrations in XIAP overexpressing neurons and XIAP-dsRed transiently transfected neurons

A. Scatterplot represents individual resting cytoplasmic Ca^{2+} levels (as measured by calculating ratio of 340nm and 380nm fluorescence in each cell) taken from 115 Wt and 214 XIAP overexpressing neurons, with horizontal line representing mean values. **B.** Scatterplot represents individual resting cytoplasmic Ca^{2+} levels taken from 141 Untransfected neurons and 25 XIAP transfected neurons, with horizontal line representing mean values. * - p<0.05, student's t-test.

basal resting cytoplasmic Ca^{2+} levels as compared to control non-XIAP overexpressing neurons.

3.4.6 XIAP overexpression lowers cytoplasmic Ca^{2+} entry in response to oxidative stress

Oxidative stress is a hallmark of several neurodegenerative diseases. It has been shown to cause lipid peroxidation, which in turn results in Ca^{2+} entry from the extracellular space and release of Ca^{2+} from intracellular stores such as the ER and mitochondria. Since the above results revealed that XIAP affects multiple aspects of Ca^{2+} dynamics within neurons, I wanted to determine if XIAP overexpression would in turn lower Ca^{2+} responses to oxidative stress, which could potentially account for the protective nature of XIAP in neurodegenerative disease and brain injury. Ca^{2+} responses were measured from primary cortical neurons from either XIAP overexpressing mice or their wildtype littermates after exposure to oxidative stress (20µM H_2O_2, 60 seconds). A significant decrease in both A.U.C. and peak Ca^{2+} response was observed in XIAP overexpressing neurons in both the presence and absence of extracellular Ca^{2+} (Figure 3.11).

3.4.7 The effect of XIAP on Ca^{2+} signalling is not specific to neurons

I wished to determine if the effects of XIAP on Ca^{2+} signalling were specific to neurons therefore, I cultured primary glia cells from the cortex of both XIAP

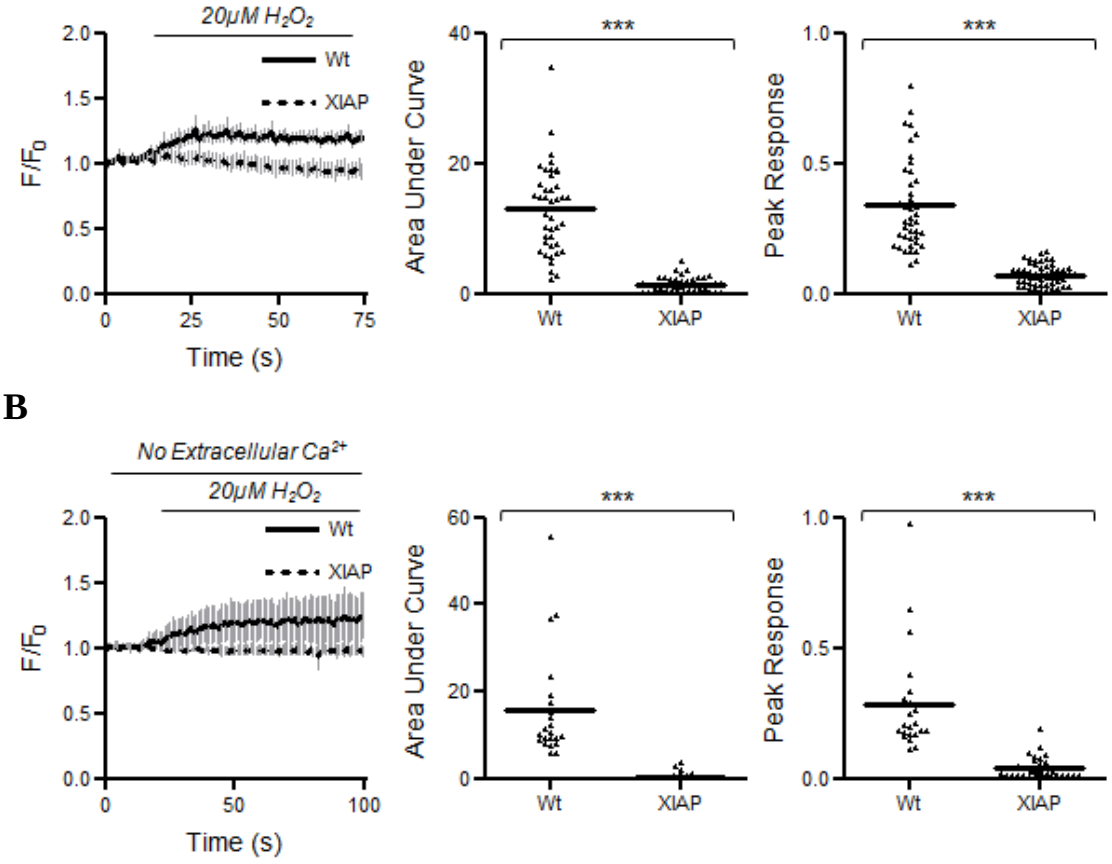

Figure 3.11. Neurons from XIAP-overexpressing mice show decreased Ca^{2+} response to oxidative stress.

A. Ca^{2+} traces taken from a sample experiment for H_2O_2 addition (20μM for 60 seconds) in wild-type (Wt) or XIAP-overexpressing (XIAP) primary mouse cortical neurons. Traces show mean ± s.d. for 14 neurons (Wt) and 26 neurons (XIAP). Scatterplots represent individual values for cells from three or more runs (Wt – 41 neurons, XIAP – 55 neurons) for area under curve (A.U.C.) and peak Ca^{2+} responses, with the horizontal line representing mean values. **B**. Ca^{2+} traces taken from a sample experiment for H_2O_2 addition (20μM for 60 seconds) in nominal extracellular Ca^{2+} in wild-type (Wt) or XIAP-overexpressing (XIAP) primary mouse cortical neurons. Traces represent mean ± s.d. for 23 neurons (Wt) and 20 neurons (XIAP). Scatterplots represent individual values for cells from three or more runs (Wt –22 neurons, XIAP – 37 neurons) for area under curve (A.U.C.) and peak Ca^{2+} responses, with the horizontal line representing mean values. For A.U.C. and peak responses, *** - P<0.0001, Student's t-test.

overexpressing mice and wildtype littermate control mice. Both A.U.C. and peak Ca^{2+} response to thapsigargin (10μM, 60 seconds) in the absence of extracellular Ca^{2+} were

significantly decreased in XIAP overexpressing glia as compared to non-transgenic controls (Figure 3.12).

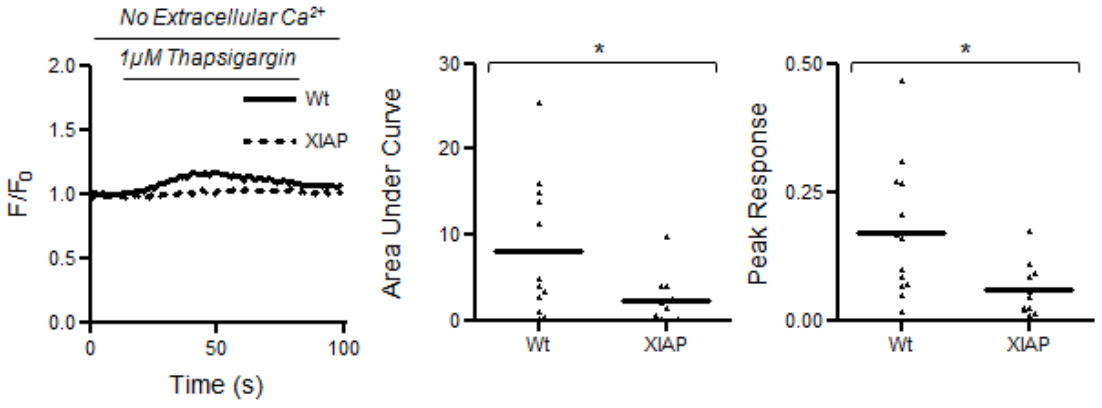

Figure 3.12. Glia from XIAP overexpressing mice show decreased Ca^{2+} response from intracellular stores

Ca^{2+} Traces taken from a sample experiment for thapsigargin addition (10μM for 60 seconds) in wild type (Wt) and XIAP-overexpressing (XIAP) glia. Traces from one Wt glia cell and one XIAP glia cell are shown. Scatterplots represent individual values for cells from three or more runs (Wt – 13 cells, XIAP – 12 cells) for area under curve (A.U.C.) and peak Ca^{2+} responses, with the horizontal line representing mean values. For A.U.C. and peak responses, * - $P<0.05$, Student's two tailed t-test

3.4.8 Inhibition of caspases does not alter glutamate induced Ca^{2+} release

Given that one of the known functions of XIAP is to bind and inhibit the activation of caspases 3, 7 and 9, I sought to determine if pharmacological inhibition of caspases in neurons would affect glutamate induced Ca^{2+} responses in a manner similar to that of XIAP overexpression.

Primary mouse cortical neurons were treated for 24 hours with the pan-caspase inhibitor Z-VAD-FMK (100μM), then stimulated with glutamate (250μM, 60 seconds) in the presence of extracellular Ca^{2+}. No significant difference in Ca^{2+} response was seen in

Z-VAD treated neurons as compared to vehicle control treated neurons in respect to both A.U.C. and peak response (Figure 3.13).

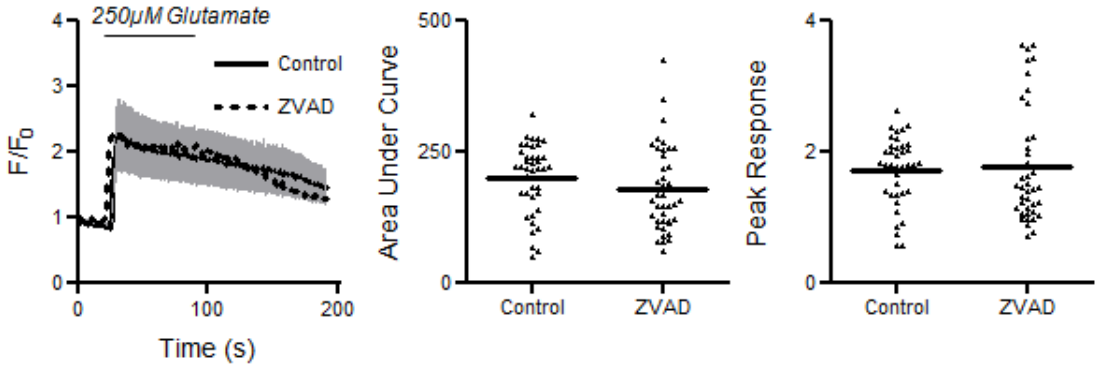

Figure 3.13. Inhibition of caspases in wild-type neurons does not alter glutamate-induced Ca^{2+} release

Ca^{2+} traces taken from a sample experiment for glutamate addition (250μM for 60 seconds) in Wt cortical neurons pretreated with ZVAD-FMK (100μM) or vehicle control (0.2% DMSO) for 24 hours; Traces represent mean ± s.d for 14 neurons (ZVAD-FMK) and 15 neurons (Control). Scatterplots represent individual values for cells from three or more runs (Control – 41 neurons, XIAP – 41 neurons) for area under curve (A.U.C.) and peak Ca^{2+} responses, with the horizontal line representing mean values.

3.5 Discussion

In this study I have shown that overexpression of XIAP alters multiple aspects of neuronal Ca^{2+}signalling. This is a novel aspect of XIAP function that has not previously been shown with respect to XIAP or any of the other members of the IAP family. Modulation of XIAP expression resulted in a large and varied effect on neuronal Ca^{2+} signalling that could not be narrowed to one particular mechanism. It seems unlikely that XIAP could modulate expression of so many different Ca^{2+} channels on both the plasma membrane and ER membrane, although this cannot be ruled out at this time. It is unlikely that the observed changes in Ca^{2+} signalling are due to direct buffering of $Ca^{2+}$by

XIAP, as XIAP has not been previously shown to have Ca^{2+}-binding properties. Another possibility is that overexpression of XIAP may be deleterious to the neurons, meaning that the disruptions in Ca^{2+} signalling are a non-specific toxicity response. I however do not believe that this is a likely scenario, as I did not observe any differences in viability between XIAP overexpressing neurons and control neurons (data not shown). Further studies using mutant variants of XIAP that separate caspase inhibiting domains from domains responsible for modulation of signalling pathways may shed more light on the potential mechanism. Given that the closely related IAP family protein NAIP was shown to interact with the Ca^{2+} binding protein hippocalcin, it would also be interesting to determine if XIAP directly interacts with any Ca^{2+} binding/modulating proteins. Furthermore, it would be interesting to determine if XIAP can modulate any of the several Ca^{2+} sensitive processes within the brain, such as neurotransmitter release, neuronal excitability, or learning and memory. Since XIAP alters multiple aspects of Ca^{2+} signalling, I expect that many of these processes are affected by XIAP.

XIAP and other members of the closely related IAP family have not previously been shown to directly alter Ca^{2+} signalling in neurons or any other cell type, thus this study is interesting as it reveals a novel function of this protein. Given the close relationship between cellular Ca^{2+} signalling and the process of apoptosis, the fact that XIAP modulates Ca^{2+} signalling may be another mechanism by which XIAP can prevent induction of apoptosis. The Bcl-2 family of apoptosis modulating proteins have been shown to affect cellular Ca^{2+} signals, so there is precedence for proteins involved in the apoptotic process to modulate Ca^{2+} signalling [266]. Modulation of cellular Ca^{2+}

signalling is an important mechanism by which a cell responds to apoptotic signals and decides whether to proceed with the apoptotic pathway, and XIAP appears to play an important role in this.

Interestingly, my experiments revealed that overexpression of XIAP in neurons resulted in an almost complete inhibition of Ca^{2+} entry into the cytoplasm in response to oxidative stress. XIAP has been shown to inhibit apoptosis through more than one mechanism, and these experiments reveal that perhaps XIAP may also be able to prevent cell injury and death by blocking disruption of Ca^{2+} signalling caused by oxidative stress. However, further experiments will be required to determine if XIAP can prevent cell death by preventing destructive changes in Ca^{2+} signalling in response to stress, independent of preventing apoptosis by inhibition of caspase activity and modulation of receptor signalling. This further illustrates the need to determine which domain of XIAP is responsible for alterations in Ca^{2+} signalling. Once this has been determined, a stable cell line could be established that only expresses the Ca^{2+} modulating portion of the XIAP protein, and it can be determined if these cells are still protected against cell death.

I also found that XIAP-mediated modulation of Ca^{2+} signalling was not isolated to neurons. Primary glia cells from XIAP-overexpressing mice also showed decreased Ca^{2+} release from ER stores. Given the fact that Ca^{2+} is such a ubiquitous messenger in numerous diverse cellular functions (examples of which are muscle contraction and cellular adhesion, among many others) it would be interesting to determine the effect XIAP has on Ca^{2+} signalling in non-brain cells, and subsequently how XIAP could modulate Ca^{2+}-sensitive physiological processes of these cells.

I have also demonstrated in this study that direct inhibition of neuronal caspase activity does not alter neuronal Ca^{2+} response to glutamate. This suggests that XIAP-mediated alteration of Ca^{2+} signalling is independent to the function of binding to and inhibiting caspase activation, in particular caspases 3, 7 and 9. XIAP has been shown to inhibit apoptosis through several mechanisms independent of caspase inhibition, in particular through activation of TGF-β, JNK, and NF-κB signalling pathways. It is possible that XIAP alters neuronal Ca^{2+} signalling through modulation of these pathways. However, given the fact that XIAP has been shown to interact with a large number of different proteins, it is also possible that XIAP is causing this effect via interaction with other protein(s) that modulate Ca^{2+} balance in the cell. Examination of the role of the TGF-β, JNK, and NF-κB signalling pathways in Ca^{2+} signalling may partially answer these questions, while studies examining which other proteins directly interact with XIAP would also be informative.

In conclusion, I have shown that cortical neurons from XIAP overexpressing mice as well as XIAP-dsRed transiently transfected neurons exhibit differences in multiple aspects of Ca^{2+} signalling as compared to control neurons. This effect is also seen in other neuronal cell types and is likely not due to the ability of XIAP to inhibit caspases. Given the prevalence of Ca^{2+} dyshomeostasis in multiple neurodegenerative diseases, XIAP may play an important role in protecting neurons from neurodegenerative processes.

Chapter 4

L-Theanine Modulates Neuronal Ca^{2+} Signalling

4.1 Abstract

L-theanine, a compound found in green tea, has a structure similar to the neurotransmitter glutamate. L-theanine has been shown to be protective in several models of ischemic neuronal injury involving excitotoxic mechanisms. Although L-theanine has previously been shown to be a competitive antagonist of both NMDA and AMPA receptors, the mechanism by which L-theanine can exert neuroprotective effects has not been conclusively elucidated. Because a known aspect of neuronal excitotoxicity is enhanced Ca^{2+} entry through NMDA receptors and subsequent overload of neuronal cytoplasmic Ca^{2+}, I hypothesized that L-theanine would alter neuronal Ca^{2+} signalling induced by glutamate.

I observed that a 24 hour pretreatment of human SH-SY5Y cells with 600μM and 1.2mM L-theanine significantly lowered glutamate induced Ca^{2+} response from intracellular stores, but did not lower Ca^{2+} entry due to glutamate receptor activation. ER Ca^{2+} responses to caffeine were also significantly lowered in L-theanine treated SH-SY5Y cells, as well as Ca^{2+} release from intracellular stores after exposure to the Ca^{2+} ionophore ionomycin. Primary mouse cortical neurons treated with L-theanine for 24 hours also exhibited significantly reduced Ca^{2+} release from intracellular stores, confirming what was seen with SH-SY5Ys. Furthermore, acute 30 minute treatment of cortical neurons with 1.2mM L-theanine also lowered neuronal Ca^{2+} release from intracellular stores in response to glutamate, suggesting a mechanism independent to novel protein synthesis for L-theanine mediated alterations of neuronal Ca^{2+} signalling. Thus, L-theanine mediated protection of neurons from excitotoxic insult may be due to

reduced load of intracellular Ca^{2+} stores. Further studies are required to determine the role of Ca^{2+} stores in excitotoxicity.

4.2 Introduction

L-theanine, or γ-glutamylethylamide, is a compound found in green tea (*Camellia sinensis*) with a chemical structure similar to that of the neurotransmitter glutamate. L-theanine has been shown to be a competitive antagonist of glutamate receptors [267]. L-theanine binds and inhibits both AMPA and NMDA receptors, with 10-fold higher inhibition of AMPA receptors as compared to NMDA receptors [268]. Recent studies have shown that L-theanine may also bind to group I metabotropic glutamate receptors (mGluR1) [269].

Neuronal death by glutamate induced excitotoxicity is thought to be involved in several disorders of the brain, including stroke, AD and ALS. L-theanine has been shown to be neuroprotective in ischemic models of excitotoxic insult. In one *in vivo* study, pre-administration of L-theanine was shown to prevent degeneration of gerbil CA1 pyramidal hippocampal neurons after transient forebrain ischemia [270]. L-Theanine was also shown to decrease the size of cerebral infarcts in mice after middle cerebral artery occlusion [271]. In addition, in an *in vitro* model of excitotoxicity, L-theanine was shown to inhibit delayed death of rat cortical neurons after exposure to glutamate [269].

The mechanism by which L-theanine can prevent excitotoxic injury to neurons is poorly understood. Although L-theanine has been shown to directly bind to and antagonize glutamate receptors, it is currently not known what effect this might have on

overall brain function. As such, it is also not known how L-theanine protects neurons from excitotoxic insult. Ca^{2+} is thought to play a crucial role in glutamate-induced excitotoxicity, in which overstimulation of NMDA and AMPA receptors by glutamate results in an overload of Ca^{2+} in the neuron [261], which can have a profound impact on neuronal function. In this study I tested the hypothesis that exposure of neurons to L-theanine would alter neuronal Ca^{2+} responses to glutamate stimulation. I demonstrate that while 24 hour treatment of SH-SY5Y neuroblastoma cells with two different concentrations of L-theanine does not alter the Ca^{2+} response to glutamate through extracellular Ca^{2+} channels, it does result in decreased Ca^{2+} response from intracellular stores. These effects were also observed in primary mouse cortical neurons pretreated with L-theanine. Acute 30 minute treatment of neurons with L-theanine reduced intracellular Ca^{2+} responses to a similar extent as the 24 hour treatment, indicating that the mechanisms by which L-theanine alters neuronal Ca^{2+} signalling may be independent of changes in gene transcription and protein synthesis.

4.3 Materials and Methods

4.3.1 Animals and cell culture

Human SH-SY5Y neuroblastoma cells were cultured as described in Chapter 2. A C57/Bl6 mouse colony was maintained at the Atlantic Veterinary College, University of Prince Edward Island. Primary cortical neurons were isolated and cultured as described in Chapter 2. Experiments were performed following 7-9 days of *in vitro*

culture. For Ca^{2+} imaging experiments, SH-SY5Ys or primary cortical neurons were plated at a density of 8 x 10^5 cells on 60mm coverslips.

4.3.2 Single cell Ca^{2+} imaging

Primary cortical neurons and SH-SY5Y cells were imaged and data was analyzed as described in Chapter 2.

4.3.3 Statistical Analysis

Data were analyzed using GraphPad Prism, version 4 (San Diego, CA). For Ca^{2+} imaging of neurons and SH-SY5Ys, student's two-tailed t-test was performed to determine the difference between mean area under the curve (A.U.C.) and peak Ca^{2+} response from multiple independent experiments.

4.4 Results

4.4.1 L-theanine reduces glutamate induced Ca^{2+} signalling from intracellular stores in SH-SY5Y cells.

Since it has been well documented that disruption of intracellular Ca^{2+} signalling is a hallmark of excitotoxic injury and subsequent cell death in neurons, experiments were performed to determine if L-theanine treatment of neurons would alter neuronal Ca^{2+} response to glutamate. I pretreated SH-SY5Y neuroblastoma cells for 24 hours with L-theanine. L-theanine was removed from the cells, and then Ca^{2+} response to 750µM glutamate (60 seconds) in the presence of extracellular Ca^{2+} was measured. No

significant difference in integrated A.U.C. or peak response was seen in SH-SY5Ys pretreated with either 600µM (Figure 4.1A) or 1.2mM (Figure 4.1B) L-theanine as compared to untreated control cells.

Ca^{2+} responses elicited by glutamate are largely due to entry of Ca^{2+} through NMDA and to a lesser extent AMPA receptors. However, glutamate can also stimulate Ca^{2+} release from ER stores through stimulation of mGluR. To determine if pretreatment of SH-SY5Ys with L-theanine altered Ca^{2+} response to glutamate from ER stores, I repeated the experiments from Figure 4.1, in the absence of extracellular Ca^{2+} to eliminate responses through NMDA or AMPA channels. Pretreatment with 600µM L-theanine for 24 hours significantly lowered A.U.C. of responses after stimulation with 750µM glutamate as compared to untreated control cells (Figure 4.2A), while pretreatment with 1.2 mM L-theanine significantly lowered both A.U.C. and peak response to glutamate as compared to untreated control cells (Figure 4.2B).

4.4.2 Treatment of SH-SY5Ys with L-theanine lowers the amount of releasable ER Ca^{2+}

Given that L-theanine pretreatment of SH-SY5Ys reduced glutamate induced Ca^{2+} release from intracellular stores, I wanted to investigate further the effect of L-theanine on intracellular Ca^{2+} stores. To specifically determine if L-theanine affects Ca^{2+} signalling from the ER, I directly stimulated RyRs with caffeine. SH-SY5Ys were pretreated with L-theanine for 24 hours, then Ca^{2+} responses to caffeine

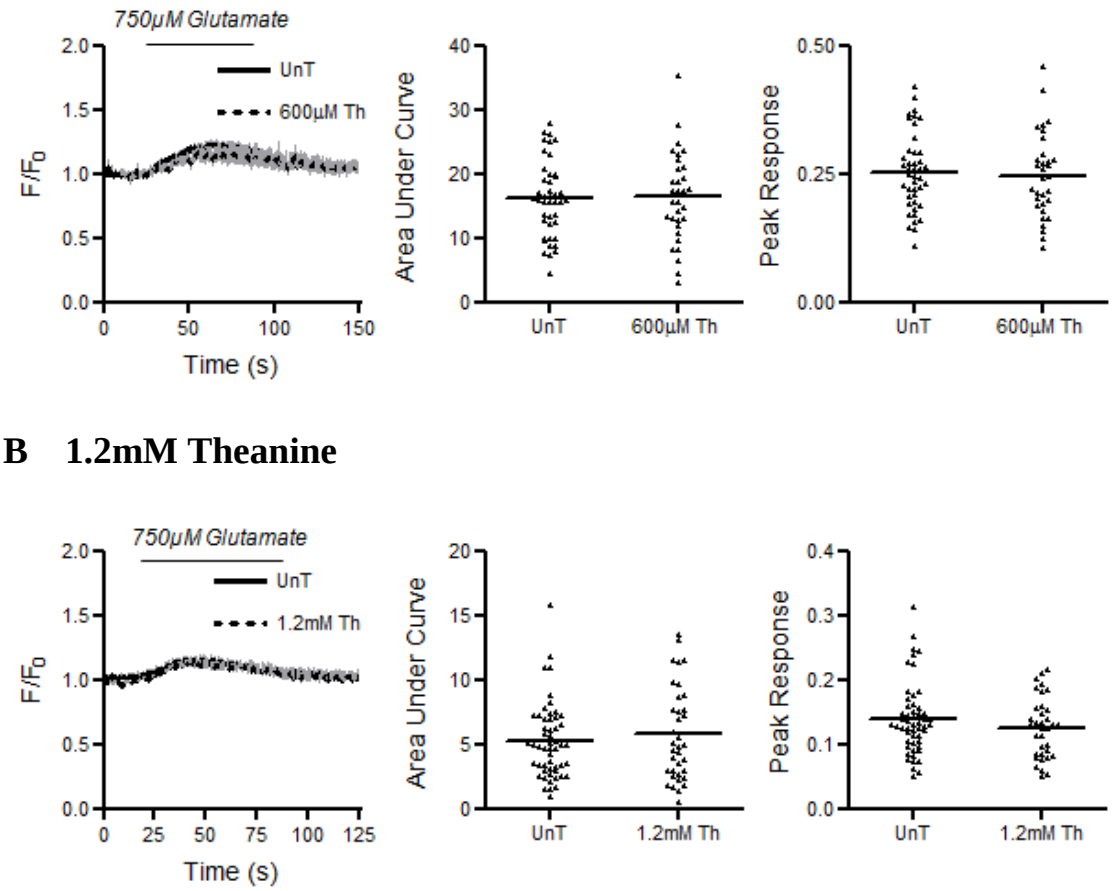

Figure 4.1. L-theanine treatment of SH-SY5Y cells does not alter Ca^{2+} response to glutamate through plasma membrane channels

A. Traces taken from a sample experiment for glutamate addition (750µM for 60 seconds) in the presence of extracellular Ca^{2+} in SH-SY5Ys pretreated for 24hrs with 600µM L-theanine. For these and all sample traces shown, 340nm / 380nm ratios were normalized to the first value of each trace; traces represent mean ± s.d. for 17 cells (UnT) and 12 cells (L-theanine). Quantification of the area under the curve (A.U.C.) and the peak Ca^{2+} response was from at least 2 separate runs from at least 3 independent experiments. Scatterplots represent individual values for cells from multiple runs (UnT: 43 cells; L-theanine 32 cells) for A.U.C. and peak Ca^{2+} responses, with the horizontal line representing mean values. **B.** Traces taken from a sample experiment for glutamate addition (750µM for 60 seconds) in the presence of extracellular Ca^{2+} in SH-SY5Ys pretreated for 24hrs with 1.2mM L-theanine, mean ± s.d. for 16 cells (UnT) and 6 cells (L-theanine). Quantification of the area under the curve (A.U.C.) and the peak Ca^{2+} response was from at least 2 separate runs from at least 3 independent experiments. Scatterplots represent individual values for cells from multiple runs (UnT: 53 cells; L-theanine 36 cells) for A.U.C. and peak Ca^{2+} responses, with the horizontal line representing mean values.

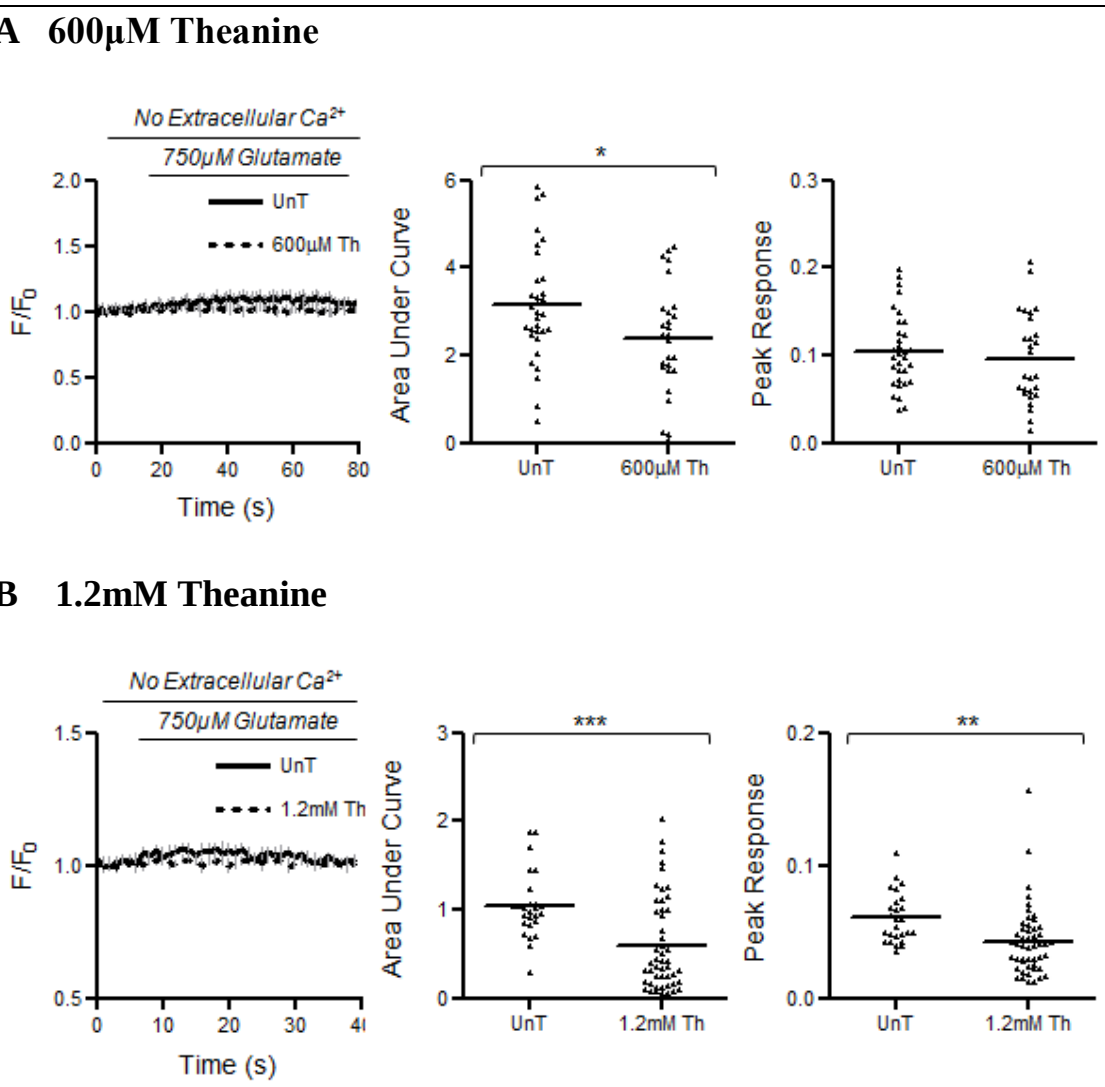

Figure 4.2: L-theanine treatment of SH-SY5Ys lowers Ca^{2+} response to glutamate from intracellular stores

A. Traces taken from a sample experiment for glutamate addition (750 µM for 60 seconds) in the absence of extracellular Ca^{2+} in SH-SY5Ys pretreated for 24 hours with 600µM L-theanine. Traces represent mean ± s.d. for 17 cells (UnT) and 3 cells (L-theanine). Quantification of the area under the curve (A.U.C.) and the peak Ca^{2+} response was from at least 2 separate runs from at least 3 independent experiments. Scatterplots represent individual values for cells from multiple runs (UnT: 32 cells; L-theanine 27 cells) for A.U.C. and peak Ca^{2+} responses, with the horizontal line representing mean values.
B. Traces taken from a sample experiment for glutamate addition (750µM for 60 seconds) in the absence of extracellular Ca^{2+} in SH-SY5Ys pretreated for 24 hours with 1.2mM L-theanine, mean ± s.d. for 9 cells (UnT) and 26 cells (L-theanine). Quantification of the area under the curve (A.U.C.) and the peak Ca^{2+} response was from at least 2 separate runs from at least 3 independent experiments. Scatterplots represent individual values for cells from multiple runs (UnT: 26 cells; L-theanine 49 cells) for A.U.C. and peak Ca^{2+} responses, with the horizontal line representing mean values.

(20mM, 1 minute) in the absence of extracellular Ca^{2+} were measured. Pretreatment with 600µM L-theanine significantly lowered peak Ca^{2+} response to caffeine (Figure 4.3A), while pretreatment with 1.2mM L-theanine had a larger effect, significantly lowering both A.U.C. and peak response to caffeine (Figure 4.3B). The manner in which L-theanine lowers releasable ER Ca^{2+} may be due to a general decrease in total stored intracellular Ca^{2+}. To test if this was the case, I pretreated SH-SY5Ys with L-theanine (1.2mM, 24 hours) and stimulated Ca^{2+} release in the absence of extracellular Ca^{2+} with ionomycin (25µM, 60 seconds), which is a Ca^{2+} ionophore that liberates Ca^{2+} from all intracellular compartments independent of receptor function. A significant decrease in both A.U.C and peak Ca^{2+} response was seen in L-theanine treated cells as compared to untreated cells after stimulation with ionomycin (Figure 4.4). This indicates that both releasable ER Ca^{2+} and total stored intracellular Ca^{2+} are lowered by treatment with L-theanine.

4.4.3 L-theanine pretreatment lowers intracellular Ca^{2+} response to glutamate in primary cortical neurons.

I next determined if the pretreatment with L-theanine in primary neuronal cultures would have a similar effect on release of Ca^{2+} from intracellular stores as observed in the SH-SY5Y cells. To determine this, I cultured primary cortical neurons from embryonic C57 mice for 7 days, and then pretreated the neurons with L-theanine (1.2mM) for 24 hours. The neurons were then stimulated with glutamate (250µM, 60 seconds) in either the presence or absence of extracellular Ca^{2+}. Consistent with the SH-SY5Y experiments,

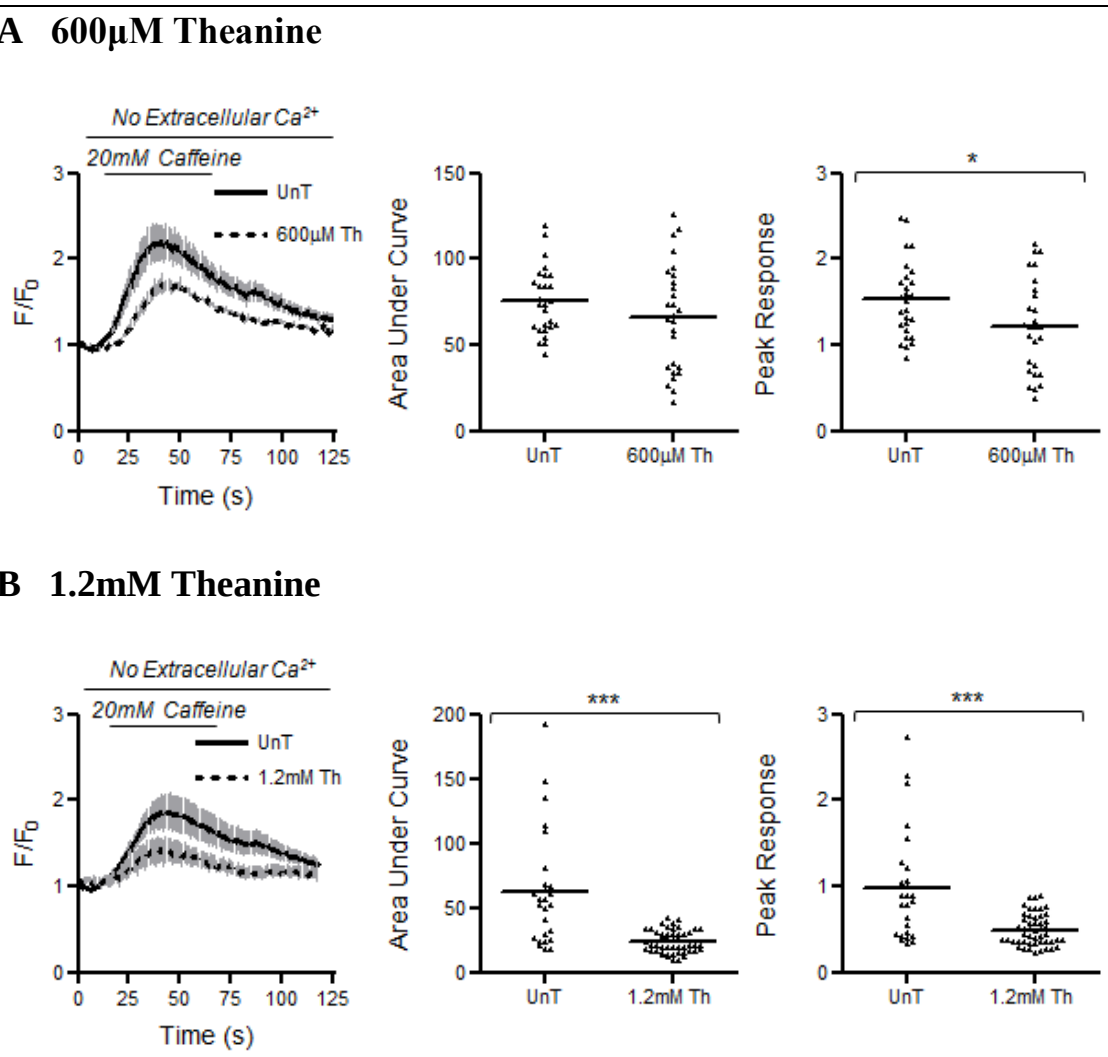

Figure 4.3. L-theanine treatment of SH-SY5Ys lowers Ca^{2+} response from ER RyR channels.

A. Traces taken from a sample experiment for caffeine addition (20mM for 60 seconds) in the absence of extracellular Ca^{2+} in SH-SY5Ys pretreated for 24 hours with 600µM L-theanine. Traces represent mean ± s.d. for 8 cells (UnT) and 3 cells (L-theanine). Quantification of the area under the curve (A.U.C.) and the peak Ca^{2+} response was from at least 2 separate runs from at least 3 independent experiments. Scatterplots represent individual values for cells from multiple runs (UnT: 27 cells; L-theanine 27 cells) for A.U.C. and peak Ca^{2+} responses, with the horizontal line representing mean values. **B**. Traces taken from a sample experiment for caffeine addition (20mM for 60 seconds) in the absence of extracellular Ca^{2+} in SH-SY5Ys pretreated for 24 hours with 1.2mM L-theanine. Traces represent mean ± s.d. for 12 cells (UnT) and 26 cells (L-theanine). Quantification of the area under the curve (A.U.C.) and the peak Ca^{2+} response was from at least 2 separate runs from at least 3 independent experiments. Scatterplots represent individual values for cells from multiple runs (UnT: 26 cells; L-theanine 49 cells) for A.U.C. and peak Ca^{2+} responses, with the horizontal line representing mean values. *-$p<0.05$, ***-$p<0.001$, student's t-test.

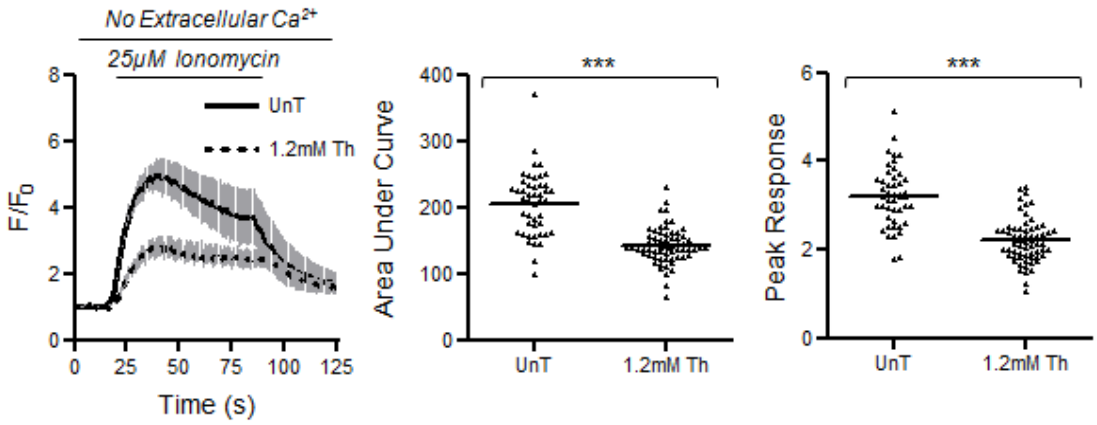

Figure 4.4. L-theanine treatment of SH-SY5Ys lowers ER Ca^{2+} response to thapsigargin and total amount of Ca^{2+} in intracellular stores.

Traces taken from a sample experiment for ionomycin addition (25 μM for 60 seconds) in the absence of extracellular Ca^{2+} in SH-SY5Ys pretreated for 24 hours with 1.2mM L-theanine. Traces represent mean ± s.d. for 8 cells (UnT) and 28 cells (L-theanine). Quantification of the area under the curve (A.U.C.) and the peak Ca^{2+} response was from at least 2 separate runs from at least 3 independent experiments. Scatterplots represent individual values for cells from multiple runs (UnT: 46 cells; L-theanine 65 cells) for A.U.C. and peak Ca^{2+} responses, with the horizontal line representing mean values. *-$p<0.05$, ***-$p<0.001$, student's t-test

Ca^{2+} responses due to glutamate in the presence of extracellular Ca^{2+} were not significantly different between in L-theanine treated and untreated neurons (Figure 4.5A). However, glutamate-induced Ca^{2+} release in the absence of extracellular Ca^{2+} was significantly reduced in neurons pretreated with L-theanine compared to untreated control neurons, with a significant reduction in peak response and trend towards decrease in A.U.C. (Figure 4.5B).

4.4.4 L-theanine acutely modulates Ca^{2+} release from intracellular stores in primary cortical neurons.

I also wished to determine whether L-theanine treatment could have a more

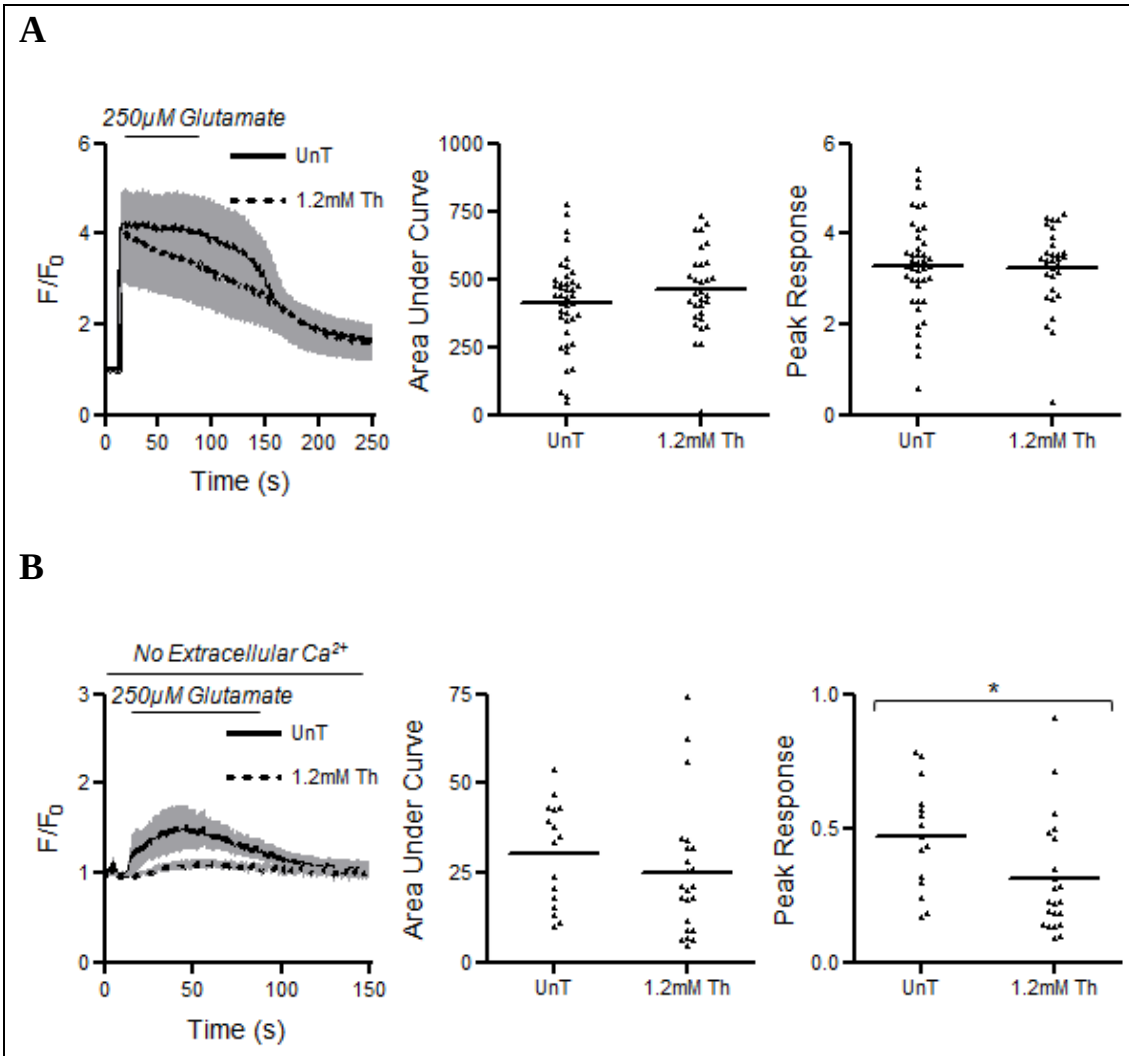

Figure 4.5. L-theanine treatment of primary cortical neurons decreases intracellular Ca^{2+} response to glutamate.

A. Traces taken from a sample experiment for glutamate addition (250 μM for 60 seconds) in the presence of extracellular Ca^{2+} in primary cortical neurons pretreated for 24 hours with 1.2mM L-theanine. Traces represent mean ± s.d. for 16 cells (UnT) and 11 cells (L-theanine). Quantification of the area under the curve (A.U.C.) and the peak Ca^{2+} response was from at least 2 separate runs from at least 3 independent experiments. Scatterplots represent individual values for cells from multiple runs (UnT: 41 cells; L-theanine 31 cells) for A.U.C. and peak Ca^{2+} responses, with the horizontal line representing mean values. **B.** Traces taken from a sample experiment for glutamate addition (250 μM for 60 seconds) in the absence of extracellular Ca^{2+} in primary cortical neurons pretreated for 24 hours with 1.2mM L-theanine. Traces represent mean ± s.d. for 7 cells (UnT) and 8 cells (L-theanine). Quantification of the area under the curve (A.U.C.) and the peak Ca^{2+} response was from at least 2 separate runs from at least 3 independent experiments. Scatterplots represent individual values for cells from multiple runs (UnT: 15 cells; L-theanine 22 cells) for A.U.C. and peak Ca^{2+} responses, with the horizontal line representing mean values. *-$p<0.05$, student's t-test

immediate effect on Ca^{2+} signalling in our neuronal cultures. As such, I pretreated primary cortical neurons for 30 minutes with L-theanine (1.2mM), then stimulated the neurons with glutamate (250µM, 60 seconds) in the continued presence of L-theanine. Similar to what was observed with the 24 hour treatment of L-theanine, acute exposure to L-theanine did not have a significant effect on neuronal Ca^{2+} response to glutamate in the presence of extracellular Ca^{2+} (Figure 4.6A), but did significantly lower both A.U.C. and peak response to glutamate in the absence of extracellular Ca^{2+} (Figure 4.6B).

4.5 Discussion

I have shown that treatment with L-theanine can reduce glutamate induced Ca^{2+} release from intracellular stores in both SH-SY5Y neuroblastoma cells and in mouse primary cortical neurons. No difference in glutamate induced Ca^{2+} signalling was observed in L-theanine treated cells when the experiments were performed in the presence of extracellular Ca^{2+}. Ca^{2+} response to the Ca^{2+}-ionophore ionomycin in the absence of extracellular Ca^{2+} was also reduced. These results suggest that L-theanine treatment reduces Ca^{2+} signalling from the ER, possibly by lowering the total concentration of Ca^{2+} within intracellular stores. It is important to note that for the above experiments, L-theanine was removed from the media before the Ca^{2+} imaging experiments took place, suggesting that L-theanine can alter Ca^{2+} signalling through an action other than direct competitive antagonism of glutamate receptors. However, an acute exposure of neurons to L-theanine, with L-theanine remaining present in the media during all imaging experiments, was also able to reduce Ca^{2+} responses to glutamate

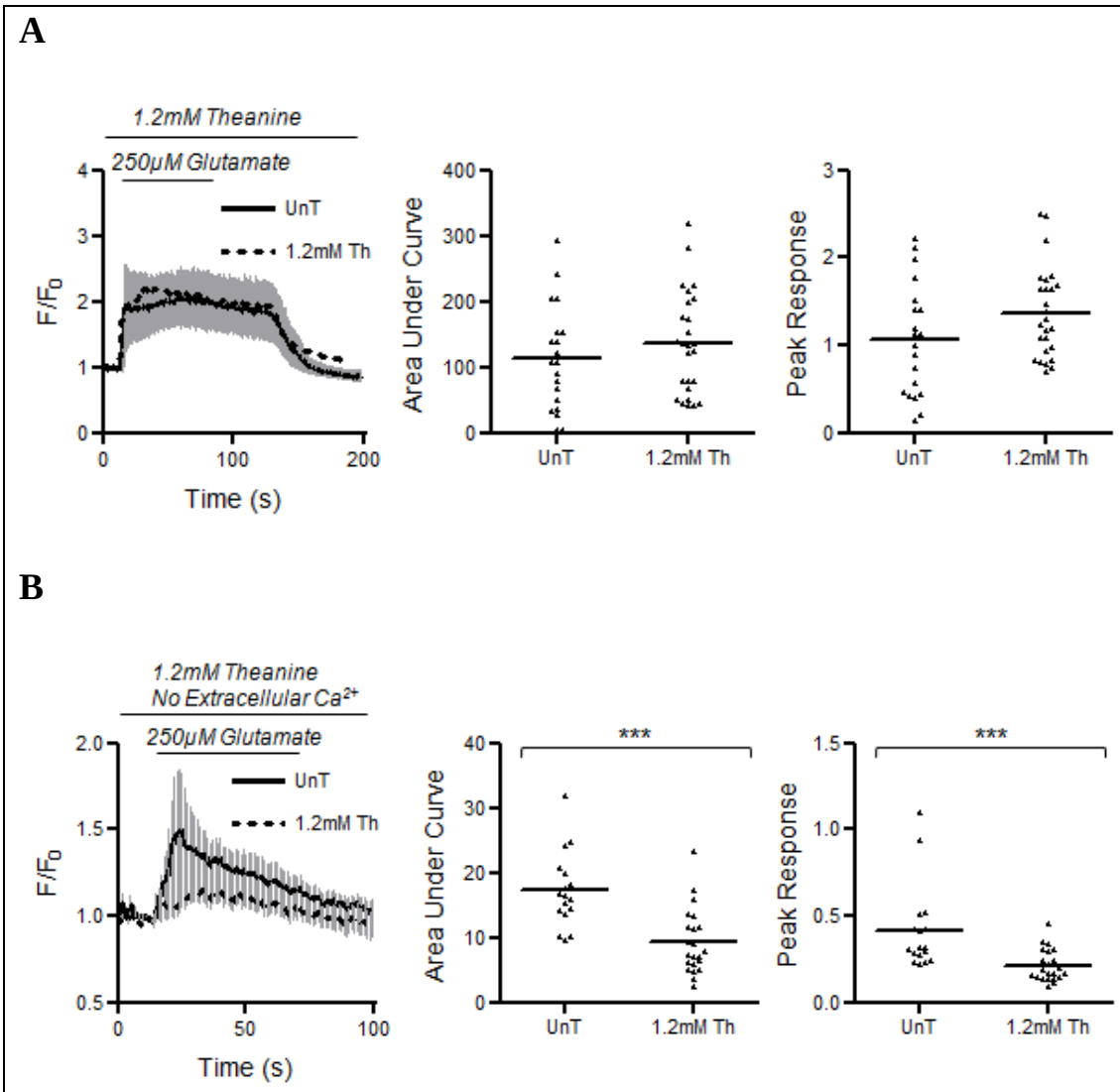

Figure 4.6. Short term L-theanine treatment of primary cortical neurons decreases intracellular Ca^{2+} response to glutamate

A. Traces taken from a sample experiment for glutamate addition (250μM for 60 seconds) in the presence of extracellular Ca^{2+} and 1.2mM L-theanine in primary cortical neurons. Neurons were pretreated for 30 minutes with 1.2mM L-theanine. Traces represent mean ± s.d. for 6 cells (UnT) and 9 cells (L-theanine). Quantification of the area under the curve (A.U.C.) and the peak Ca^{2+} response was from at least 2 separate runs from at least 3 independent experiments. Scatterplots represent individual values for cells from multiple runs (UnT: 20 cells; L-theanine 26 cells) for A.U.C. and peak Ca^{2+} responses, with the horizontal line representing mean values. **B.** Traces taken from a sample experiment for glutamate addition (250μM for 60 seconds) in the absence of extracellular Ca^{2+} and 1.2mM L-theanine in primary cortical neurons. Neurons were pretreated for 30 minutes with 1.2mM L-theanine; Traces represent mean ± s.d. for 6 cells (UnT) and 8 cells (L-theanine). Quantification of the area under the curve (A.U.C.) and the peak Ca^{2+} response was from at least 2 separate runs from at least 3 independent experiments. Scatterplots represent individual values for cells from multiple runs (UnT: 17 cells; L-theanine 22 cells) for A.U.C. and peak Ca^{2+} responses, with the horizontal line representing mean values. ***-$p<0.001$, student's t-test.

in the absence of extracellular Ca^{2+}. Thus it appears that L-theanine can have a rapid effect on Ca^{2+} release from intracellular stores, suggesting that L-theanine can mediate quick alterations in cell signalling or receptor function. It would be interesting in future experiments to examine if the there are rapid modifications of ER Ca^{2+} channel or signalling proteins after L-theanine treatments, such as alterations in phosphorylation state.

The fact that L-theanine can modulate Ca^{2+}-signalling from ER stores makes it a possible preventative tool and therapeutic agent for several neurodegenerative disorders. In addition to ischemic injury, where L-theanine has already been shown to be therapeutically effective in animal models, other possible conditions for which L-theanine may be beneficial include AD and ALS. Ca^{2+}-mediated excitotoxic neuronal injury is implicated in both of these disorders, and disruption on Ca^{2+} signalling from the ER has been shown to be important in AD in particular. It is worth noting that orally administered L-theanine has been shown to cross the blood-brain barrier [272], which is crucial for a compound to be useful as a drug for a neurodegenerative disease. Thus, it would be interesting to determine the effects that a long-term feeding trial of L-theanine would have on disease progression in animal models of these disorders.

In conclusion, both acute and longer term treatment with the green tea compound L-theanine was shown to alter neuronal Ca^{2+} signalling from intracellular stores, and in particular was shown to lower the amount of Ca^{2+} release from ER Ca^{2+} pools. Further studies are required to determine the mechanism by which L-theanine can have these effects on neuronal Ca^{2+} signalling.

Chapter 5

General Discussion

5.1 Summary of findings

This thesis examined disruption of Ca^{2+} signalling in neurodegeneration, and identification of both endogenous and exogenous modulators of neuronal Ca^{2+} signalling. Three specific hypotheses were tested.

The first hypothesis was that *CRT disrupts Ca^{2+} signalling and induces neurodegeneration in AD*. I observed that CRT expression was increased in the cortex of mice expressing a familial AD associated form of mutant APP. This increase in CRT was seen at 12 and 16 weeks of age, which corresponded with the age of plaque deposition and cognitive decline seen in these mice. SH-SY5Y cells exposed to oxidative stress or toxic forms of Aβ also exhibited increased expression of CRT. However, similar treatments on primary cortical neurons failed to induce increases in CRT expression. I next examined the cellular consequences of increased CRT expression due to AD-related stressors in SH-SY5Y, specifically in terms of Ca^{2+} signalling and cell viability. Changes in Ca^{2+} signalling were observed upon exposure of SH-SY5Y cells to Aβ, specifically with increased Ca^{2+} release from ER Ca^{2+} stores through RyRs and decreased carbachol- induced Ca^{2+} release from ER stores. Changes in Ca^{2+} signalling due to knockdown or overexpression of CRT generally did not correspond with what was seen in terms of treatment with Aβ, except for an increase in RyR associated Ca^{2+} responses which was common to both experimental models. Overexpression of CRT also did not significantly alter the susceptibility of SH-SY5Ys to cell death from exposure to oxidative stress or Aβ. Thus, further studies to determine the mechanisms and consequences of increased CRT in AD are required.

The second hypothesis tested was that *XIAP is a modulator of neuronal Ca^{2+} signalling*. I demonstrated that overexpression of XIAP in neurons resulted in widespread reductions in Ca^{2+} signalling from plasma membrane Ca^{2+} channels including VGCC, ROC, and SOC. XIAP also lowered Ca^{2+} signalling from intracellular stores, while resting cytoplasmic Ca^{2+} levels were slightly elevated. Similar effects were seen in XIAP overexpressing astrocytes. The mechanism by which XIAP alters neuronal Ca^{2+} signalling appears to be independent to inhibition of caspase activation. Further studies will be needed to determine the mechanism by which XIAP modulates neuronal Ca^{2+} signalling.

The final hypothesis tested was that *L-theanine is a modulator of neuronal Ca^{2+} signalling*. I demonstrated that pretreatment of neuronal cells with the glutamate receptor antagonist L-theanine lowered intracellular Ca^{2+} signalling in response to glutamate stimulation, but did not appear to have an effect on signalling from plasma membrane glutamate receptors. Both acute and longer treatment with L-theanine had this effect on neuronal Ca^{2+} signalling, suggesting a mechanism independent of new protein synthesis.

5.2 Future considerations

The demonstration that CRT is increased in models of AD adds to the large body of literature demonstrating that there are widespread changes in Ca^{2+}-signalling in AD. It is likely that further studies will show altered levels/functions of other molecules associated with Ca^{2+}-signalling in AD and other neurodegenerative diseases, given the complexity of control of neuronal Ca^{2+} signalling. As the study on the Ca^{2+} modulating

functions of XIAP demonstrates, there are also likely many endogenous molecules/proteins associated with neuronal Ca^{2+}-signalling that are as yet undiscovered. Because disruption of Ca^{2+} signalling is such a prominent feature of many neurodegenerative diseases, it is crucial that we continue to attempt to fully understand both the mechanisms by which neurons regulate Ca^{2+} signalling and also the mechanisms by which this can be disrupted in neurodegenerative diseases.

There are few approved therapeutic strategies targeting alterations in Ca^{2+}-signalling in neurodegenerative disease. For AD, there are two approved drugs that have shown clinical benefits to AD patients that target changes in neuronal Ca^{2+} signalling. One is nimodipine, a blocker of L-type VGCCs [273]. The other is the NMDA receptor antagonist memantine [274]. There is one drug targeting Ca^{2+} approved for treatment of ALS. Riluzole can prevent increases in intracellular Ca^{2+} by blocking VGCC and NMDA receptors and has been shown to be of clinical benefit to ALS patients [161]. These three drugs demonstrate that disruptions in Ca^{2+} signalling are a valid target for treatment of neurodegenerative diseases. It is worth noting that the above mentioned drugs all inhibit Ca^{2+} influx through the plasma membrane. However, alteration of Ca^{2+} signalling from ER stores is also an important aspect of several neurodegenerative diseases. To date, there are no clinically effective drugs for neurodegenerative diseases that target these disruptions in ER Ca^{2+} signalling. This thesis has demonstrated that molecules such as XIAP and L-theanine can effectively modulate ER Ca^{2+} signalling. These and other molecules with similar effects on ER Ca^{2+} signalling may prove to be of therapeutic benefit in neurodegenerative disease. Another important consideration is that

the above mentioned drug therapies function to slow disease progression, but do nothing to treat the underlying cause of the disease. Indeed, these therapies are only employed once significant damage to neurons has already been done [275]. This is why it is crucial that research continues into preventative therapies for neurodegenerative disease that are effective in stopping the initial damage to neurons that occurs in these disease states. Compounds like L-theanine that show little to no toxicity could be administered in a long-term fashion prior to the development of neurodegenerative symptoms in persons at risk of developing neurodegenerative disease. Figure 5.1 illustrates the various aspects of neuronal Ca^{2+} signalling that are disrupted in neurodegenerative disease, and which of these disruptions have the potential to be reversed by therapies involving XIAP or L-Theanine.

Finally, it is also vital to continue studies examining how neuronal Ca^{2+} signals are utilized to control the various aspects of neuronal physiology. Much progress has been made in understanding the role of Ca^{2+} in a wide range of processes including neuronal excitability, synapse plasticity, second messenger signalling, gene transcription, and induction of cell death. Also important are studies concerning how the nature of the neuronal Ca^{2+} signals can differentially affect different neuronal processes. For example, it is now known that factors such as the amplitude, frequency, and subcellular location of Ca^{2+} signals are important in allowing neurons to have very specific control of different Ca^{2+} modulated processes [22]. Determining how a neuron can "decode" these signals is important for the understanding of basic neuronal function and how disruption of these signals can be so damaging to neurons and general brain activity.

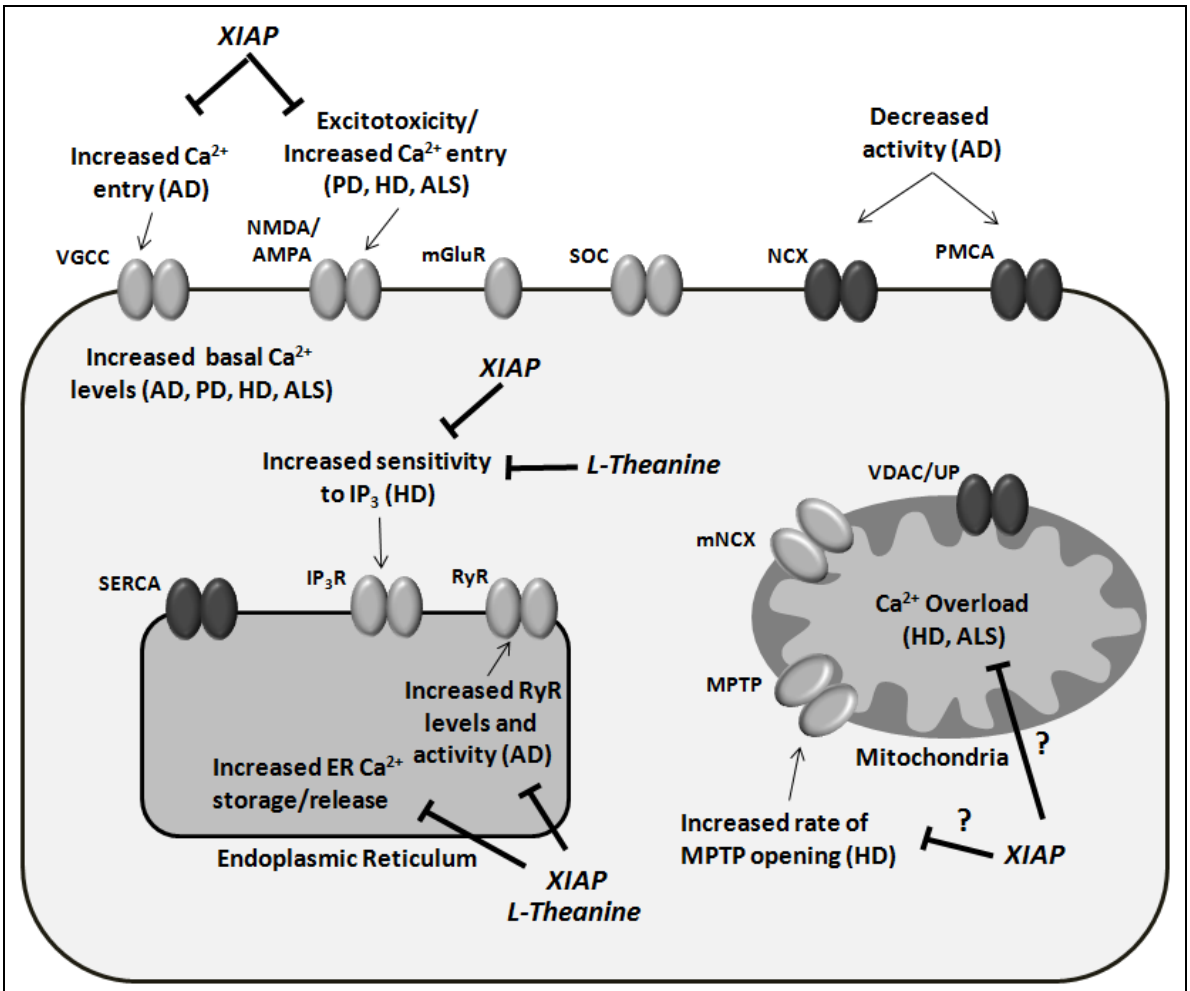

Figure 5.1 Therapeutic targets for XIAP and L-Theanine in neurodegeneration

Several aspects of neuronal Ca^{2+} signaling are disrupted in neurodegenerative diseases such as Alzheimer's disease (AD), Parkinson's disease (PD), Huntington's disease (HD), and Amyotrophic Lateral Sclerosis (ALS). This thesis has demonstrated that both XIAP and L-Theanine modulate neuronal Ca^{2+} signalling and thus may be of potential therapeutic benefit for the prevention and treatment of neurodegenerative disease. For example, XIAP decreases the extent of Ca^{2+} entry into the cytoplasm through several channels. As such, XIAP may be able to protect neurons from increased Ca^{2+} movement through VGCCs and from ER Ca^{2+} overload and increased release from RyR channels in AD, excitotoxicity in PD, HD, and ALS, and increased Ca^{2+} movement through IP_3Rs in HD. L-Theanine was shown to lower the extent of releaseable Ca^{2+} from ER stores, thus may protect neurons from ER Ca^{2+} overload and increased release from RyRs in AD, and and increased Ca^{2+} movement through IP_3Rs in HD. Although not demonstrated in this thesis, XIAP also has the potential to prevent mitochondrial Ca^{2+} overload in HD and ALS, and lower Ca^{2+} release through MPTP, which is overactivated in HD.

This thesis has presented data concerning the role of three molecules, CRT, XIAP, and L-theanine, in the regulation of neuronal Ca^{2+} signalling. While I have determined novel

specific actions of each of these molecules, further studies will be needed to determine their full importance and mechanisms of action in neuronal Ca^{2+} modulated processes.

References

1. Berridge, M.J., P. Lipp, and M.D. Bootman, *The versatility and universality of calcium signalling.* Nat Rev Mol Cell Biol, 2000. **1**(1): p. 11-21.
2. Petersen, O.H., M. Michalak, and A. Verkhratsky, *Calcium signalling: past, present and future.* Cell Calcium, 2005. **38**(3-4): p. 161-9.
3. Jeffs, G.J., et al., *The role of the Na(+)/Ca(2+) exchanger (NCX) in neurons following ischaemia.* J Clin Neurosci, 2007. **14**(6): p. 507-14.
4. Lee, S.L., A.S. Yu, and J. Lytton, *Tissue-specific expression of Na(+)-Ca2+ exchanger isoforms.* J Biol Chem, 1994. **269**(21): p. 14849-52.
5. Philipson, K.D. and D.A. Nicoll, *Sodium-calcium exchange: a molecular perspective.* Annu Rev Physiol, 2000. **62**: p. 111-33.
6. Monteith, G.R., Y. Wanigasekara, and B.D. Roufogalis, *The plasma membrane calcium pump, its role and regulation: new complexities and possibilities.* J Pharmacol Toxicol Methods, 1998. **40**(4): p. 183-90.
7. Blaustein, M.P., et al., *Na/Ca exchanger and PMCA localization in neurons and astrocytes: functional implications.* Ann N Y Acad Sci, 2002. **976**: p. 356-66.
8. Carafoli, E., *Calcium pump of the plasma membrane.* Physiol Rev, 1991. **71**(1): p. 129-53.
9. Greeb, J. and G.E. Shull, *Molecular cloning of a third isoform of the calmodulin-sensitive plasma membrane Ca2+-transporting ATPase that is expressed predominantly in brain and skeletal muscle.* J Biol Chem, 1989. **264**(31): p. 18569-76.

10. Brown, B.J., et al., *Primary structure of human plasma membrane Ca(2+)-ATPase isoform 3.* Biochim Biophys Acta, 1996. **1283**(1): p. 10-3.

11. Keeton, T.P., S.E. Burk, and G.E. Shull, *Alternative splicing of exons encoding the calmodulin-binding domains and C termini of plasma membrane Ca(2+)-ATPase isoforms 1, 2, 3, and 4.* J Biol Chem, 1993. **268**(4): p. 2740-8.

12. Strehler, E.E., et al., *Plasma membrane Ca2+ ATPases as dynamic regulators of cellular calcium handling.* Ann N Y Acad Sci, 2007. **1099**: p. 226-36.

13. Catterall, W.A., et al., *International Union of Pharmacology. XLVIII. Nomenclature and structure-function relationships of voltage-gated calcium channels.* Pharmacol Rev, 2005. **57**(4): p. 411-25.

14. Dolphin, A.C., *Beta subunits of voltage-gated calcium channels.* J Bioenerg Biomembr, 2003. **35**(6): p. 599-620.

15. Dubel, S.J., et al., *Plasma membrane expression of T-type calcium channel alpha(1) subunits is modulated by high voltage-activated auxiliary subunits.* J Biol Chem, 2004. **279**(28): p. 29263-9.

16. Nowycky, M.C., A.P. Fox, and R.W. Tsien, *Three types of neuronal calcium channel with different calcium agonist sensitivity.* Nature, 1985. **316**(6027): p. 440-3.

17. Pessia, M., *Ion channels and electrical activity*, in *Molecular biology of the neuron*, R.W. Davies, and Morris, B.J., Editor. 2004, Oxford University Press: New York. p. 103-137.

18. *Molecular and Functional Diversity of Ion Channels and Receptors. Proceedings of a conference. New York City, New York, USA. May 14-17, 1998.* Ann N Y Acad Sci, 1999. **868**: p. 1-774.

19. Stephenson, F.A., *Structure and trafficking of NMDA and GABAA receptors.* Biochem Soc Trans, 2006. **34**(Pt 5): p. 877-81.

20. Rao, V.R. and S. Finkbeiner, *NMDA and AMPA receptors: old channels, new tricks.* Trends Neurosci, 2007. **30**(6): p. 284-91.

21. Bradley, J., et al., *Splice variants of the NR1 subunit differentially induce NMDA receptor-dependent gene expression.* J Neurosci, 2006. **26**(4): p. 1065-76.

22. Berridge, M.J., *Neuronal calcium signaling.* Neuron, 1998. **21**(1): p. 13-26.

23. Papadia, S., et al., *Nuclear Ca2+ and the cAMP response element-binding protein family mediate a late phase of activity-dependent neuroprotection.* J Neurosci, 2005. **25**(17): p. 4279-87.

24. Zhang, S.J., et al., *Decoding NMDA Receptor Signaling: Identification of Genomic Programs Specifying Neuronal Survival and Death.* Neuron, 2007. **53**(4): p. 549-62.

25. Cull-Candy, S., L. Kelly, and M. Farrant, *Regulation of Ca2+-permeable AMPA receptors: synaptic plasticity and beyond.* Curr Opin Neurobiol, 2006. **16**(3): p. 288-97.

26. Perkinton, M.S., T.S. Sihra, and R.J. Williams, *Ca(2+)-permeable AMPA receptors induce phosphorylation of cAMP response element-binding protein through a phosphatidylinositol 3-kinase-dependent stimulation of the mitogen-*

activated protein kinase signaling cascade in neurons. J Neurosci, 1999. **19**(14): p. 5861-74.

27. Santos, A.E., et al., *Excitotoxicity mediated by Ca2+-permeable GluR4-containing AMPA receptors involves the AP-1 transcription factor.* Cell Death Differ, 2006. **13**(4): p. 652-60.

28. Parekh, A.B. and J.W. Putney, Jr., *Store-operated calcium channels.* Physiol Rev, 2005. **85**(2): p. 757-810.

29. Prakriya, M., et al., *Orai1 is an essential pore subunit of the CRAC channel.* Nature, 2006. **443**(7108): p. 230-3.

30. Yeromin, A.V., et al., *Molecular identification of the CRAC channel by altered ion selectivity in a mutant of Orai.* Nature, 2006. **443**(7108): p. 226-9.

31. Vig, M., et al., *CRACM1 multimers form the ion-selective pore of the CRAC channel.* Curr Biol, 2006. **16**(20): p. 2073-9.

32. Liou, J., et al., *STIM is a Ca2+ sensor essential for Ca2+-store-depletion-triggered Ca2+ influx.* Curr Biol, 2005. **15**(13): p. 1235-41.

33. Roos, J., et al., *STIM1, an essential and conserved component of store-operated Ca2+ channel function.* J Cell Biol, 2005. **169**(3): p. 435-45.

34. Lewis, R.S., *The molecular choreography of a store-operated calcium channel.* Nature, 2007. **446**(7133): p. 284-7.

35. Nakanishi, S., et al., *Glutamate receptors: brain function and signal transduction.* Brain Res Brain Res Rev, 1998. **26**(2-3): p. 230-5.

36. Terasaki, M., et al., *Continuous network of endoplasmic reticulum in cerebellar Purkinje neurons.* Proc Natl Acad Sci U S A, 1994. **91**(16): p. 7510-4.

37. Parys, J.B., et al., *Regulation of inositol 1,4,5-triphosphate-induced Ca^{2+} release by Ca^{2+}*, in *Calcium: The molecular basis of calcium action in biology and medicine,* R. Pochet, Editor. 2000, Kluwer Academic Publishers: Dordrecht. p. 179-190.

38. Sharp, A.H., et al., *Differential immunohistochemical localization of inositol 1,4,5-trisphosphate- and ryanodine-sensitive Ca2+ release channels in rat brain.* J Neurosci, 1993. **13**(7): p. 3051-63.

39. Finch, E.A., T.J. Turner, and S.M. Goldin, *Calcium as a coagonist of inositol 1,4,5-trisphosphate-induced calcium release.* Science, 1991. **252**(5004): p. 443-6.

40. Tanimura, A. and R.J. Turner, *Calcium release in HSY cells conforms to a steady-state mechanism involving regulation of the inositol 1,4,5-trisphosphate receptor Ca2+ channel by luminal [Ca2+]*. J Cell Biol, 1996. **132**(4): p. 607-16.

41. Zucchi, R. and S. Ronca-Testoni, *The sarcoplasmic reticulum Ca2+ channel/ryanodine receptor: modulation by endogenous effectors, drugs and disease states.* Pharmacol Rev, 1997. **49**(1): p. 1-51.

42. McPherson, P.S. and K.P. Campbell, *Characterization of the major brain form of the ryanodine receptor/Ca2+ release channel.* J Biol Chem, 1993. **268**(26): p. 19785-90.

43. Rossi, D., et al., *Ryanodine-sensitive calcium release channels*, in *Calcium: The molecular basis of calcium action in biology and medicine*, R. Pochet, Editor. 2000, Kluwer Academic Publishers: Dordrecht. p. 205-219.

44. Selkoe, D.J. and M.S. Wolfe, *Presenilin: running with scissors in the membrane.* Cell, 2007. **131**(2): p. 215-21.

45. Tu, H., et al., *Presenilins form ER Ca2+ leak channels, a function disrupted by familial Alzheimer's disease-linked mutations.* Cell, 2006. **126**(5): p. 981-93.

46. Misquitta, C.M., D.P. Mack, and A.K. Grover, *Sarco/endoplasmic reticulum Ca2+ (SERCA)-pumps: link to heart beats and calcium waves.* Cell Calcium, 1999. **25**(4): p. 277-90.

47. Brandl, C.J., et al., *Adult forms of the Ca2+ATPase of sarcoplasmic reticulum. Expression in developing skeletal muscle.* J Biol Chem, 1987. **262**(8): p. 3768-74.

48. Grover, A.K. and I. Khan, *Calcium pump isoforms: diversity, selectivity and plasticity. Review article.* Cell Calcium, 1992. **13**(1): p. 9-17.

49. Wu, K.D., et al., *Localization and quantification of endoplasmic reticulum Ca(2+)-ATPase isoform transcripts.* Am J Physiol, 1995. **269**(3 Pt 1): p. C775-84.

50. Chang, D.T. and I.J. Reynolds, *Mitochondrial trafficking and morphology in healthy and injured neurons.* Prog Neurobiol, 2006. **80**(5): p. 241-68.

51. Nicholls, D.G., et al., *Interactions between mitochondrial bioenergetics and cytoplasmic calcium in cultured cerebellar granule cells.* Cell Calcium, 2003. **34**(4-5): p. 407-24.

52. Rizzuto, R. and T. Pozzan, *Microdomains of intracellular Ca2+: molecular determinants and functional consequences.* Physiol Rev, 2006. **86**(1): p. 369-408.

53. Gincel, D., H. Zaid, and V. Shoshan-Barmatz, *Calcium binding and translocation by the voltage-dependent anion channel: a possible regulatory mechanism in mitochondrial function.* Biochem J, 2001. **358**(Pt 1): p. 147-55.

54. Cesar Mde, C. and J.E. Wilson, *All three isoforms of the voltage-dependent anion channel (VDAC1, VDAC2, and VDAC3) are present in mitochondria from bovine, rabbit, and rat brain.* Arch Biochem Biophys, 2004. **422**(2): p. 191-6.

55. Lemasters, J.J. and E. Holmuhamedov, *Voltage-dependent anion channel (VDAC) as mitochondrial governator--thinking outside the box.* Biochim Biophys Acta, 2006. **1762**(2): p. 181-90.

56. Kirichok, Y., G. Krapivinsky, and D.E. Clapham, *The mitochondrial calcium uniporter is a highly selective ion channel.* Nature, 2004. **427**(6972): p. 360-4.

57. Hajnoczky, G., et al., *Mitochondrial calcium signalling and cell death: approaches for assessing the role of mitochondrial Ca2+ uptake in apoptosis.* Cell Calcium, 2006. **40**(5-6): p. 553-60.

58. Gunter, K.K. and T.E. Gunter, *Transport of calcium by mitochondria.* J Bioenerg Biomembr, 1994. **26**(5): p. 471-85.

59. Nicholls, D.G. and I.D. Scott, *The regulation of brain mitochondrial calcium-ion transport. The role of ATP in the discrimination between kinetic and membrane-potential-dependent calcium-ion efflux mechanisms.* Biochem J, 1980. **186**(3): p. 833-9.

60. Wang, G.J. and S.A. Thayer, *Sequestration of glutamate-induced Ca2+ loads by mitochondria in cultured rat hippocampal neurons.* J Neurophysiol, 1996. **76**(3): p. 1611-21.

61. Kim, B. and S. Matsuoka, *Mitochondrial Ca2+ flux through Na+/Ca2+ exchange.* Ann N Y Acad Sci, 2007. **1099**: p. 507-11.

62. Carafoli, E., et al., *The release of calcium from heart mitochondria by sodium.* J Mol Cell Cardiol, 1974. **6**(4): p. 361-71.

63. Wingrove, D.E. and T.E. Gunter, *Kinetics of mitochondrial calcium transport. I. Characteristics of the sodium-independent calcium efflux mechanism of liver mitochondria.* J Biol Chem, 1986. **261**(32): p. 15159-65.

64. Bernardi, P., *Mitochondrial transport of cations: channels, exchangers, and permeability transition.* Physiol Rev, 1999. **79**(4): p. 1127-55.

65. Massari, S. and G.F. Azzone, *The equivalent pore radius of intact and damaged mitochondria and the mechanism of active shrinkage.* Biochim Biophys Acta, 1972. **283**(1): p. 23-9.

66. Crompton, M., *The mitochondrial permeability transition pore and its role in cell death.* Biochem J, 1999. **341 (Pt 2)**: p. 233-49.

67. Brustovetsky, N., et al., *Calcium-induced cytochrome c release from CNS mitochondria is associated with the permeability transition and rupture of the outer membrane.* J Neurochem, 2002. **80**(2): p. 207-18.

68. Schmidt, H., et al., *Mutational analysis of dendritic Ca2+ kinetics in rodent Purkinje cells: role of parvalbumin and calbindin D28k.* J Physiol, 2003. **551**(Pt 1): p. 13-32.

69. Celio, M.R., *Calbindin D-28k and parvalbumin in the rat nervous system.* Neuroscience, 1990. **35**(2): p. 375-475.

70. Gelebart, P., M. Opas, and M. Michalak, *Calreticulin, a Ca2+-binding chaperone of the endoplasmic reticulum.* Int J Biochem Cell Biol, 2005. **37**(2): p. 260-6.

71. Lancaster, B. and P.R. Adams, *Calcium-dependent current generating the afterhyperpolarization of hippocampal neurons.* J Neurophysiol, 1986. **55**(6): p. 1268-82.

72. Sah, P., *Role of calcium influx and buffering in the kinetics of Ca(2+)-activated K+ current in rat vagal motoneurons.* J Neurophysiol, 1992. **68**(6): p. 2237-47.

73. Ishii, Y., T. Kawai, and M. Watanabe, *Inhibitory effects of cyclopiazonic acid on the spike after-hyperpolarization in rat sympathetic neurons.* Jpn J Pharmacol, 1992. **58**(4): p. 451-6.

74. Fujimoto, S., et al., *Calcium localization in the sympathetic ganglion of the bullfrog and effects of caffeine.* Brain Res, 1980. **202**(1): p. 21-32.

75. Tzingounis, A.V., et al., *Hippocalcin gates the calcium activation of the slow afterhyperpolarization in hippocampal pyramidal cells.* Neuron, 2007. **53**(4): p. 487-93.

76. Hashimoto, T., T. Ishii, and H. Ohmori, *Release of Ca2+ is the crucial step for the potentiation of IPSCs in the cultured cerebellar Purkinje cells of the rat.* J Physiol, 1996. **497 (Pt 3)**: p. 611-27.

77. Staple, J., and Catsicas, S., *Molecular biology of neurotransmitter release*, in *Molecular biology of the neuron*, R.W. Davies, and Morris, B.J., Editor. 2004, Oxford University Press: New York. p. 140-163.

78. O'Connor, V., G.J. Augustine, and H. Betz, *Synaptic vesicle exocytosis: molecules and models.* Cell, 1994. **76**(5): p. 785-7.

79. Sutton, R.B., et al., *Crystal structure of a SNARE complex involved in synaptic exocytosis at 2.4 A resolution.* Nature, 1998. **395**(6700): p. 347-53.

80. Yoshihara, M. and J.T. Littleton, *Synaptotagmin I functions as a calcium sensor to synchronize neurotransmitter release.* Neuron, 2002. **36**(5): p. 897-908.

81. Emptage, N.J., C.A. Reid, and A. Fine, *Calcium stores in hippocampal synaptic boutons mediate short-term plasticity, store-operated Ca2+ entry, and spontaneous transmitter release.* Neuron, 2001. **29**(1): p. 197-208.

82. Bliss, T.V. and G.L. Collingridge, *A synaptic model of memory: long-term potentiation in the hippocampus.* Nature, 1993. **361**(6407): p. 31-9.

83. Morris, B.J., *Neuronal plasticity*, in *Molecular biology of the neuron*, R.W. Davies, and Morris, B.J., Editor. 2004, Oxford University Press: New York. p. 353-382.

84. Malenka, R.C. and M.F. Bear, *LTP and LTD: an embarrassment of riches.* Neuron, 2004. **44**(1): p. 5-21.

85. Xia, Z. and D.R. Storm, *The role of calmodulin as a signal integrator for synaptic plasticity.* Nat Rev Neurosci, 2005. **6**(4): p. 267-76.

86. LaPorte, D.C., B.M. Wierman, and D.R. Storm, *Calcium-induced exposure of a hydrophobic surface on calmodulin.* Biochemistry, 1980. **19**(16): p. 3814-9.

87. Barria, A., et al., *Regulatory phosphorylation of AMPA-type glutamate receptors by CaM-KII during long-term potentiation.* Science, 1997. **276**(5321): p. 2042-5.

88. Lisman, J.E. and A.M. Zhabotinsky, *A model of synaptic memory: a CaMKII/PP1 switch that potentiates transmission by organizing an AMPA receptor anchoring assembly.* Neuron, 2001. **31**(2): p. 191-201.

89. Plant, K., et al., *Transient incorporation of native GluR2-lacking AMPA receptors during hippocampal long-term potentiation.* Nat Neurosci, 2006. **9**(5): p. 602-4.

90. Matsuzaki, M., et al., *Structural basis of long-term potentiation in single dendritic spines.* Nature, 2004. **429**(6993): p. 761-6.

91. Atkins, C.M., et al., *Cytoplasmic polyadenylation element binding protein-dependent protein synthesis is regulated by calcium/calmodulin-dependent protein kinase II.* J Neurosci, 2004. **24**(22): p. 5193-201.

92. Impey, S., et al., *Cross talk between ERK and PKA is required for Ca2+ stimulation of CREB-dependent transcription and ERK nuclear translocation.* Neuron, 1998. **21**(4): p. 869-83.

93. Montminy, M.R. and L.M. Bilezikjian, *Binding of a nuclear protein to the cyclic-AMP response element of the somatostatin gene.* Nature, 1987. **328**(6126): p. 175-8.

94. Finkbeiner, S. and M.E. Greenberg, *Ca2+ channel-regulated neuronal gene expression.* J Neurobiol, 1998. **37**(1): p. 171-89.

95. Silva, A.J., et al., *CREB and memory.* Annu Rev Neurosci, 1998. **21**: p. 127-48.

96. Walton, M.R. and I. Dragunow, *Is CREB a key to neuronal survival?* Trends Neurosci, 2000. **23(**2): p. 48-53.

97. Bading, H. and M.E. Greenberg, *Stimulation of protein tyrosine phosphorylation by NMDA receptor activation.* Science, 1991. **253**(5022): p. 912-4.

98. Rosen, L.B., et al., *Membrane depolarization and calcium influx stimulate MEK and MAP kinase via activation of Ras.* Neuron, 1994. **12**(6): p. 1207-21.

99. Hardingham, G.E., *Synapse-to-nucleus calcium signalling*, in *Molecular biology of the neuron*, R.W. Davies, and Morris, B.J., Editor. 2004, Oxford University Press: New York. p. 249-269.

100. Kang, H., et al., *An important role of neural activity-dependent CaMKIV signaling in the consolidation of long-term memory.* Cell, 2001. **106**(6): p. 771-83.

101. Ho, N., et al., *Impaired synaptic plasticity and cAMP response element-binding protein activation in Ca2+/calmodulin-dependent protein kinase type IV/Gr-deficient mice.* J Neurosci, 2000. **20**(17): p. 6459-72.

102. Ribar, T.J., et al., *Cerebellar defects in Ca2+/calmodulin kinase IV-deficient mice.* J Neurosci, 2000. **20(**22): p. RC107.

103. Impey, S., et al., *Phosphorylation of CBP mediates transcriptional activation by neural activity and CaM kinase IV.* Neuron, 2002. **34**(2): p. 235-44.

104. Ginty, D.D., A. Bonni, and M.E. Greenberg, *Nerve growth factor activates a Ras-dependent protein kinase that stimulates c-fos transcription via phosphorylation of CREB.* Cell, 1994. **77**(5): p. 713-25.

105. Beattie, E.C., et al., *Regulation of AMPA receptor endocytosis by a signaling mechanism shared with LTD.* Nat Neurosci, 2000. **3**(12): p. 1291-300.

106. Massey, P.V. and Z.I. Bashir, *Long-term depression: multiple forms and implications for brain function.* Trends Neurosci, 2007. **30**(4): p. 176-84.

107. Mackenzie, G.G. and P.I. Oteiza, *Zinc and the cytoskeleton in the neuronal modulation of transcription factor NFAT.* J Cell Physiol, 2007. **210**(1): p. 246-56.

108. Pongs, O., et al., *Frequenin--a novel calcium-binding protein that modulates synaptic efficacy in the Drosophila nervous system.* Neuron, 1993. **11**(1): p. 15-28.

109. Gomez, M., et al., *Ca2+ signaling via the neuronal calcium sensor-1 regulates associative learning and memory in C. elegans.* Neuron, 2001. **30**(1): p. 241-8.

110. Sippy, T., et al., *Acute changes in short-term plasticity at synapses with elevated levels of neuronal calcium sensor-1.* Nat Neurosci, 2003. **6**(10): p. 1031-8.

111. Weiss, J.L., D.A. Archer, and R.D. Burgoyne, *Neuronal Ca2+ sensor-1/frequenin functions in an autocrine pathway regulating Ca2+ channels in bovine adrenal chromaffin cells.* J Biol Chem, 2000. **275**(51): p. 40082-7.

112. Tsujimoto, T., et al., *Neuronal calcium sensor 1 and activity-dependent facilitation of P/Q-type calcium currents at presynaptic nerve terminals.* Science, 2002. **295**(5563): p. 2276-9.

113. Hui, H., et al., *Calcium-sensing mechanism in TRPC5 channels contributing to retardation of neurite outgrowth.* J Physiol, 2006. **572**(Pt 1): p. 165-72.

114. Nakamura, T.Y., et al., *Novel role of neuronal Ca2+ sensor-1 as a survival factor up-regulated in injured neurons.* J Cell Biol, 2006. **172**(7): p. 1081-91.

115. Kobayashi, M., et al., *Hippocalcin-deficient mice display a defect in cAMP response element-binding protein activation associated with impaired spatial and associative memory.* Neuroscience, 2005. **133**(2): p. 471-84.

116. Palmer, C.L., et al., *Hippocalcin functions as a calcium sensor in hippocampal LTD.* Neuron, 2005. **47**(4): p. 487-94.

117. Mercer, E.A., et al., *NAIP interacts with hippocalcin and protects neurons against calcium-induced cell death through caspase-3-dependent and -independent pathways.* Embo J, 2000. **19**(14): p. 3597-607.

118. Burgoyne, R.D., *Neuronal calcium sensor proteins: generating diversity in neuronal Ca2+ signalling.* Nat Rev Neurosci, 2007. **8**(3): p. 182-93.

119. Kasri, N.N., et al., *Regulation of InsP3 receptor activity by neuronal Ca2+-binding proteins.* Embo J, 2004. **23**(2): p. 312-21.

120. Zhou, H., et al., *Ca2+-binding protein-1 facilitates and forms a postsynaptic complex with Cav1.2 (L-type) Ca2+ channels.* J Neurosci, 2004. **24**(19): p. 4698-708.

121. Lee, A., et al., *Differential modulation of Ca(v)2.1 channels by calmodulin and Ca2+-binding protein 1.* Nat Neurosci, 2002. **5**(3): p. 210-7.

122. Orrenius, S., B. Zhivotovsky, and P. Nicotera, *Regulation of cell death: the calcium-apoptosis link.* Nat Rev Mol Cell Biol, 2003. **4**(7): p. 552-65.

123. Choi, D.W., *Excitotoxic cell death.* J Neurobiol, 1992. **23**(9): p. 1261-76.

124. Waxman, E.A. and D.R. Lynch, *N-methyl-D-aspartate receptor subtypes: multiple roles in excitotoxicity and neurological disease.* Neuroscientist, 2005. **11**(1): p. 37-49.

125. Kruman, I., Q. Guo, and M.P. Mattson, *Calcium and reactive oxygen species mediate staurosporine-induced mitochondrial dysfunction and apoptosis in PC12 cells.* J Neurosci Res, 1998. **51**(3): p. 293-308.

126. Khan, A.A., et al., *Lymphocyte apoptosis: mediation by increased type 3 inositol 1,4,5-trisphosphate receptor.* Science, 1996. **273**(5274): p. 503-7.

127. Kaufman, R.J., *Orchestrating the unfolded protein response in health and disease.* J Clin Invest, 2002. **110**(10): p. 1389-98.

128. Pahl, H.L. and P.A. Baeuerle, *The ER-overload response: activation of NF-kappa B.* Trends Biochem Sci, 1997. **22**(2): p. 63-7.

129. Ferri, K.F. and G. Kroemer, *Organelle-specific initiation of cell death pathways.* Nat Cell Biol, 2001. **3**(11): p. E255-63.

130. Johnson, S., et al., *The ins and outs of calreticulin: from the ER lumen to the extracellular space.* Trends Cell Biol, 2001. **11**(3): p. 122-9.

131. Korge, P. and J.N. Weiss, *Thapsigargin directly induces the mitochondrial permeability transition.* Eur J Biochem, 1999. **265**(1): p. 273-80.

132. Kroemer, G., B. Dallaporta, and M. Resche-Rigon, *The mitochondrial death/life regulator in apoptosis and necrosis.* Annu Rev Physiol, 1998. **60**: p. 619-42.

133. Kroemer, G. and J.C. Reed, *Mitochondrial control of cell death.* Nat Med, 2000. **6**(5): p. 513-9.

134. Li, P., et al., *Cytochrome c and dATP-dependent formation of Apaf-1/caspase-9 complex initiates an apoptotic protease cascade.* Cell, 1997. **91**(4): p. 479-89.

135. Raynaud, F. and A. Marcilhac, *Implication of calpain in neuronal apoptosis. A possible regulation of Alzheimer's disease.* Febs J, 2006. **273**(15): p. 3437-43.

136. Christakos, S., et al., *Activation of programmed cell death by calcium: Protection against cell death by the calcium binding protein, calbindin-D_{28k},* in *Calcium: The molecular basis of calcium action in biology and medicine*, R. Pochet, Editor. 2000, Kluwer Academic Publishers: Dordrecht. p. 259-275.

137. Wang, H.G., et al., *Ca2+-induced apoptosis through calcineurin dephosphorylation of BAD.* Science, 1999. **284**(5412): p. 339-43.

138. Szabadkai, G. and R. Rizzuto, *Participation of endoplasmic reticulum and mitochondrial calcium handling in apoptosis: more than just neighborhood?* FEBS Lett, 2004. **567**(1): p. 111-5.

139. Kettenmann, H.a.R., B.R., *Neuroglia*. 2nd ed. 2005, New York: Oxford University Press.

140. Perea, G. and A. Araque, *Glial calcium signaling and neuron-glia communication.* Cell Calcium, 2005. **38**(3-4): p. 375-82.

141. Araque, A., G. Carmignoto, and P.G. Haydon, *Dynamic signaling between astrocytes and neurons.* Annu Rev Physiol, 2001. **63**: p. 795-813.

142. Cotrina, M.L., Nedergaard, N, *Intracellular calcium control mechanisms in glia*. 2nd ed. Neuroglia, ed. B.R. H. Kettenman. 2005, New York: Oxford University Press. pp. 229-239.

143. Porter, J.T. and K.D. McCarthy, *Astrocytic neurotransmitter receptors in situ and in vivo.* Prog Neurobiol, 1997. **51**(4): p. 439-55.

144. Deitmer, J.W., A.J. Verkhratsky, and C. Lohr, *Calcium signalling in glial cells.* Cell Calcium, 1998. **24**(5-6): p. 405-16.

145. Araque, A. and G. Perea, *Glial modulation of synaptic transmission in culture.* Glia, 2004. **47**(3): p. 241-8.

146. Erickson, C.A. and C.A. Barnes, *The neurobiology of memory changes in normal aging.* Exp Gerontol, 2003. **38**(1-2): p. 61-9.

147. Toescu, E.C. and A. Verkhratsky, *The importance of being subtle: small changes in calcium homeostasis control cognitive decline in normal aging.* Aging Cell, 2007. **6**(3): p. 267-73.

148. Kirischuk, S., et al., *Age-associated changes of cytoplasmic calcium homeostasis in cerebellar granule neurons in situ: investigation on thin cerebellar slices.* Exp Gerontol, 1996. **31**(4): p. 475-87.

149. Thibault, O. and P.W. Landfield, *Increase in single L-type calcium channels in hippocampal neurons during aging.* Science, 1996. **272**(5264): p. 1017-20.

150. Murchison, D., D.C. Zawieja, and W.H. Griffith, *Reduced mitochondrial buffering of voltage-gated calcium influx in aged rat basal forebrain neurons.* Cell Calcium, 2004. **36**(1): p. 61-75.

151. Toescu, E.C. and A. Verkhratsky, *Neuronal ageing from an intraneuronal perspective: roles of endoplasmic reticulum and mitochondria.* Cell Calcium, 2003. **34**(4-5): p. 311-23.

152. Toescu, E.C., A. Verkhratsky, and P.W. Landfield, *Ca2+ regulation and gene expression in normal brain aging.* Trends Neurosci, 2004. **27**(10): p. 614-20.

153. Zaidi, A., et al., *Age-related decrease in brain synaptic membrane Ca2+-ATPase in F344/BNF1 rats.* Neurobiol Aging, 1998. **19**(5): p. 487-95.

154. Mattson, M.P., *Calcium and neurodegeneration.* Aging Cell, 2007. **6**(3): p. 337-50.

155. Yankner, B.A., *Mechanisms of neuronal degeneration in Alzheimer's disease.* Neuron, 1996. **16**(5): p. 921-32.

156. Mattson, M.P., *Pathways towards and away from Alzheimer's disease.* Nature, 2004. **430**(7000): p. 631-9.

157. Wolfe, M.S. and S.Y. Guenette, *APP at a glance.* J Cell Sci, 2007. **120**(Pt 18): p. 3157-61.

158. Murray, F.E., et al., *Elemental analysis of neurofibrillary tangles in Alzheimer's disease using proton-induced X-ray analysis.* Ciba Found Symp, 1992. **169**: p. 201-10; discussion 210-6.

159. Nixon, R.A., et al., *Calcium-activated neutral proteinase (calpain) system in aging and Alzheimer's disease.* Ann N Y Acad Sci, 1994. **747**: p. 77-91.

160. Grynspan, F., et al., *Active site-directed antibodies identify calpain II as an early-appearing and pervasive component of neurofibrillary pathology in Alzheimer's disease.* Brain Res, 1997. **763**(2): p. 145-58.

161. Johnson, G.V., et al., *Transglutaminase activity is increased in Alzheimer's disease brain.* Brain Res, 1997. **751**(2): p. 323-9.

162. Kelliher, M., et al., *Alterations in the ryanodine receptor calcium release channel correlate with Alzheimer's disease neurofibrillary and beta-amyloid pathologies.* Neuroscience, 1999. **92**(2): p. 499-513.

163. Hensley, K., et al., *A model for beta-amyloid aggregation and neurotoxicity based on free radical generation by the peptide: relevance to Alzheimer disease.* Proc Natl Acad Sci U S A, 1994. **91**(8): p. 3270-4.

164. Mark, R.J., et al., *Amyloid beta-peptide impairs ion-motive ATPase activities: evidence for a role in loss of neuronal Ca2+ homeostasis and cell death.* J Neurosci, 1995. **15**(9): p. 6239-49.

165. Mark, R.J., et al., *Amyloid beta-peptide impairs glucose transport in hippocampal and cortical neurons: involvement of membrane lipid peroxidation.* J Neurosci, 1997. **17**(3): p. 1046-54.

166. Mattson, M.P., *Calcium and neurodegeneration.* Aging Cell, 2007. **6**(3): p. 337-50.

167. Price, S.A., B. Held, and H.A. Pearson, *Amyloid beta protein increases Ca2+ currents in rat cerebellar granule neurones.* Neuroreport, 1998. **9**(3): p. 539-45.

168. Stutzmann, G.E., et al., *Dysregulated IP3 signaling in cortical neurons of knock-in mice expressing an Alzheimer's-linked mutation in presenilin1 results in exaggerated Ca2+ signals and altered membrane excitability.* J Neurosci, 2004. **24**(2): p. 508-13.

169. Guo, Q., et al., *Alzheimer's presenilin mutation sensitizes neural cells to apoptosis induced by trophic factor withdrawal and amyloid beta-peptide: involvement of calcium and oxyradicals.* J Neurosci, 1997. **17**(11): p. 4212-22.

170. Chan, S.L., et al., *Presenilin-1 mutations increase levels of ryanodine receptors and calcium release in PC12 cells and cortical neurons.* J Biol Chem, 2000. **275**(24): p. 18195-200.

171. Smith, I.F., et al., *Enhanced caffeine-induced Ca2+ release in the 3xTg-AD mouse model of Alzheimer's disease.* J Neurochem, 2005. **94**(6): p. 1711-8.

172. Stutzmann, G.E., et al., *Enhanced ryanodine-mediated calcium release in mutant PS1-expressing Alzheimer's mouse models.* Ann N Y Acad Sci, 2007. **1097**: p. 265-77.

173. Supnet, C., et al., *Amyloid-beta-(1-42) increases ryanodine receptor-3 expression and function in neurons of TgCRND8 mice.* J Biol Chem, 2006. **281**(50): p. 38440-7.

174. Haughey, N.J. and M.P. Mattson, *Alzheimer's amyloid beta-peptide enhances ATP/gap junction-mediated calcium-wave propagation in astrocytes.* Neuromolecular Med, 2003. **3**(3): p. 173-80.

175. DeKosky, S.T., S.W. Scheff, and S.D. Styren, *Structural correlates of cognition in dementia: quantification and assessment of synapse change.* Neurodegeneration, 1996. **5**(4): p. 417-21.

176. Begley, J.G., et al., *Altered calcium homeostasis and mitochondrial dysfunction in cortical synaptic compartments of presenilin-1 mutant mice.* J Neurochem, 1999. **72**(3): p. 1030-9.

177. Barrow, P.A., et al., *Functional phenotype in transgenic mice expressing mutant human presenilin-1.* Neurobiol Dis, 2000. **7**(2): p. 119-26.

178. Greenamyre, J.T. and T.G. Hastings, *Biomedicine. Parkinson's--divergent causes, convergent mechanisms.* Science, 2004. **304**(5674): p. 1120-2.

179. Moore, D.J., et al., *Molecular pathophysiology of Parkinson's disease.* Annu Rev Neurosci, 2005. **28**: p. 57-87.

180. Polymeropoulos, M.H., et al., *Mutation in the alpha-synuclein gene identified in families with Parkinson's disease.* Science, 1997. **276**(5321): p. 2045-7.

181. Beal, M.F., *Excitotoxicity and nitric oxide in Parkinson's disease pathogenesis.* Ann Neurol, 1998. **44**(3 Suppl 1): p. S110-4.

182. Mouatt-Prigent, A., Y. Agid, and E.C. Hirsch, *Does the calcium binding protein calretinin protect dopaminergic neurons against degeneration in Parkinson's disease?* Brain Res, 1994. **668**(1-2): p. 62-70.

183. Yamada, T., et al., *Relative sparing in Parkinson's disease of substantia nigra dopamine neurons containing calbindin-D28K.* Brain Res, 1990. **526**(2): p. 303-7.

184. Furukawa, K., et al., *Plasma membrane ion permeability induced by mutant alpha-synuclein contributes to the degeneration of neural cells.* J Neurochem, 2006. **97**(4): p. 1071-7.

185. Walker, F.O., *Huntington's disease.* Lancet, 2007. **369**(9557): p. 218-28.

186. *A novel gene containing a trinucleotide repeat that is expanded and unstable on Huntington's disease chromosomes. The Huntington's Disease Collaborative Research Group.* Cell, 1993. **72**(6): p. 971-83.

187. Ross, C.A., *Polyglutamine pathogenesis: emergence of unifying mechanisms for Huntington's disease and related disorders.* Neuron, 2002. **35**(5): p. 819-22.

188. Bezprozvanny, I. and M.R. Hayden, *Deranged neuronal calcium signaling and Huntington disease.* Biochem Biophys Res Commun, 2004. **322**(4): p. 1310-7.

189. Panov, A.V., et al., *Early mitochondrial calcium defects in Huntington's disease are a direct effect of polyglutamines.* Nat Neurosci, 2002. **5**(8): p. 731-6.

190. Hodgson, J.G., et al., *A YAC mouse model for Huntington's disease with full-length mutant huntingtin, cytoplasmic toxicity, and selective striatal neurodegeneration.* Neuron, 1999. **23**(1): p. 181-92.

191. Oliveira, J.M., et al., *Mitochondrial dysfunction in Huntington's disease: the bioenergetics of isolated and in situ mitochondria from transgenic mice.* J Neurochem, 2007. **101**(1): p. 241-9.

192. Zeron, M.M., et al., *Increased sensitivity to N-methyl-D-aspartate receptor-mediated excitotoxicity in a mouse model of Huntington's disease.* Neuron, 2002. **33**(6): p. 849-60.

193. Zeron, M.M., et al., *Potentiation of NMDA receptor-mediated excitotoxicity linked with intrinsic apoptotic pathway in YAC transgenic mouse model of Huntington's disease.* Mol Cell Neurosci, 2004. **25**(3): p. 469-79.

194. Tang, T.S., et al., *Huntingtin and huntingtin-associated protein 1 influence neuronal calcium signaling mediated by inositol-(1,4,5) triphosphate receptor type 1.* Neuron, 2003. **39**(2): p. 227-39.

195. Rowland, L.P. and N.A. Shneider, *Amyotrophic lateral sclerosis.* N Engl J Med, 2001. **344**(22): p. 1688-700.

196. Heath, P.R. and P.J. Shaw, *Update on the glutamatergic neurotransmitter system and the role of excitotoxicity in amyotrophic lateral sclerosis.* Muscle Nerve, 2002. **26**(4): p. 438-58.

197. Agar, J. and H. Durham, *Relevance of oxidative injury in the pathogenesis of motor neuron diseases.* Amyotroph Lateral Scler Other Motor Neuron Disord, 2003. **4**(4): p. 232-42.

198. von Lewinski, F. and B.U. Keller, *Ca2+, mitochondria and selective motoneuron vulnerability: implications for ALS.* Trends Neurosci, 2005. **28**(9): p. 494-500.

199. Alexianu, M.E., et al., *The role of calcium-binding proteins in selective motoneuron vulnerability in amyotrophic lateral sclerosis.* Ann Neurol, 1994. **36**(6): p. 846-58.

200. Beers, D.R., et al., *Parvalbumin overexpression alters immune-mediated increases in intracellular calcium, and delays disease onset in a transgenic model of familial amyotrophic lateral sclerosis.* J Neurochem, 2001. **79**(3): p. 499-509.

201. Ho, B.K., et al., *Expression of calbindin-D28K in motoneuron hybrid cells after retroviral infection with calbindin-D28K cDNA prevents amyotrophic lateral sclerosis IgG-mediated cytotoxicity.* Proc Natl Acad Sci U S A, 1996. **93**(13): p. 6796-801.

202. Carri, M.T., et al., *Expression of a Cu,Zn superoxide dismutase typical of familial amyotrophic lateral sclerosis induces mitochondrial alteration and increase of cytosolic Ca2+ concentration in transfected neuroblastoma SH-SY5Y cells.* FEBS Lett, 1997. **414**(2): p. 365-8.

203. Carriedo, S.G., H.Z. Yin, and J.H. Weiss, *Motor neurons are selectively vulnerable to AMPA/kainate receptor-mediated injury in vitro.* J Neurosci, 1996. **16**(13): p. 4069-79.

204. Carriedo, S.G., et al., *AMPA exposures induce mitochondrial Ca(2+) overload and ROS generation in spinal motor neurons in vitro.* J Neurosci, 2000. **20**(1): p. 240-50.

205. Ostwald, T.J. and D.H. MacLennan, *Isolation of a high affinity calcium-binding protein from sarcoplasmic reticulum.* J Biol Chem, 1974. **249**(3): p. 974-9.

206. Fliegel, L., et al., *Molecular cloning of the high affinity calcium-binding protein (calreticulin) of skeletal muscle sarcoplasmic reticulum.* J Biol Chem, 1989. **264**(36): p. 21522-8.

207. Fliegel, L., et al., *The high-affinity calcium binding protein of sarcoplasmic reticulum. Tissue distribution, and homology with calregulin.* Biochim Biophys Acta, 1989. **982**(1): p. 1-8.

208. Baksh, S. and M. Michalak, *Expression of calreticulin in Escherichia coli and identification of its Ca2+ binding domains.* J Biol Chem, 1991. **266**(32): p. 21458-65.

209. Nakamura, K., et al., *Functional specialization of calreticulin domains.* J Cell Biol, 2001. **154**(5): p. 961-72.

210. Williams, D.B., *Beyond lectins: the calnexin/calreticulin chaperone system of the endoplasmic reticulum.* J Cell Sci, 2006. **119**(Pt 4): p. 615-23.

211. Nigam, S.K., et al., *A set of endoplasmic reticulum proteins possessing properties of molecular chaperones includes Ca(2+)-binding proteins and members of the thioredoxin superfamily.* J Biol Chem, 1994. **269**(3): p. 1744-9.

212. Otteken, A. and B. Moss, *Calreticulin interacts with newly synthesized human immunodeficiency virus type 1 envelope glycoprotein, suggesting a chaperone function similar to that of calnexin.* J Biol Chem, 1996. **271**(1): p. 97-103.

213. Michalak, M., J.M. Robert Parker, and M. Opas, *Ca2+ signaling and calcium binding chaperones of the endoplasmic reticulum.* Cell Calcium, 2002. **32**(5-6): p. 269-78.

214. Bedard, K., et al., *Cellular functions of endoplasmic reticulum chaperones calreticulin, calnexin, and ERp57.* Int Rev Cytol, 2005. **245**: p. 91-121.

215. Conway, E.M., et al., *Heat shock-sensitive expression of calreticulin. In vitro and in vivo up-regulation.* J Biol Chem, 1995. **270**(28): p. 17011-6.

216. Llewellyn, D.H., et al., *Induction of calreticulin expression in HeLa cells by depletion of the endoplasmic reticulum Ca2+ store and inhibition of N-linked glycosylation.* Biochem J, 1996. **318 (Pt 2)**: p. 555-60.

217. Waser, M., et al., *Regulation of calreticulin gene expression by calcium.* J Cell Biol, 1997. **138**(3): p. 547-57.

218. Mery, L., et al., *Overexpression of calreticulin increases intracellular Ca2+ storage and decreases store-operated Ca2+ influx.* J Biol Chem, 1996. **271**(16): p. 9332-9.

219. Arnaudeau, S., et al., *Calreticulin differentially modulates calcium uptake and release in the endoplasmic reticulum and mitochondria.* J Biol Chem, 2002. **277**(48): p. 46696-705.

220. Liu, H., et al., *Endoplasmic reticulum chaperones GRP78 and calreticulin prevent oxidative stress, Ca2+ disturbances, and cell death in renal epithelial cells.* J Biol Chem, 1997. **272**(35): p. 21751-9.

221. Llewelyn Roderick, H., et al., *Role of calreticulin in regulating intracellular Ca2+ storage and capacitative Ca2+ entry in HeLa cells.* Cell Calcium, 1998. **24**(4): p. 253-62.

222. Bastianutto, C., et al., *Overexpression of calreticulin increases the Ca2+ capacity of rapidly exchanging Ca2+ stores and reveals aspects of their lumenal microenvironment and function.* J Cell Biol, 1995. **130**(4): p. 847-55.

223. Hayashida, Y., et al., *Calreticulin represses E-cadherin gene expression in Madin-Darby canine kidney cells via Slug.* J Biol Chem, 2006. **281**(43): p. 32469-84.

224. Xu, W., et al., *Calreticulin modulates capacitative Ca2+ influx by controlling the extent of inositol 1,4,5-trisphosphate-induced Ca2+ store depletion.* J Biol Chem, 2000. **275**(47): p. 36676-82.

225. Coppolino, M.G., et al., *Calreticulin is essential for integrin-mediated calcium signalling and cell adhesion.* Nature, 1997. **386**(6627): p. 843-7.

226. Liu, H., et al., *Endoplasmic reticulum stress proteins block oxidant-induced Ca2+ increases and cell death.* J Biol Chem, 1998. **273**(21): p. 12858-62.

227. Liu, N., et al., *Decreasing calreticulin expression lowers the Ca2+ response to bradykinin and increases sensitivity to ionomycin in NG-108-15 cells.* J Biol Chem, 1994. **269**(46): p. 28635-9.

228. Mesaeli, N. and C. Phillipson, *Impaired p53 expression, function, and nuclear localization in calreticulin-deficient cells.* Mol Biol Cell, 2004. **15**(4): p. 1862-70.

229. Chishti, M.A., et al., *Early-onset amyloid deposition and cognitive deficits in transgenic mice expressing a double mutant form of amyloid precursor protein 695.* J Biol Chem, 2001. **276**(24): p. 21562-70.

230. Garavito-Aguilar, Z.V., et al., *Differential thapsigargin-sensitivities and interaction of Ca2+ stores in human SH-SY5Y neuroblastoma cells.* Brain Res, 2004. **1011**(2): p. 177-86.

231. Giacomello, M., et al., *Reduction of Ca2+ stores and capacitative Ca2+ entry is associated with the familial Alzheimer's disease presenilin-2 T122R mutation and anticipates the onset of dementia.* Neurobiol Dis, 2005. **18**(3): p. 638-48.

232. Leissring, M.A., et al., *Capacitative calcium entry deficits and elevated luminal calcium content in mutant presenilin-1 knockin mice.* J Cell Biol, 2000. **149**(4): p. 793-8.

233. Yoo, A.S., et al., *Presenilin-mediated modulation of capacitative calcium entry.* Neuron, 2000. **27**(3): p. 561-72.

234. Shaner, N.C., et al., *Improved monomeric red, orange and yellow fluorescent proteins derived from Discosoma sp. red fluorescent protein.* Nat Biotechnol, 2004. **22**(12): p. 1567-72.

235. Arrasate, M. and S. Finkbeiner, *Automated microscope system for determining factors that predict neuronal fate.* Proc Natl Acad Sci U S A, 2005. **102**(10): p. 3840-5.

236. Kennedy, T.E., et al., *Long-term sensitization training in Aplysia leads to an increase in calreticulin, a major presynaptic calcium-binding protein.* Neuron, 1992. **9**(6): p. 1013-24.

237. Taguchi, J., et al., *Different expression of calreticulin and immunoglobulin binding protein in Alzheimer's disease brain.* Acta Neuropathol, 2000. **100**(2): p. 153-60.

238. Li, X., L. Song, and R.S. Jope, *Cholinergic stimulation of AP-1 and NF kappa B transcription factors is differentially sensitive to oxidative stress in SH-SY5Y*

neuroblastoma: relationship to phosphoinositide hydrolysis. J Neurosci, 1996. **16**(19): p. 5914-22.

239. Huang, H.M., H.C. Ou, and S.J. Hsieh, *Amyloid beta peptide impaired carbachol but not glutamate-mediated phosphoinositide pathways in cultured rat cortical neurons.* Neurochem Res, 2000. **25**(2): p. 303-12.

240. Zatti, G., et al., *The presenilin 2 M239I mutation associated with familial Alzheimer's disease reduces Ca2+ release from intracellular stores.* Neurobiol Dis, 2004. **15**(2): p. 269-78.

241. Murayama, K., et al., *Neural Cell Lines*, in *Protocols for Neural Cell Culture*, S. Fedoroff, Editor. 2001, Humana Press, Inc.: Totowa, NJ. p. 219-228.

242. Duckett, C.S., et al., *A conserved family of cellular genes related to the baculovirus iap gene and encoding apoptosis inhibitors.* Embo J, 1996. **15**(11): p. 2685-94.

243. Deveraux, Q.L., et al., *X-linked IAP is a direct inhibitor of cell-death proteases.* Nature, 1997. **388**(6639): p. 300-4.

244. Deveraux, Q.L., et al., *IAPs block apoptotic events induced by caspase-8 and cytochrome c by direct inhibition of distinct caspases.* Embo J, 1998. **17**(8): p. 2215-23.

245. Deveraux, Q.L., et al., *Cleavage of human inhibitor of apoptosis protein XIAP results in fragments with distinct specificities for caspases.* Embo J, 1999. **18**(19): p. 5242-51.

246. Birkey Reffey, S., et al., *X-linked inhibitor of apoptosis protein functions as a cofactor in transforming growth factor-beta signaling.* J Biol Chem, 2001. **276**(28): p. 26542-9.

247. Sanna, M.G., et al., *IAP suppression of apoptosis involves distinct mechanisms: the TAK1/JNK1 signaling cascade and caspase inhibition.* Mol Cell Biol, 2002. **22**(6): p. 1754-66.

248. Levkau, B., et al., *xIAP induces cell-cycle arrest and activates nuclear factor-kappaB : new survival pathways disabled by caspase-mediated cleavage during apoptosis of human endothelial cells.* Circ Res, 2001. **88**(3): p. 282-90.

249. Yamaguchi, K., et al., *XIAP, a cellular member of the inhibitor of apoptosis protein family, links the receptors to TAB1-TAK1 in the BMP signaling pathway.* Embo J, 1999. **18**(1): p. 179-87.

250. Hofer-Warbinek, R., et al., *Activation of NF-kappa B by XIAP, the X chromosome-linked inhibitor of apoptosis, in endothelial cells involves TAK1.* J Biol Chem, 2000. **275**(29): p. 22064-8.

251. Lewis, J., et al., *Uncoupling of the signaling and caspase-inhibitory properties of X-linked inhibitor of apoptosis.* J Biol Chem, 2004. **279**(10): p. 9023-9.

252. Wang, X., et al., *X-linked inhibitor of apoptosis (XIAP) protein protects against caspase activation and tissue loss after neonatal hypoxia-ischemia.* Neurobiol Dis, 2004. **16**(1): p. 179-89.

253. Xu, D., et al., *Attenuation of ischemia-induced cellular and behavioral deficits by X chromosome-linked inhibitor of apoptosis protein overexpression in the rat hippocampus.* J Neurosci, 1999. **19**(12): p. 5026-33.

254. Trapp, T., et al., *Transgenic mice overexpressing XIAP in neurons show better outcome after transient cerebral ischemia.* Mol Cell Neurosci, 2003. **23**(2): p. 302-13.

255. Korhonen, L., N. Belluardo, and D. Lindholm, *Regulation of X-chromosome-linked inhibitor of apoptosis protein in kainic acid-induced neuronal death in the rat hippocampus.* Mol Cell Neurosci, 2001. **17**(2): p. 364-72.

256. Tanaka, T., et al., *Neurobiological studies of dementia--biological markers and neuroprotective strategies for Alzheimer disease.* Acta Neurol Taiwan, 2006. **15**(1): p. 68-71.

257. Eberhardt, O., et al., *Protection by synergistic effects of adenovirus-mediated X-chromosome-linked inhibitor of apoptosis and glial cell line-derived neurotrophic factor gene transfer in the 1-methyl-4-phenyl-1,2,3,6-tetrahydropyridine model of Parkinson's disease.* J Neurosci, 2000. **20**(24): p. 9126-34.

258. Ishigaki, S., et al., *X-Linked inhibitor of apoptosis protein is involved in mutant SOD1-mediated neuronal degeneration.* J Neurochem, 2002. **82**(3): p. 576-84.

259. Wootz, H., et al., *XIAP decreases caspase-12 cleavage and calpain activity in spinal cord of ALS transgenic mice.* Exp Cell Res, 2006. **312**(10): p. 1890-8.

260. Kugler, S., et al., *The X-linked inhibitor of apoptosis (XIAP) prevents cell death in axotomized CNS neurons in vivo.* Cell Death Differ, 2000. **7**(9): p. 815-24.

261. Arundine, M. and M. Tymianski, *Molecular mechanisms of calcium-dependent neurodegeneration in excitotoxicity.* Cell Calcium, 2003. **34**(4-5): p. 325-37.

262. Leissring, M.A., et al., *Calsenilin reverses presenilin-mediated enhancement of calcium signaling.* Proc Natl Acad Sci U S A, 2000. **97**(15): p. 8590-3.

263. Paschen, W. and T. Mengesdorf, *Endoplasmic reticulum stress response and neurodegeneration.* Cell Calcium, 2005. **38**(3-4): p. 409-15.

264. Pringle, A.K., *In, out, shake it all about: elevation of [Ca2+]i during acute cerebral ischaemia.* Cell Calcium, 2004. **36**(3-4): p. 235-45.

265. Hu, P., et al., *Critical role of endogenous Akt/IAPs and MEK1/ERK pathways in counteracting endoplasmic reticulum stress-induced cell death.* J Biol Chem, 2004. **279**(47): p. 49420-9.

266. Pinton, P. and R. Rizzuto, *Bcl-2 and Ca2+ homeostasis in the endoplasmic reticulum.* Cell Death Differ, 2006. **13**(8): p. 1409-18.

267. Kakuda, T., *Neuroprotective effects of the green tea components theanine and catechins.* Biol Pharm Bull, 2002. **25**(12): p. 1513-8.

268. Kakuda, T., et al., *Inhibition by theanine of binding of [3H]AMPA, [3H]kainate, and [3H]MDL 105,519 to glutamate receptors.* Biosci Biotechnol Biochem, 2002. **66**(12): p. 2683-6.

269. Nagasawa, K., et al., *Possible involvement of group I mGluRs in neuroprotective effect of theanine.* Biochem Biophys Res Commun, 2004. **320**(1): p. 116-22.

270. Kakuda, T., et al., *Protective effect of gamma-glutamylethylamide (theanine) on ischemic delayed neuronal death in gerbils.* Neurosci Lett, 2000. **289**(3): p. 189-92.

271. Egashira, N., et al., *Neuroprotective effect of gamma-glutamylethylamide (theanine) on cerebral infarction in mice.* Neurosci Lett, 2004. **363**(1): p. 58-61.

272. Yokogoshi, H., et al., *Effect of theanine, r-glutamylethylamide, on brain monoamines and striatal dopamine release in conscious rats.* Neurochem Res, 1998. **23**(5): p. 667-73.

273. Tollefson, G.D., *Short-term effects of the calcium channel blocker nimodipine (Bay-e-9736) in the management of primary degenerative dementia.* Biol Psychiatry, 1990. **27**(10): p. 1133-42.

274. Bullock, R., *Efficacy and safety of memantine in moderate-to-severe Alzheimer disease: the evidence to date.* Alzheimer Dis Assoc Disord, 2006. **20**(1): p. 23-9.

275. Golde, T.E., *Disease modifying therapy for AD?* J Neurochem, 2006. **99**(3): p. 689-707.